

Fall 12-2016

**Examining the Combined Effects of Dissolved Oxygen,
Temperature, and Body Size on the Physiological Responses of a
Model Macrobenthic Polychaete Species, *Capitella teleta***

Kelsey Burns Gillam
University of Southern Mississippi

Follow this and additional works at: <https://aquila.usm.edu/dissertations>



Part of the [Comparative and Evolutionary Physiology Commons](#), [Integrative Biology Commons](#), [Laboratory and Basic Science Research Commons](#), [Marine Biology Commons](#), [Other Physiology Commons](#), and the [Terrestrial and Aquatic Ecology Commons](#)

Recommended Citation

Gillam, Kelsey Burns, "Examining the Combined Effects of Dissolved Oxygen, Temperature, and Body Size on the Physiological Responses of a Model Macrobenthic Polychaete Species, *Capitella teleta*" (2016). *Dissertations*. 892.
<https://aquila.usm.edu/dissertations/892>

This Dissertation is brought to you for free and open access by The Aquila Digital Community. It has been accepted for inclusion in Dissertations by an authorized administrator of The Aquila Digital Community. For more information, please contact Joshua.Cromwell@usm.edu.

EXAMINING THE COMBINED EFFECTS OF DISSOLVED OXYGEN,
TEMPERATURE, AND BODY SIZE ON THE PHYSIOLOGICAL RESPONSES OF A
MODEL MACROBENTHIC POLYCHAETE SPECIES, *CAPITELLA TELETA*

by

Kelsey Burns Gillam

A Dissertation
Submitted to the Graduate School
and the Department of Biological Sciences
at The University of Southern Mississippi
in Partial Fulfillment of the Requirements
for the Degree of Doctor of Philosophy

Approved:

Dr. Chet F. Rakocinski, Committee Chair
Professor, Ocean Science and Technology

Dr. Mark S. Peterson, Committee Member
Professor, Ocean Science and Technology

Dr. Robert J. Griffitt, Committee Member
Associate Professor, Ocean Science and Technology

Dr. Andrew N. Evans, Committee Member
Assistant Professor, Ocean Science and Technology

Dr. Karen S. Coats
Dean of the Graduate School

December 2016

COPYRIGHT BY

Kelsey Burns Gillam

2016

Published by the Graduate School



ABSTRACT

EXAMINING THE COMBINED EFFECTS OF DISSOLVED OXYGEN, TEMPERATURE, AND BODY SIZE ON THE PHYSIOLOGICAL RESPONSES OF A MODEL MACROBENTHIC POLYCHAETE SPECIES, *CAPITELLA TELETA*

by Kelsey Burns Gillam

December 2016

While the scientific community is in consensus that coastal systems are threatened by climate change, few climate change studies test the effects of more than one variable directly related to climate change. The dissolved oxygen (DO) levels of the ocean are currently subject to both global warming and eutrophication; 94% of all hypoxia zones are expected to experience $\geq 2^{\circ}\text{C}$ increase by 2035. This dissertation aims to examine how a model organism responds to simultaneous thermal and DO stress involving four levels of DO (100%, 70%, 50%, and 20%) saturation and three temperatures (15°C, 20°C, and 25°C).

The polychaete, *Capitella teleta*, maintained aerobic respiration at low DO levels under natural temperatures, 15°C and 20°C, but reduced its respiration by 40% at 25°C under hypoxia (20% saturation). The main anaerobic pathway of *C. teleta* was mediated by strombine dehydrogenase, in addition to weak activity by three additional pyruvate oxidoreductases. Anaerobic respiration at 25°C under normoxia was symptomatic of functional anaerobiosis, suggesting this species may be near its critical limit. Total energy production based on combined aerobic and anaerobic respiration suggests that large individuals (range from 0.003-0.012 g) may be limited under low DO and high temperatures.

Specific growth rates under starvation ranged from -2.34 to -69.31% d and were significantly influenced by temperature. Weight loss was significantly greater during the first 24 h and declined over 72 h. Weight losses were unrelated to body size. Under fed conditions, specific growth rates varied from -50.58 to 30.76%; a significant interaction occurred between DO level and body size. Small individuals lost less weight with increasing DO, whereas large individuals consistently exhibited negative growth rates across DO levels. There was a significant interaction between DO level and time, in that during the first 48 h growth was negative at lower DO levels, but positive at high DO levels.

Egestion rates were significantly influenced by temperature, DO, and time. Egestion rates at low DO respond strongly to increasing temperature and decrease over time. Overall, *C. teleta* was capable of surviving low DO and high temperatures; however, the species was near its critical thermal limit at 25°C.

ACKNOWLEDGMENTS

I would like to thank my advisor, Dr. Chet Rakocinski for introducing me to the world of hypoxia and polychaetes. We had our highs and lows, but they helped mold me into the scientist I am today. I would like to thank my Ph.D. committee members, Dr. Patricia Biesiot, Dr. Andy Evans, Dr. Joe Griffitt, and Dr. Mark S. Peterson, for their expertise and help along the way. They pushed me to be the best I could be and to produce the best science possible. I would particularly like to thank Dr. Joe Griffitt for allowing me to invade his lab for over a year (even after putting a hole in his floor). A huge “thank you” goes to Alyssa Bennett who worked by my side on many of the experiments and has helped to expand the polychaete ecophysiology research program. Acknowledgment must be given to all the summer interns who helped me, Ashley Meredith, Tyler Sanders, Alex Thomas, and Joyce Baptista. Gratitude is also extended to Dr. Patrick Biber and Dr. Kevin Dillon for the use of their space. Last but not least, thank you to all of my friends at GCRL, especially Corey Russo and Carley Knight, for moral support and many graduate school memories.

DEDICATION

This dissertation is dedicated to the most amazing and inspiring family in the world: Andrea Burns, Fred Pokrzywa, Anna Marie Pokrzywa, and Haley Burns. It is also dedicated to Patrick Gillam, who during this journey was first my lab mate, then my best friend, fiancé, and finally husband. You were my crutch when I fell down and my rock throughout my pursuit of this degree. All of you helped me laugh during the tears, celebrate during the accomplishments, and remember to always focus on the light at the end of the tunnel. Without this team of support “Dr.” Kelsey Gillam would never exist.

TABLE OF CONTENTS

ABSTRACT	ii
ACKNOWLEDGMENTS	iv
DEDICATION	v
LIST OF TABLES	xiii
LIST OF ILLUSTRATIONS	xvii
LIST OF ABBREVIATIONS	xxv
CHAPTER I - INTRODUCTION	1
1.1 Temperature and Hypoxia.....	1
1.2 Physiological Response to Increasing Temperature and Decreasing Dissolved Oxygen.....	3
1.3 Body Size Relationships	6
1.4 Model Species	7
1.5 Conclusion	9
CHAPTER II – SYNERGYSTIC INTERACTIONS OF DISSOLVED OXYGEN AND TEMPERATURE ON THE ALLOMETRIC AEROBIC RESPIRATORY RESPONSE OF A MODEL TOLERANT POLYCHAETE, <i>CAPITELLA TELETA</i>	11
2.1 Introduction.....	11
2.2 Materials and Methods.....	14
2.2.1 Model Species.....	14

2.2.2 Experimental Setup.....	16
2.2.3 Respiration Measurements.....	18
2.2.4 Analysis.....	21
2.3 Results.....	22
2.3.1 Effects of Temperature and Dissolved Oxygen on VO ₂	22
2.3.2 Allometric Relationships	26
2.3.3 Critical Sizes of Ontogenetic Shifts in Allometric Mass-Specific Respiration Curves.	28
2.4 Discussion	30
2.4.1 Physiological Relationships	30
2.4.2 Allometric Relationships	32
2.4.3 Conclusion	35
CHAPTER III – ANAEROBIC ENZYMATIC ACTIVITY AND TOTAL CATABOLIC ENERGY PRODUCTION BY A MODEL TOLERANT POLYCHAETE, <i>CAPITELLA</i> <i>TELETA</i> , EXPOSED TO COMBINED LEVELS OF DISSOLVED OXYGEN AND TEMPERATURE IN RELATION TO BODY SIZE	
3.1 Introduction.....	36
3.2 Materials and Methods.....	40
3.2.1 Experimental Setup.....	40
3.2.2 Enzyme Activity Assays	40

3.2.3 Analysis.....	42
3.3 Results.....	42
3.3.1 Anaerobic Pathways.....	42
3.3.2 Body Size Effects.....	44
3.3.3 Catabolic Energy Production	46
3.4 Discussion	49
3.4.1 Anaerobic Enzymatic Activity.....	49
3.4.2 Conclusion	50
CHAPTER IV – THE EFFECT OF STARVATION ON GROWTH, EGESTION, AND MORTALITY OF THE MODEL TOLERANT POLYCHAETE, <i>CAPITELLA TELETA</i> , UNDER COMBINED LEVELS OF DISSOLVED OXYGEN, TEMPERATURE, AND BODY SIZE.....	52
4.1 Introduction.....	52
4.2 Material and Methods	54
4.2.1 Model Species.....	54
4.2.2 Culture Maintenance	55
4.2.3 Experimental Treatments	55
4.2.4 Treatment Control.....	57
4.2.5 Flow-through System.....	58
4.2.6 Starvation Experiments.....	60

4.2.7 Quantifying Egestion	61
4.2.8 Data Analysis	62
4.3 Results.....	64
4.3.1 Specific Growth Results	64
4.3.2 Daily Weight Loss	67
4.3.3 Fecal Counts and Egestion Rates	68
4.3.4 Body-Size Egestion Relationships	70
4.3.5 Egestion vs. Degrowth	74
4.3.6 Mortality	76
4.4 Discussion	78
4.4.1 Conclusion	82
CHAPTER V GROWTH, EGESTION, AND MORTALITY OF A MODEL	
TOLERANT POLYCHAETE, <i>CAPITELLA TELETA</i> , TO VARYING LEVELS OF	
DISSOLVED OXYGEN, TEMPERATURE, AND BODY SIZE	84
5.1 Introduction.....	84
5.2 Materials and Methods.....	86
5.2.1 Model Species	86
5.2.2 Culture Maintenance	87
5.2.3 Experimental Treatments	87
5.2.4 Regulation of Treatment Conditions and Flow-through System	89

5.2.5 Growth Experiments	89
5.2.6 Growth Data Analysis.....	90
5.2.7 Egestion Analysis.....	91
5.3 Results.....	94
5.3.1 Growth Rates	94
5.3.1.1 Specific Growth Rates	94
5.3.1.2 Daily Percent Growth	96
5.3.2 Egestion Rates.....	97
5.3.3 Gross Production Efficiency	103
5.3.4 Mortality	104
5.4 Discussion.....	106
5.4.1 Specific Growth and Egestion Rate	106
5.4.2 Conclusion	109
CHAPTER VI MAKING THE CONNECTIONS: HOW DO COMPLEMENTARY PHYSIOLOGICAL RESPONSES PRODUCE A STRESS RESPONSE IN THE POLYCHAETE, <i>CAPITELLA TELETA</i> , UNDER DISSOLVED OXYGEN AND THERMAL STRESS	110
6.1 Introduction.....	110
6.1.1 Stress Bioenergetic Framework	110
6.1.2 Physiological Stress of Dissolved Oxygen and Temperature	112

6.2 Materials and Methods.....	113
6.2.1 Surface Plots and OCLTT Analysis.....	113
6.2.2 Contribution Analysis	114
6.3 Results.....	115
6.3.1 General Comparisons.....	115
6.3.2 ATP Supply and Demand	117
6.3.3 Relative Importance of Independent Variables.....	120
6.4 Discussion	122
6.4.1 Ecophysiological Connections.....	122
6.4.2 Overall Outlook and Conclusions.....	126
APPENDIX A – INSTRUCTIONS FOR CULTURING <i>CAPITELLA TELETA</i> PER CAROLA NOJI FROM RUTGERS UNIVERSITY	128
APPENDIX B COMPARISONS OF 24H AND 168 MASS-SPECIFIC RESPIRATION OF <i>CAPITELLA TELETA</i>	130
APPENDIX C – RELATIONSHIPS BETWEEN TOTAL VOLUME EGESTED AND THE TOTAL WEIGHT EGESTED OF <i>CAPITELLA TELETA</i>	131
APPENDIX D Q-Q PLOTS OF GROSS PRODUCTION EFFICIENCY OF <i>CAPITELLA TELETA</i>	132
APPENDIX E SHAPIRO-WILK TEST AND Q-Q PLOT FOR DAILY GROWTH OF <i>CAPITELLA TELETA</i>	133

REFERENCES	135
------------------	-----

LIST OF TABLES

Table 2.1 Treatment levels of dissolved oxygen and temperature for respiration measurements (\pm SD).....	18
Table 2.2 Q_{10} values for mass-specific oxygen consumption rates in <i>Capitella teleta</i> under multiple dissolved oxygen and temperature treatments at small and large body sizes.) ..	24
Table 2.3 Nonlinear regression equations relating VO_2 (mg O ₂ /g/hr-1) to body weight (g) in <i>Capitella teleta</i> exposed to multiple dissolved oxygen and temperature treatments. Regressions equations fit in the form of $VO_2 = aW^b$, where W is weight (mg) n= number of samples; r^2 = correlation coefficient. Non mass-specific allometric exponent b is calculated as $b = 1 + b'$.	27
Table 2.4 The critical sizes for ontogenetic breaks and scaling exponents for smaller and larger size ranges of <i>Capitella teleta</i> at four dissolved oxygen saturations and three temperatures. Statistically significant breaks denoted by *.	29
Table 3.1 Treatment levels of dissolved oxygen and temperature for anaerobic respiration measurements (mean + standard error).....	40
Table 3.2 Anaerobic enzymatic activity (mean + SD) of four pyruvate oxidoreductases (SDH = strombine dehydrogenase, ADH = alanopine dehydrogenase, ODH = opine dehydrogenase, and LDH = lactate dehydrogenase) at two temperature and four dissolved oxygen saturation levels (%).	43
Table 3.3 Q_{10} values from 15° to 25° C for four pyruvate oxidoreductases (SDH = strombine dehydrogenase, ADH = alanopine dehydrogenase, ODH = opine dehydrogenase, and LDH = lactate dehydrogenase) at four dissolved oxygen saturations. No Q_{10} exists for SDH and ADH 100% due to no enzymatic activity measured at 15°C.	44

Table 3.4 Enzymatic activity (mean + SE) of strombine dehydrogenase for two body size groups exposed to two temperatures and four dissolved oxygen saturation levels (%). ..	45
Table 3.5 Allometric relationships for anaerobic enzymatic activity of strombine dehydrogenase for <i>Capitella teleta</i> exposed to two temperature and four dissolved oxygen saturation levels (%). Equation in form of $y = aW^b$; n= number of samples; r^2 = correlation coefficient (mean + SE). Whole organism allometric exponent b is calculated as $b = 1 + b'$. ..	46
Table 3.6 Mass-specific catabolic energy (mmol ATP/ g WW/ d) produced by aerobic respiration vs. the two main anaerobic pyruvate oxidoreductases for <i>Capitella teleta</i> (mean + SE). Total = mean energy available. WW = wet weight.	48
Table 4.1 Mean DO and temperature conditions (\pm SE) for the twelve oxygen saturation \times temperature treatments.....	58
Table 4.2 Summary of the daily specific growth (SG % d ⁻¹) and total weight loss of <i>Capitella teleta</i> during starvation while exposed to 12 treatment combinations comprising four DO saturation and three temperature levels (\pm SE).....	66
Table 4.3 The Q ₁₀ values of the specific degrowth rate (% d) of <i>Capitella teleta</i> during starvation while exposed to 12 treatment combinations comprising four DO saturation and three temperature levels	66
Table 4.4 The Q ₁₀ values for the egestion rate (ug d ⁻¹) of <i>Capitella teleta</i> spanning three temperature intervals over four DO saturation levels.	70
Table 4.5 Regressions between the geometric mean body size and sediment egested (ug) during the first 24 h of starvation of <i>Capitella teleta</i> . Regressions are fit as: $y = Mx + b$,	

where y is sediment egested and x is the geometric mean body size. Statistically significant regressions are denoted by *.	72
Table 4.6 Correlations between daily specific growth (%) and total sediment egested (ug) during the first 24 h of starvation for <i>Capitella teleta</i> . Statistically significant correlations are denoted by *.	75
Table 5.1 Mean experimental temperature (°C) and DO levels (mg/L) for the 5 d growth experiment (\pm SE).	88
Table 5.2 Mean specific growth rates (% d) of <i>Capitella teleta</i> under four dissolved (\pm SE).	94
Table 5.3 Linear regressions between the initial wet weight (g) and specific growth rate (% d) for <i>Capitella teleta</i> at four dissolved oxygen saturations. Relationships are in linear form: $y = Mx + b$ where y= specific growth and x= initial wet weight.	96
Table 5.4 Allometric relationships between body size (g) and egestion rate ($\mu\text{g d}^{-1}$) for <i>Capitella teleta</i> across three temperatures (i.e., pooled over 4 DO levels) spanning four days. Regressions in the form: $y = aX^b$ where y= egestion rate ($\mu\text{g d}^{-1}$) and X = wet weight (g).	102
Table 6.1 Summary of body size effects on the physiology of <i>Capitella teleta</i> .	117
Table 6.2 Relative importance of egestion, respiration, and body size on specific growth models for <i>Capitella teleta</i> at four DO saturations. Model form: Specific growth (% d) = Egestion ($\mu\text{g d}^{-1}$) + Respiration ($\text{mg O}_2 \text{ d}$) + initial wet weight (g).	121
Table C.1 Correlations between the total volume egested ($\text{mm}^3 \text{ d}^{-1}$) and total weight egested ($\mu\text{g d}^{-1}$) for <i>Capitella teleta</i> after 24 hours of starvation when exposed to three temperatures and four dissolved oxygen saturations.	131

Table E.1 The Shapiro-Wilk test of normality for daily growth data from four dissolved oxygen saturation levels, three temperatures, and four time intervals. * = statistically significant at $p = 0.05$	133
---	-----

LIST OF ILLUSTRATIONS

Figure 1.1 The physical and biological effects of climate change drivers on eutrophication and other hypoxia-related factors (from Alteri and Gedan 2015).	3
Figure 1.2 Projected temperature increases within hypoxic zones of the United States by 2100 (from Alteri and Gedan 2015).....	3
Figure 1.3 A) Sea surface temperatures during the last half of 2012 and the first half of 2013; the highest recorded temperatures in the past 150 years were observed between August and September 2012. B) Sea surface temperatures for the Gulf of Maine from late 2013 to early 2014. Gray bars represent the long term mean SST + 1 and 2 SD. The red line represents surface temperatures above mean and the blue line represents temperatures below mean. C) Deviation from long-term mean sea surface temperature for the Gulf of Maine and George’s Bank, USA during Spring 2013. http://nefsc.noaa.gov/ecosys/advisory/current/sst.html	9
Figure 2.1 Comparison of the FireSting fiber optic respirometer (blue diamond; n = 10) to the Qubit Clark’s electrode respirometer (red square; n = 20) saw no apparent difference in a) respiration measurement or b) respiration residuals at 20°C and 100% oxygen saturation.....	19
Figure 2.2 Mass-specific respiration rates of <i>Capitella teleta</i> at three temperatures crossed with four dissolved oxygen saturations.....	23
Figure 2.3 Interaction effects between dissolved oxygen and temperature on Q ₁₀ values for oxygen consumption rates in A) small and B) large <i>Capitella teleta</i>	25

Figure 2.4 Respiration capacity ($VO_{2x}/VO_{2(100\%)}$) for small and large size categories of <i>Capitella teleta</i> at three temperatures (A = 15°C, B = 20°C, and C = 25°C) and four dissolved oxygen saturations.	25
Figure 2.5 A) Allometric exponent, b , and B) constant, a , (of $VO_2 = aW^b$) for 12 (three temperature crossed with four dissolved oxygen saturation) treatments.	28
Figure 2.6 The body size of <i>Capitella teleta</i> where shifts in allometric weight exponent (b) occur when exposed to 12 treatments (three temperatures and four dissolved oxygen levels. Graph includes points that are statistically significant or marginally significant ($p < 0.1$)).	29
Figure 2.7 The allometric scaling exponent b (of $VO_2 = aW^b$) A) before and B) after body size shifts of <i>Capitella teleta</i> when exposed to 12 treatments (three temperatures and four dissolved oxygen levels). Graph includes data that is statistically significant or marginally significant ($p < 0.1$)).	30
Figure 3.1 Anaerobic enzymatic activity of four pyruvate oxidoreductases (SDH = strombine dehydrogenase, ADH = alanopine dehydrogenase, ODH= opine dehydrogenase, and LDH = lactate dehydrogenase) at two temperatures (A = 15°C; B = 25°C) and four DO saturation levels (%) (\pm SE).	44
Figure 3.2 A) Allometric relationships for strombine dehydrogenase activity in <i>Capitella teleta</i> across four DO levels at 15°C (mean \pm SE); B) allometric mass-specific curves (20% = solid line and 50% = dashed line).	45
Figure 3.3 A) mass-specific allometric relationships for strombine dehydrogenase activity in <i>Capitella teleta</i> at 25°C (mean \pm SE); B) allometric curves (20% = solid line, 50% = dashed line, 70% = bold solid line, 100% = dotted bold line).	46

Figure 3.4 Catabolic energy produced by aerobic respiration for <i>Capitella teleta</i> exposed to two temperatures (A=15°C; B=25°C) and two dissolved oxygen saturations (20% and 100%) (WW= wet weight; mean + SE).	47
Figure 3.5 Relative contribution (mmol ATP/g WW/ d) of aerobic and anaerobic respiration to the total catabolic potential energy production of <i>Capitella teleta</i> exposed to 20% and 100% dissolved oxygen saturation and two temperature levels (A and B = 15°C; C and D = 25°C; WW= wet weight).	48
Figure 4.1 Variation in the twelve DO (mg/L) and temperature treatments over four days during starvation experiment (lines on bottom panel represent same temperature treatments as in upper panel).	56
Figure 4.2 Flow-through experimental layout for one of the DO treatments comprising three replicates of each of three temperature treatments and body size categories. Inset illustrates a PVC experimental chamber containing a 5 mL centrifuge tube enclosure which housed one worm. Each of the four DO treatments was set up using the same layout. Red = 25°C, green = 20°C, and blue= 15°C.	57
Figure 4.3 The specific growth rate (% d) by body size of <i>Capitella teleta</i> during starvation while exposed to 12 treatment combinations comprising four DO levels and three temperature levels.	65
Figure 4.4 The specific growth rate (% d) of <i>Capitella teleta</i> under starvation pooled across (A) four DO saturation levels and (B) three temperature levels (\pm SE).	65
Figure 4.5 Total weight loss (%) based on size of <i>Capitella teleta</i> during starvation while exposed to 12 treatment combinations comprising four DO and three temperature levels.	67

Figure 4.6 Total weight loss (% loss of initial size) of <i>Capitella teleta</i> under starvation pooled across (A) four DO saturations and (B) three temperatures (\pm SE).	67
Figure 4.7 Daily weight loss (%) of <i>Capitella teleta</i> over 96 h of starvation. Statistical significance was observed for (A) pooled temperature treatments; (B) temperature-specific effects (\pm SE).	68
Figure 4.8 The (A) fecal count and corresponding (B) estimated sediment egested by <i>Capitella teleta</i> during the first 24 h of starvation under 12 treatment combinations of three temperature and four DO saturation levels (\pm SD).	69
Figure 4.9 Relationships between body size and the total sediment egested (μ g) during the first 24 hrs of starvation for <i>Capitella teleta</i> exposed to combinations of four DO (100%, =70%, =50%, =20%) and three temperature levels. Body size was calculated as the geometric mean of measurements for initial and 24hr later time points.....	71
Figure 4.10 Body size trends in the sediment egested by <i>Capitella teleta</i> during the first 24 h of starvation at three temperatures and four DO saturations (A) small subjects; (B) medium subjects; and (C) large subjects.	73
Figure 4.11 Weight loss (%) after 24 h of starvation in relation to total egested sediment (μ g) for <i>Capitella teleta</i> when exposed to 12 treatment combinations of four dissolved oxygen and three temperature levels.....	74
Figure 4.12 The gross production efficiency (GPE) (% weight lost per total μ g sediment egested) for <i>Capitella teleta</i> after 24 h of starvation when exposed to 12 treatment combinations of four dissolved oxygen saturation and three temperature levels (\pm SE)...	75

Figure 4.13 Relationship between body size (g) and gross production efficiency (% weight lost per μg sediment egested) of <i>Capitella teleta</i> after 24 h of starvation when exposed to four dissolved oxygen saturations (20%, 50%, 70%, and 100%).....	76
Figure 4.14 Total mortality over four days for <i>Capitella teleta</i> under starvation when exposed to combinations of three temperatures (15°C, 20°C, and 25°C) and four dissolved oxygen concentrations (100%, 70%, 50%, and 20%).....	77
Figure 4.15 The mortality of three body sizes (small= diamond, medium= square, and large= triangle) of <i>Capitella teleta</i> after 4d of starvation at two temperatures (20°C and 25°C) and two oxygen saturations (20% and 100%).	78
Figure 4.16 Total weight loss at mortality vs. body size for <i>Capitella teleta</i> under starvation at combined treatments comprising three temperatures (25°C, 20°C, and 15°C) and four dissolved oxygen saturations (100%, 70%, 50%, and 20%).	78
Figure 5.1 Variation in DO (mg/L) over 5 days for growth experiments at three temperature and four dissolved oxygen saturation levels (A = 100%, B = 70%, C = 50%, and D = 20%).	89
Figure 5.2 Specific growth rates for three body size classes of <i>Capitella teleta</i> under four dissolved oxygen saturations (20%, 50%, 70%, and 100%). (A) mean \pm SE; (B) body size trend lines.....	95
Figure 5.3 Specific growth rates of <i>Capitella teleta</i> exposed to three temperatures (\pm SE).	95
Figure 5.4 Relationships between the initial wet weight (g) and specific growth rate (% d) of <i>Capitella teleta</i> at four dissolved oxygen saturations.....	96

Figure 5.5 Daily growth (%) of <i>Capitella teleta</i> exposed to four dissolved oxygen saturations (20%, 50%, 70%, and 100%) for four days. (A) mean \pm SE; (B) mean DO % growth trend lines.	97
Figure 5.6 The mean daily egestion rate ($\mu\text{g d}^{-1}$) of <i>Capitella teleta</i> under four dissolved oxygen saturation and three temperature levels (\pm SE).	98
Figure 5.7 The Q_{10} value of the mean daily egestion rate ($\mu\text{g d}$) of <i>Capitella teleta</i> under four dissolved oxygen saturations (A=20%, B=50%, C=70%, D=100%) crossed with three temperatures. The 15-20°C 100% DO is missing due to supersaturated conditions resulting in no feeding and high mortality ($Q_{10}=15.3$).	98
Figure 5.8 The egestion rate capacity of <i>Capitella teleta</i> at 24 and 96 hours under four dissolved oxygen saturations crossed with three temperatures. (A) 20% DO; (B) 50% DO; (C) 70% DO; (D) 100% DO. The 70% and 100% treatments (bold box) have a different Y-axis relative to lower DO treatments. Red lines mark a ratio of 1, or no change in egestion.	99
Figure 5.9 Log transformed-egestion ($\mu\text{g d}^{-1}$) of <i>Capitella teleta</i> over four days under three temperatures and four dissolved oxygen saturations.	100
Figure 5.10 Log transformed-egestion ($\mu\text{g d}^{-1}$) of <i>Capitella teleta</i> over four days under three temperatures and two body sizes (small < 0.003, large > 0.003).	101
Figure 5.11 Relationships between the body size (g) and log-transformed egestion rate ($\mu\text{g d}^{-1}$) for <i>Capitella teleta</i> when exposed to three temperatures (i.e., pooled over 4 DO levels) over four days.	102
Figure 5.12 Mean gross production efficiency for <i>Capitella teleta</i> exposed to four dissolved oxygen saturation levels at three temperatures (\pm SD).	103

Figure 5.13 Gross production efficiency versus body size for <i>Capitella teleta</i> exposed to four dissolved oxygen saturation levels over four days. (A) 100% DO; (B) 70% DO; (C) 50% DO; and (D) 20% DO.....	104
Figure 5.14 Survivorship (% alive) of <i>Capitella teleta</i> after four days of exposure to 12 treatment combinations of three temperatures and four dissolved oxygen saturations. .	105
Figure 5.15 Survivorship (% alive) of <i>Capitella teleta</i> over four days while exposed to 100% DO at three temperatures.	105
Figure 5.16 Survivorship (% alive) of three size classes of <i>Capitella teleta</i> after four days of exposure to 100% DO at three temperatures.	106
Figure 6.1 Bioenergetic framework combining the Dynamic Energy Budget (DEB) and oxygen- and capacity-limited thermal tolerance concept (OCLTT) for assessing stress based on organismal physiology (Sokolova et al. 2012).	112
Figure 6.2 Surface plots of relationships between observed growth, respiration, and egestion for <i>Capitella teleta</i> at three temperatures and four dissolved oxygen saturations. (A) 100% DO; (B) 70% DO; (C) 50% DO; and (D) 20% DO).....	116
Figure 6.3 Percent ATP contribution from aerobic and anaerobic respiration for <i>Capitella teleta</i> . A) 15°C small body size, B) 25°C small body size, C) 15°C large body size, and D) 25°C large body size.....	119
Figure 6.4 Sum ATP production (mmol ATP/min) from aerobic and anaerobic respiration for <i>Capitella teleta</i>	119
Figure 6.5 Percent contribution of maintenance and specific growth to the total ATP demand <i>Capitella teleta</i>	120

Figure 6.6 Contribution of egestion, respiration, and initial body size to the explained variability of specific growth rate models of <i>Capitella teleta</i> under four DO saturation levels. A) 100% DO, B) 70% DO, C) 50% DO, and D) 20% DO.....	122
Figure B.1 Comparison of 24h and 168h mass-specific respiration for <i>Capitella teleta</i> at 20°C and 25°C and multiple levels of dissolved oxygen saturations. Confidence levels were constructed with 24h data only.	130
Figure D.1 Q-Q plot for cube root transformed gross production efficiency data from the 100% dissolved oxygen treatment. Data failed the Shapiro-Wilk normality test ($W = 0.88$; $p = 0.024$).....	132
Figure D.2 Q-Q plot for cube root transformed gross production efficiency data from the 25°C treatment. Data failed the Shapiro-Wilk normality test ($W = 0.928$; $p = 0.042$)...	132
Figure E.1 Q-Q plots of treatments that failed the Shapiro-Wilk normality test. Plots include the treatments A) 70% dissolved oxygen, B) 25°C, and C) day 4.	134

LIST OF ABBREVIATIONS

ADH	Alanopine Dehydrogenase
<i>ATP</i>	Adenosine triphosphate
<i>DEB</i>	Dynamic Energy Budget
<i>DO</i>	Dissolved Oxygen
GCRL	Gulf Coast Research Lab
GPE	Gross Production Efficiency
LDH	Lactase Dehydrogenase
OCLTT	Oxygen- and Capacity-limited Thermal Tolerance Concept
ODH	Octopine Dehydrogenase
PVC	Polyvinyl Chloride
Q_{10}	Temperature Coefficient
USM	The University of Southern Mississippi
SD	Standard Deviation
SE	Standard Error
SG	Specific Growth
SDH	Strombine Dehydrogenase
VO_2	Maximal Oxygen Consumption
WW	Wet Weight

CHAPTER I - INTRODUCTION

“As global warming and eutrophication reduce oxygenation of the world oceans, there is a pressing need to understand the functional consequences of oxygen depletion in marine ecosystems.” -Levin (2003)

1.1 Temperature and Hypoxia

Atmospheric concentrations of greenhouse gases are increasing due to anthropogenic activities resulting in changes to the climate of the world (Matear and Hirst 2003). The surface of the Earth has been progressively getting warmer for the past three decades, with global air and sea surface temperatures rising 0.65-1.06°C in the past century alone (Field 2014). Subsequently, the world's oceans have declined 4-7% in dissolved oxygen (DO) concentration, as dictated by the basic principles of water chemistry, which state gas solubility decreases with increasing temperature (Matear and Hirst 2003, Weiss 1970). While the scientific community is in strong consensus that coastal systems are threatened by anthropogenic climate change, only 2.2% of all climate change studies test for non-independent effects of more than one variable directly related to climate change (Field 2014, Harley et al. 2006, Levin 2003). As a result of sea surface temperatures increasing by 0.3-0.7°C by 2035 (up to 4.8°C by 2100), 94% of global hypoxic zones are expected to experience 2°C or greater increase in temperature by the end of the century. Thus, there is a critical need to understand the combined effects of DO and temperature within the world's oceans (Alteri and Gedan 2015, Field 2014).

Global oceanic decreases in DO due to temperature occur in conjunction with historically occurring local zones of reduced oxygen resulting from anthropogenic eutrophication. Hypoxia is defined by the DO concentration threshold of 2.0 ml O₂ l⁻¹;

and in extreme cases, may be followed by anoxia, as defined by the DO threshold of 0.0 ml O₂ l⁻¹ (Diaz and Rosenberg 1995). Two main processes facilitate the onset and maintenance of hypoxia: 1) effects of water column stratification on the isolation of bottom water layers from surface layers, and the inhibition of oxygen diffusion between the layers and 2) the decomposition of organic matter by aerobic bacteria leading to oxygen depletion in bottom sediments (Rabalais et al. 2002). The effect of temperature on water stratification alone is enough to worsen hypoxia where it presently exists and trigger its occurrence in other coastal areas (Alteri and Gedan 2015, Rabalais et al. 2009). However, temperature will also affect more than just water stratification. Hypoxia responds to multiple aspects of climate change as they influence physical and biological properties affecting the onset of hypoxia, including increases in river runoff, effects on water column stability, increased stratification, and reduced ventilation (Figure 1.1) (Conley et al. 2007, Miller and Russel 1992, Sarmiento et al. 1998). Worsening conditions are predicted for 65% of U.S. estuaries due solely to increased eutrophication in combination with warming of $\geq 4^{\circ}\text{C}$ in water temperature (Figure 1.2) (Alteri and Gedan 2015, Bricker et al. 2008). During an era that is predicted to face increased temperatures along with frequency and magnitude of hypoxia, it is essential for management to understand how organisms will respond to combined thermal and oxygen stresses.

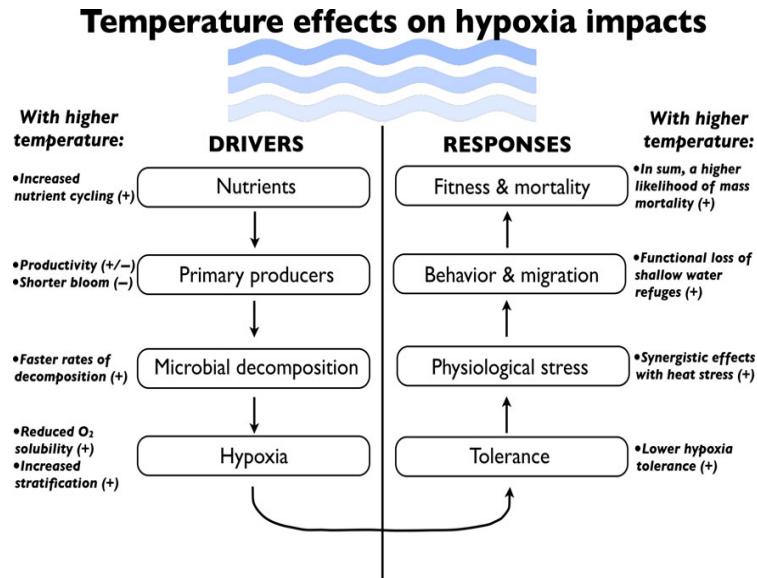


Figure 1.1 The physical and biological effects of climate change drivers on eutrophication and other hypoxia-related factors (from Alteri and Gedan 2015).

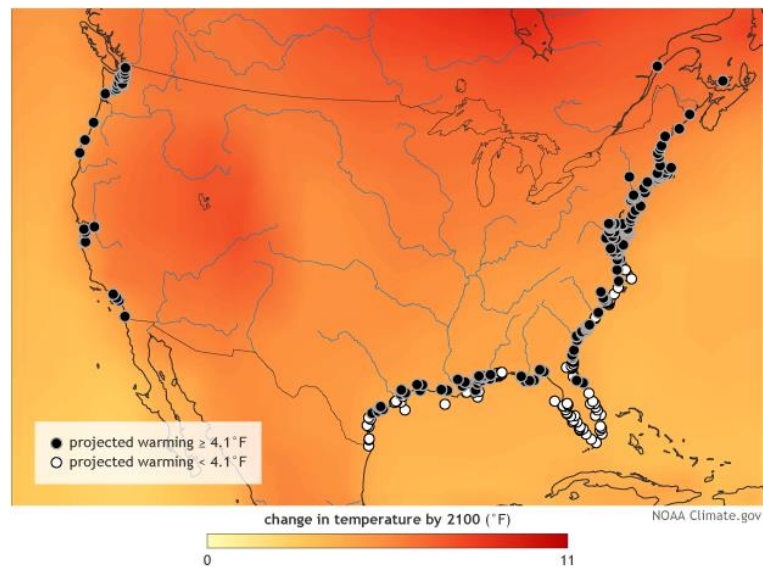


Figure 1.2 Projected temperature increases within hypoxic zones of the United States by 2100 (from Alteri and Gedan 2015).

1.2 Physiological Response to Increasing Temperature and Decreasing Dissolved Oxygen

The physiological effects of temperature and hypoxia are well known as single stressors for marine invertebrates (Burnett and Stickle 2001, Pörtner 2002, Pörtner 2009,

and Grieshaber et al. 1994). Physiologically, temperature elicits a bi-phasic response, initially elevating vital rates up to a critical threshold marked by protein damage, enhanced membrane fluidity, and failure in organ function (Harley et al. 2006, Pörtner 2001). Aerobic respiration increases with increasing temperature due to Q_{10} effects on metabolic rates (Alteri and Gedan 2015, Brown et al. 2004). Because DO physically decreases with temperature, elevated water temperature simultaneously decreases oxygen availability while increasing aerobic metabolic demand. Consequently, hypoxia tolerance decreases as temperature increases (Alteri and Gedan 2015, Vanquer-Sunyer and Duarte 2011). Functional hypoxia occurs at the critical thermal limit defined by where the organism cannot physiologically acquire enough oxygen, through either ventilation or its blood capacity limits. However, the biological impact of temperature varies from species to species. In particular, species living close to their physiological thermal limits, such as many eurythermal species, may show less capacity to physiologically acclimate to changing temperatures (Hartley et al. 2006, Pörtner 2001, Stillman 2002, Tomanek and Somero 1999). Conversely, when exposed to environmental hypoxia, organisms respond by means of reduced movement and ingestion, a complex of responses known as metabolic depression. Further, organisms may increase anaerobic respiration or respond with more complex cellular mechanisms, such as acidosis, in order to reduce cellular oxygen demand (Burnett and Stickle 2001, Pörtner et al. 2005).

When concurrently faced with multiple stressors, a tradeoff in physiological responses must occur for optimal survival; however, very little is known about how organisms face concurrent thermal and DO stressors. Although the literature on impacts of climate change on marine systems has grown exponentially since the early 1990's,

only 2.2% of all climate change studies test for non-independent, or synergistic, effects of more than one variable related to climate change (Harley et al. 2006). Synergistic effects can arise in one of two ways: 1) the impact of one factor is strengthened or weakened by interaction with an additional factor, or 2) the combination of the factors pushes an individual or population past a critical threshold that would otherwise not have been reached by one factor alone (Harley et al. 2006). Organisms facing combined increases in temperature with decreases in DO concentrations could face both functional and environmental oxygen limitations, even while metabolic demands increase.

In this dissertation, I examine the ecophysiological responses of a model tolerant species exposed concurrently to three temperatures crossed with four DO saturations. Experiments include two naturally occurring temperatures: 1) 15°C, a mid-point within the range of tolerance (also a common culturing temperature) and 2) 20°C, at the higher end of the range of temperatures experienced in the natural environment. In addition, the ecophysiological response at 25°C is examined. This temperature treatment is on the order of high temperatures which may be experienced by this polychaete within the next decade. This study will lend insights into our understanding of how this organism responds to simultaneous stressors, as well as the magnitude in these responses as increasing water temperatures become more prevalent. Specifically, this study examines the comprehensive ecophysiological response of a model tolerant polychaete species as a combination of several responses, including respiration, egestion (proxy for ingestion), mortality, and growth under fed and starved conditions, when exposed to two concurrent stressors of DO and temperature.

1.3 Body Size Relationships

Body size is well known to be a fundamental ecological trait that underpins vital bioenergetic rates and has been used to infer mechanistic connections in an assortment of macrobenthic indicators (Schwinghamer 1981, Edgar 1990, Rasmussen 1993, Brey et al. 1996, Persson and De Roos 2007, Rakocinski 2009). One cannot simply view “small individuals as scaled-down versions of adults”, as different sized animals must cope with very different environmental demands, as often expressed by size-dependent shifts in physiological rates (Forbes 1989). Allometry concerns how organismal traits scale disproportionately in relation to body size (Shingleton, 2010). Allometric relationships can often be described by a power relationship: $y=aX^b$, where y is the trait of interest; a is a constant multiplier; X is the animal’s mass; and b is the scaling exponent. The allometric parameters, a and b , are often used to infer biological meaning from the relationships. For example, the scaling exponent b is often interpreted as a reflection of follow Klieber’s Law, or the $\frac{3}{4}$ rule ($b=0.75$), which suggests functional relationships between fractal branching networks and body size; or as the $\frac{2}{3}$ rule ($b=0.67$), which connotes functional relationships with surface area (Shumway 1979, Forbes 1989, Brown et al. 2004, Kooijman et al. 2008). However, there has been much speculation as to the universal applicability of metabolic scaling theory, due to the wide range of intra- and interspecific scaling exponents reported throughout the literature (White et al. 2007, Glazier 2005, Glazier 2006). Variability in constant and scaling exponents have been reported in response to life history, starvation, temperature, and ontogeny (Everett and Crawford 2010, Glazier 2005, Shumway 1979, White et al. 2007).

The paradigm of macrobenthic community response to hypoxia, known as the Pearson-Rosenberg (P-R) model (Pearson and Rosenberg, 1978), is characterized by a shift from a community containing many large, long-lived burrowing equilibrium organisms to one dominated by small, opportunistic, short-lived surface and subsurface species. This community response potentially also reflects individual level physiological responses to abiotic stress. Such mechanistic connections could be revealed with a deeper understanding of how allometric ecophysiological responses of individuals might contribute to the population response. Thus, examining changes in allometric relationships in the face of multiple stressors can lead to the generation of hypotheses and predictions in terms of ecophysiological constraints, as well as to related modeling efforts (Forbes 1989).

1.4 Model Species

The polychaete species *Capitella teleta* (previously identified as *Capitella* sp. I) is an opportunistic species often associated with disturbed and eutrophic habitats in the northeastern United States, Japan, and the Mediterranean (Blake et al., 2009). This small deposit-feeding polychaete ranges from 20-40 mm and 3-12 mg (Grassle and Grassle 1976), and lives within mucus-lined burrows while feeding on surface and near-surface sediments (Levin 1984). This sibling species in the capitellid complex is regarded as the capitellid showing the most rapid individual growth (>20% d), short generation times (37-50 d at 15°C), and multiple broods per year. All of these traits facilitate its explosive population growth (104 m²) (Grassle and Grassle 1974, Blake et al. 2009). *Capitella teleta* is one of the most frequently cited polychaetes, including studies of its biology, physiology, genetics and ecology (Blake et al. 2009). Physiologically, *C. teleta* was

extensively studied as a model organism of ingestion responses in deposit feeding organisms, particularly by Forbes (1989), and Tenore and Chesney (1985). More recently, *C. teleta* has been used extensively for toxicology studies, using such agents as nonylphenol (Jager and Selk 2011), polycyclic aromatic hydrocarbons (Linke-Gamenick et al. 1999), and metal contaminants (Selck et al. 1999), as well as for studies of invertebrate development (Meyer and Seaver 2010).

The native US habitat of *C. teleta* typically ranges seasonally in sea surface temperature from ~5°C to 20°C. However, in 2012 NOAA issued an advisory report for the Northeast Atlantic Shelf citing the highest recorded sea-surface temperatures in 150 years, and temperatures above long-term means in 2013 (Figure 1.3A-B). Since 2012, sea surface temperatures were higher on mean through most of the year, with anomalies ranging from 1-3°C (Figure 1.3 C). These trends illustrate that organisms must not only be able to acclimate to increases in the mean water temperature, but must also cope with an increased frequency and magnitude of extreme thermal events (Sommer et al. 1997). Furthermore, with the exception of the Mississippi River region, the highest nitrogen loads into coastal systems of the US occur in the mid-Atlantic region, spanning Cape Cod to Chesapeake Bay (60-80 x 10⁶ tonnes/yr vs. 400-800 x 10⁶ tonnes/yr for the MS River region) (Bricker et al. 2008). This region also exhibits the largest concentration of highly eutrophic systems due to high population densities.

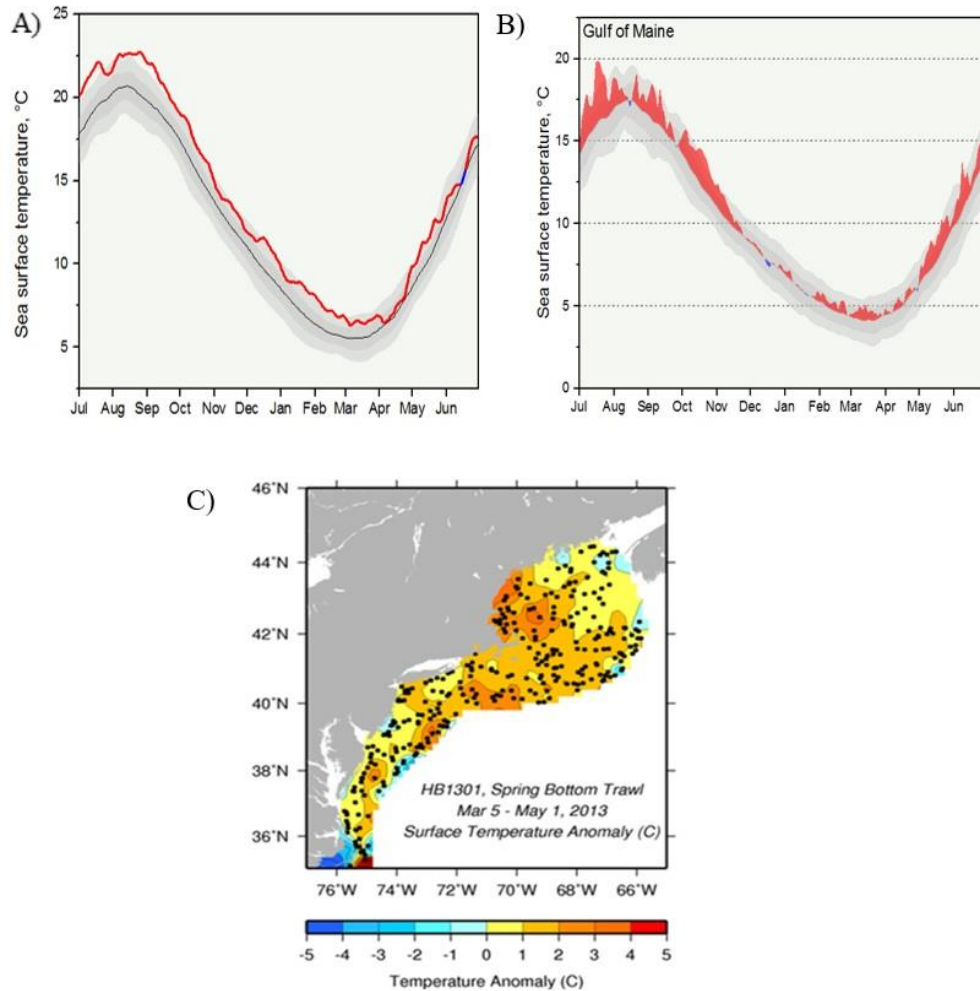


Figure 1.3 A) Sea surface temperatures during the last half of 2012 and the first half of 2013; the highest recorded temperatures in the past 150 years were observed between August and September 2012. B) Sea surface temperatures for the Gulf of Maine from late 2013 to early 2014. Gray bars represent the long term mean SST ± 1 and 2 SD. The red line represents surface temperatures above mean and the blue line represents temperatures below mean. C) Deviation from long-term mean sea surface temperature for the Gulf of Maine and George's Bank, USA during Spring 2013.
<http://nefsc.noaa.gov/ecosys/advisory/current/sst.html>

1.5 Conclusion

Levin (2003) asserted that, “as global warming and eutrophication reduce oxygenation of the world oceans, there is a pressing need to understand the functional consequences of oxygen depletion in marine ecosystems.” As underscored in the 2013

NOAA Ecosystem Advisory, "it isn't always easy to understand the big picture when you are looking at one specific part of it (*the ecosystem*) at one specific point in time.... a comparison similar to not seeing the forest when looking at a single tree in it" (Dawicki 2013). Accordingly, quantifying organismal responses to single stressors in isolation fails to convey how they interact synergistically with other stressors to elicit biological responses. Given hypoxic zones are expected to experience an increase of 2°C or more in the next century, it is important to understand the interaction effects of DO and thermal stress. Thus, this dissertation examines multiple ecophysiological responses of the model tolerant polychaete species, *C. teleta*, including respiration, egestion, mortality, and growth under fed and starved conditions, relative to concurrent DO and thermal stressors. Moreover, in order to consider non-linearity in the physiological responses, multiple levels of DO (100%, 70%, 50%, and 20% saturation) and temperature (15°C, 20°C, and 25°C) were examined. Lastly, allometric body-size relationships across the full range of body sizes (0.001 – 0.01 g) are also examined in order to understand how physiological responses scale with size. Hopefully by simultaneously accounting for these multiple dimensions, hypotheses can be made on the effects of concurrent DO and temperature as stressors at the population level.

CHAPTER II – SYNERGYSTIC INTERACTIONS OF DISSOLVED OXYGEN AND
TEMPERATURE ON THE ALLOMETRIC AEROBIC RESPIRATORY RESPONSE
OF A MODEL TOLERANT POLYCHAETE, *CAPITELLA TELETA*

2.1 Introduction

The world's oceans are experiencing dissolved oxygen (DO) declines due to ocean warming and eutrophication (Pörtner et al. 2005). Sea-surface temperatures are predicted to increase up to 4.8°C by 2100, in conjunction with a subsequent 4-7% decline in DO. In addition, eutrophication-induced hypoxic events are predicted to increase in frequency, duration, and severity (Field 2014, Matear and Hirst 2003, Diaz & Rosenberg 2008, Justic et al. 1996). The physiological separate effects of temperature and hypoxia are well researched, especially for marine invertebrates (Burnett and Stickle 2001, Pörtner 2002, Pörtner 2009, and Grieshaber et al. 1994). However, elevated eutrophication and temperature will not occur in isolation. Of all the globally recognized hypoxic zones, 94% are expected to experience future temperature increases of 2°C or more (Alteri and Gedan 2015). As the world oceans become depleted of oxygen due to combined warming and eutrophication, there is a need to understand interactive effects and functional implications (Harley et al. 2006, Levin 2003).

Ecophysiological responses of invertebrates to elevated temperature include increased ventilation, metabolic demand, biochemical rates, and reduced protein stability (Pörtner 2001, Frederick and Pörtner 2000). On the other hand, low DO can induce metabolic depression, increased anaerobic respiration, and behavioral responses, such as increased movement of the benthos at the sediment surface (Dales and Warren 1980, Llanos and Diaz 1994, Sagasti et al. 2001). When concurrently faced with these opposing

stressors, the ecophysiological response will not necessarily be a simple linear, additive outcome owing to counteracting physiological trade-offs. Nonlinear effects arise in one of two ways: 1) the impact of one factor is strengthened or weakened by interaction with another factor, or 2) the combined effect of two factors pushes an individual or population past a critical threshold that would otherwise not have been reached from one factor alone (Harley et al. 2006). Furthermore, it is especially important to recognize not only the possibility of a synergistic response, but also resultant nonlinearity due to physiological tradeoffs. Limited past studies that consider interactions involving multiple stressors include only 'high vs. low' treatment combinations, and thus preclude the detection of nonlinear responses.

Respiratory function can be affected by extrinsic (e.g., temperature) and intrinsic factors (e.g., body size) (Bridges and Brand 1980, Shumway 1983, Cammen 1987). While body size is well known to scale with vital rates throughout the animal kingdom, small individuals cannot be simply viewed as scaled-down versions of adults, as environmental demands elicit size-dependent shifts in physiological rates (Forbes 1989). Synthesis of the literature representing multiple polychaete species suggests a body-size trend such that small organisms generally exhibit higher mass-specific respiration rates than large organisms under normoxia (Shumway 1983, Cammen 1987). Allometry concerns how organismal traits scale disproportionately in relation to body size (Shingleton 2010). Allometric relationships can often be described by a power relationship: $y = aX^b$ where y is the trait of interest; a is an intercept at unit body mass; X is the animal's mass; and b is the exponent. The allometric parameters, a and b , can be used to infer biological meaning from the relationships. For example, b is often believed

to follow Klieber's Law, or the $\frac{3}{4}$ rule ($b = 0.75$), which suggests functional relationships between fractal branching networks and body size, or the $\frac{2}{3}$ rule ($b = 0.67$), which suggests functional relationships with surface area (Shumway 1979, Forbes 1989, Brown et al. 2004, Kooijman et al. 2008). The parameter a is the magnitude of y when $X = 1$ and provides a comparison for individuals of the same weight under different scenarios (Shumway 1979). Shumway (1979) observed b values relating body size to oxygen consumption among eight cold water (10°C) species of polychaetes and suggested that b may be affected by the individual's state of nutrition, temperature, life history characteristics, and season. Similarly, Shumway (1979) observed a values related to the variation to physical movement and activity of the individual. Thus, examining changes in allometric relationships allows for the generation of hypotheses and predictions concerning physiological constraints (Forbes 1989). Since allometric relationships are sensitive to temperature, DO, nutrition, etc., I hypothesize allometric relationships change in relation to physical stressors, such as temperature and DO due to changes in the overall metabolism of the organisms; however, changes in the relationships will not be simple additive responses when the organisms are subjected to more than one stressor. The study aims to determine if the intraspecific respiratory response can be characterized by one allometric curve, or if ontogenetic shifts occur due to different respiratory demands of small and large individuals.

Further, classifications based on the ability of the organism to regulate respiration in relation to DO levels also often relies on extrinsic variables and life history characteristics (Shumway 1982, Shumway 1983). An organism is classified as an oxygen conformer (oxygen dependent) when respiration rates change in relation to DO levels, or

as an oxygen regulator (oxygen independent) when respiration rate is unchanged in relation to changing DO levels (Bridges and Brand 1980, Shumway 1983, Shumway 1987). Based on the concept that it is more difficult for small organisms to maintain high mass-specific respiration rates than large organisms, small individuals should be relative oxyconformers whereas large organisms should be relative oxyregulators (Rakocinski 2009). Accordingly, Gamenick et al. (1998) observed an allometric trend among four species in the capitellid complex, whereby the smallest species conformed to declining DO whereas the three larger species exhibited different levels of regulation. In order to examine the influence of multiple stressors and body size on respiration, I aim to characterize the allometric respiratory response of tolerant polychaete, *Capitella teleta*, under multiple, interacting levels of dissolved oxygen and temperature. I hypothesize increasing temperatures will result in increased respiration rates; further, under higher increasing temperature organisms will display functional hypoxic responses (i.e., metabolic depression, reduced respiration capacity, display oxygen conforming, etc.) at higher DO levels (>50% saturation). Since smaller individuals maintain higher mass-specific respiration rates, I hypothesize smaller individuals will respond to increasing temperatures at higher DO levels more than larger counterparts, such that small individuals will display steeper oxyconforming trends and earlier signs of functional hypoxia.

2.2 Materials and Methods

2.2.1 Model Species

The model tolerant polychaete, *Capitella teleta*, (previously identified as *Capitella* sp. I) is an opportunistic species often associated with disturbed and eutrophic

habitats (Blake et al. 2009). Commonly found in the northeastern United States, Japan and the Mediterranean, *C. teleta* has been described as the capitellid sibling species with the “most rapid response to disturbed habitats, the highest rate of increase, largest maximum population size, and highest mortality” (Blake et al. 2009). Within its native habitat, sea surface temperature commonly ranges in from ~5°C to 20°C seasonally. Recently, NOAA issued an advisory report for the Northeast Atlantic Shelf citing the highest recorded sea-surface temperatures in 150 years during 2012, and temperatures during 2013 were above the long-term means along the shelf (NOAA 2013).

Most polychaetes are tube dwellers and procure oxygen by either protruding part of the body out of the tube or actively pumping water through U-shaped burrows (Mills 1978). Capitellids construct primitive burrows and rely on extending the hind end out of the burrow. In response to low DO, capitellids will extend the body farther out of the burrow in order to increase surface area contact with the surrounding waters. Further, polychaetes have diverse respiratory pigments used for both oxygen storage and oxygen transport (Mills 1978, Cammen 1987). This species has red blood cells with a moderate oxygen affinity ($P_{50} = 6.88 \pm 0.97$) and high cooperativity ($n_{50} 2.89 \pm 0.82$) (Magnum et al. 1992) allowing for success in low DO habitats. There is also a significant increase in heme b, the protein responsible for the attachment/release of oxygen, at colder temperatures (4°C vs 21°C; Barclay 2013). Barclay (2013) also observed *C. teleta* 6.2x larger at cold temperatures, and suggested the ability to unload oxygen to tissues farther removed from the surface because of higher oxygen saturation may contribute to the increased growth. Changes in maximum sizes between temperatures suggest a metabolic difference at higher temperature that could be driven by reduced heme quantity and

reduced affinity and cooperativity. Under increasing global temperatures, this species must not only be able to acclimate to upward trends in the mean water temperature, but it must also cope with an increased frequency and magnitude of extreme thermal events.

2.2.2 Experimental Setup

Stock cultures of *C. teleta* were obtained from Dr. Judy Grassle of Rutgers University and reared at 15°C and 27 ppt (Appendix A). Groups of ~50 polychaetes were maintained in 4.5” culture dishes with 15-30 mL of enriched sediment. Sediment was collected from the Mississippi Sound, passed through a 1 mm sieve and frozen in 30 mL plastic, food safe containers. Sediment was thawed and Tetramin© fish flakes were added at a ratio of 2.5 g of flake to 54 g of mud before using it for cultures. Every two weeks, cultures were maintained by replacing sediment and water.

All cultures crash in December 2012 suspected to be due concentrating microbes when evaporating natural water to 27 ppt. In order to avoid such misfortune, cultures and respiration runs were conducted in artificial seawater starting in January 2014. Data was examined to ensure that respiration was equivalent between natural and artificial waters by comparing past natural respiration data with data at the same treatment in artificial waters. Influences of microbes were accounted for through examination of blank water trials which ran between each respiration session. Microbe influence was never observed in any of the experiments.

In an attempt to standardize DO conditions, treatments were classified into four oxygen saturation categories (20%, 50%, 70%, and 100%), which were fully crossed with three temperatures (15°C, 20°C, and 25°C) (Table 1). Experimental conditions were created in a sealed air chamber (BioSpherix) into which nitrogen gas was pumped at a

predetermined rate (Proox© Model 360) for diffusion across air-water interface of specimen containers to create the appropriate DO conditions. In order to ensure the water-gas interface reached equilibrium and the DO concentration stabilized at the desired temperature, experimental conditions within the chamber were required to remain constant for 24 hr before organisms were introduced. Once the chamber stabilized after 24 hrs of constant DO saturation and temperature levels, worms were introduced within individual 60 x15mm open petri dishes filled with enriched sediment (~ 5mm with 6 g sediment). Worms had been acclimated at the treatment temperature for 24 h before being introduced to the air chamber. Initially, some worms were examined at both 24 and 168 h; however, the lack of apparent differences in respiration between these time points prompted exclusion of the latter time point for most runs (Appendix B). Containers for these long-term subjects underwent a water change every other day to limit the build-up of excretion products.

Table 2.1

Treatment levels of dissolved oxygen and temperature for respiration measurements (\pm SD).

Temperature (°C)	Oxygen Saturation (%)	Dissolved Oxygen (mg/L)
15.4 ± 2.1	20	2.41 ± 0.30
	50	4.52 ± 0.91
	70	6.10 ± 0.01
	100	7.47 ± 0.32
21.0 ± 1.3	20	1.97 ± 0.25
	50	4.21 ± 0.44
	70	5.62 ± 0.39
	100	7.15 ± 0.5
24.2 ± 1.0	20	1.91 ± 0.24
	50	3.79 ± 0.37
	70	4.99 ± 0.60
	100	7.09 ± 0.38

2.2.3 Respiration Measurements

Oxygen consumption at 20 and 25°C was measured with an OX1LP 4 mL Dissolved Oxygen Cuvette (Qubit Systems, Canada) respirometer. Respiration using this instrument was measured via a polarographic Clark-type O₂ electrode connected to a C410 LoggerPro Interface (Vernier Software and Technology, USA). For 15°C runs, oxygen consumption was measured with an optical oxygen meter FireStingO2 (PyroScience, Germany) using 10ml syringes sealed with cockstops. The fiber optic equipment was unavailable for the respiration measurements at 20°C and 25°C; however, its ability to run 3x the number of samples per day and produce more stable measurements warranted the change to this advanced apparatus. Comparisons of readings using both apparatus at 20°C and 100% DO showed similar spreads in sample residuals

when related to the 20°C 100% DO allometric relationship taken on the Qubit equipment (i.e, $y=0.0061x^{-.077}$ $r^2=0.88$), indicating congruent results (Figure 2.1).

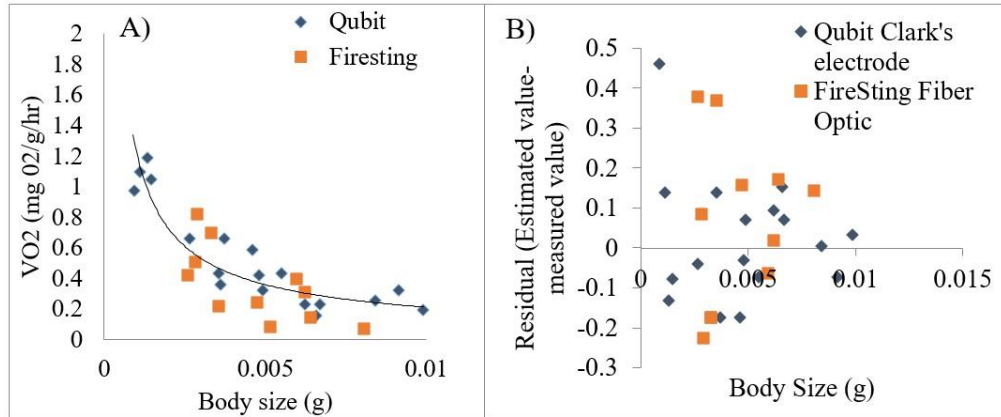


Figure 2.1 Comparison of the FireSting fiber optic respirometer (blue diamond; n = 10) to the Qubit Clark's electrode respirometer (red square; n = 20) saw no apparent difference in a) respiration measurement or b) respiration residuals at 20°C and 100% oxygen saturation.

Temperature was maintained within the Qubit respirometer by pumping water (Eheim Universal Pump 1046) through a water jacket surrounding the chamber, or by placing the sealed FireSting chamber in a water bath. The temperature was maintained at the desired treatment level with a water bath (GD100, Boekel/Grant Optima, USA). For the Qubit respirometer, a small magnetic stir bar at the bottom of the sampling chamber prevented the electrode from locally depleting oxygen. This was not necessary for the FireSting Fiber optic probe. For both respirometers, organisms were kept in small mesh cages to reduce movement, and protection from the stir bar. The organism was given 40 min to adjust to the respiratory conditions at the designated temperature and oxygen levels before starting.

The mass-specific respiration rates (VO_2 ; mg O_2 /mg/h) of individual worms were measured in complete darkness in 3 mL of salt water (27 ppt) that was preconditioned to

treatment levels in the hypoxia chamber. Before and after measurements of organisms, 40 min reference readings (i.e., without organisms) accounted for any microbial oxygen consumption and instrument drift. When using the Qubit respirometer, two separate readings of individual worms were made for 40 minutes, and the water changed in between each reading. Duplicate readings were precluded by the stability and precision of the fiber optics probe when using the FireSting respirometer. Following respiration measurements, worms were wet weighed (Ohaus Analytical Plus, Model AP2500; ± 0.00001) and frozen. As much water as possible was removed prior to weighing the organism by blotting the worm on a plastic weight dish (kim wipes were not used as it often resulted in tearing of the worm)

LoggerPro software and Excel were used to fit linear regressions to the decline in oxygen during each individual trial, with oxygen uptake defined as the slope of the line. Pilot studies and personal communications (Bryce Mendelsohn, personal communication, January 2013) determined that a minimum of 20 min was needed for the Clark's type electrode to stabilize after a water change; so, the last 10 min of each trial was routinely used to measure the rate of oxygen uptake. Differences in the Clark electrode stabilization time were likely affected by animal size, DO level, and electrode maintenance (cleaning/use). The same method for measuring the rate of oxygen uptake was used for the FireSting. The coefficient of determination (R^2) provided a Quality Control standard for respiration measurements: values of $R^2 < 0.80$ were excluded from the data set (Linke-Gamenick et al. 2000, Vismann and Hagermann 1996). Excluded runs accounting for 4.3% of all trials for both respirometers, in addition to 5.2% of the runs due to equipment malfunction, resulting in a total of 208 usable trials (of 232 trials).

The slope for oxygen consumption relationship by each individual (VO_2 ; $\text{mg O}_2/\text{mg/h}$) is defined as: $d(\text{DO})/dt = (\text{DeclineO}_2 - \text{EquipmentDrift})$. Microbial response was accounted for in the equipment drift measurement. Slopes were averaged for the duplicate readings for individuals from the Qubit respirometer. Pilot studies using this method yielded results for normoxic rates comparable with those from the literature. Mass-specific respiration, VO_2 ($\text{mg O}_2/\text{mg/h}$), was calculated as: $\text{VO}_2 = (d(\text{DO})/dt) * (V_r - V_a)/m$; where VO_2 = the rate of instantaneous oxygen consumption ($\text{mg O}_2/\text{mg/h}$); $d(\text{DO})/dt$ = rate of decrease of DO ($\text{mg O}_2/\text{L/h}$), V_r = respirometer volume (L) (with correction for mesh), V_a = volume of experimental animal (L), and m = animal mass (mg) (Qubit Reference Manual).

2.2.4 Analysis

Respiration curves for each treatment combination were obtained by response curve model fitting to the raw data using the power ($y = ax^b$) Dynamic Fit Wizard (Sigma Plot 10), which yielded allometric a and b parameters for the 12 treatment combinations. In order to identify abrupt allometric parameter shifts within respiration curves and to objectively identify relevant body size categories based on shifts, departure from single power curve scaling was determined through segmented (piecewise) linear regression on \log_{10} transformed data. Analysis was conducted in R 3.2.1 using the package ‘segmented’ (Muggeo 2014). This technique determines if size-scaling can be represented by a continuous allometric curve, and, if not, at what sizes abrupt changes require new allometric slopes (Forbes and Lopez 1989). Based on the results from segmented regression, body sizes were separated into small and large size categories based on the mean segmentation point of 0.0035 g. The complete results of the

segmented regression will be discussed in more detail below in the results. Pooled body size data was used only for calculation of Q_{10} and respiration capacity analysis. Data was analyzed using pooled body size subsets for these calculations since worms were only subjected to one treatment (1 DO x temperature interaction) and both Q_{10} and respiration capacity are based on ratios of multiple treatments that could not be viewed on an individual basis. Q_{10} values of oxygen consumption were calculated for each body size category as $Q_{10} = (R_2/R_1)^{10/(T_2-T_1)}$; where R_1 and R_2 are the rates of oxygen consumption at temperatures T_1 and T_2 respectively. Lastly, respiration capacity was calculated for each body size group x temperature x DO treatment and defined as: capacity = $VO_{2x}/VO_{2(100\%)}$; where VO_{2x} is the mean VO_2 at DO treatment X and $VO_{2(100\%)}$ is the mean VO_2 at 100% DO for any given body size x temperature treatment.

2.3 Results

2.3.1 Effects of Temperature and Dissolved Oxygen on VO_2

Mass-specific respiration (VO_2) ranged from 0.07 to 5.34 mg O_2 /g/hr for all treatments for body sizes ranging from 0.00014-0.01410 g (Figure 2.2). Smaller individuals maintained higher VO_2 rates at all treatments, with the magnitude of difference due to body size decreasing with temperature. The effect of temperature on mass-specific respiration varied with DO, increment of temperature increase (i.e., moving from 15-20°C or from 20-25°C), and body size (Figure 2.3). Further, the magnitude of respiration also appeared to be influenced by dissolved oxygen: Q_{10} values increased with increasing DO for both body sizes. On mean, large worms had higher Q_{10} values than small worms over increments of 5°C increase however, the full Q_{10} from 15-25°C was similar for both body sizes (Table 2.2). Under hypoxia, mass-specific respiration rates for

small worms did not change from 15-25°C; whereas rates doubled for large worms.

Moreover, under low DO the greatest increase in respiration (6x) occurred at 15-20° C for large worms; whereas the greatest increase in respiration (3x) occurred at 20-25° for small worms.

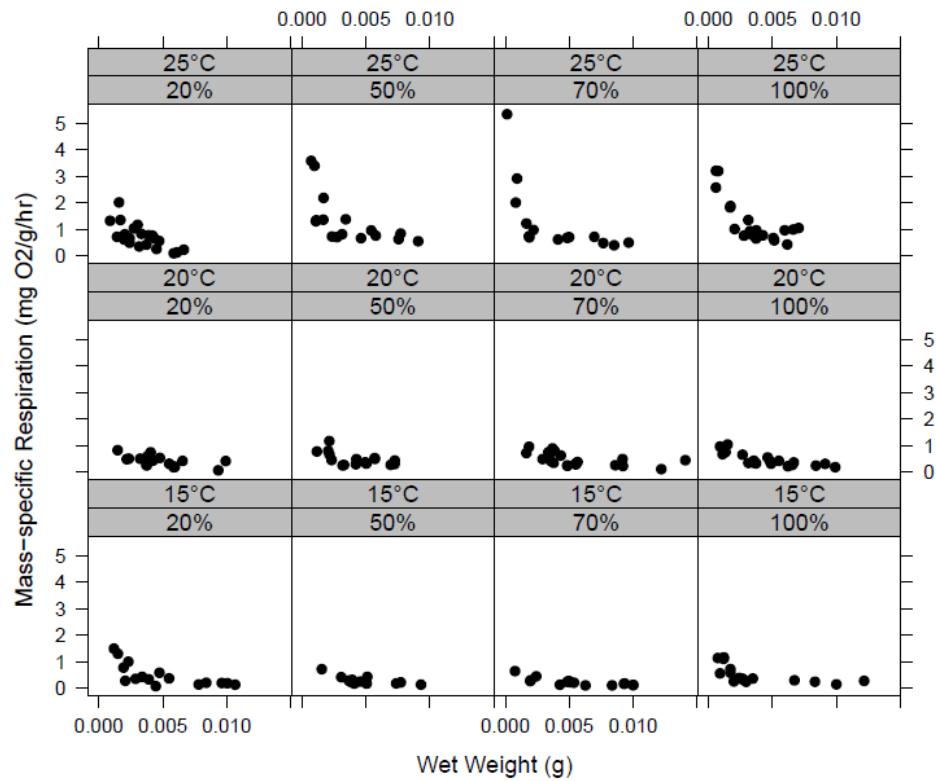


Figure 2.2 Mass-specific respiration rates of *Capitella teleta* at three temperatures crossed with four dissolved oxygen saturations.

Table 2.2

Q₁₀ values for mass-specific oxygen consumption rates in *Capitella teleta* under multiple dissolved oxygen and temperature treatments at small and large body sizes.)

	15-20°C				20-25°C				15-25°C			
	100%	70%	50%	20%	100%	70%	50%	20%	100%	70%	50%	20%
Small	1.71	4.05	2.72	0.89	4.48	3.84	4.32	2.78	2.91	4.73	3.58	1.18
Large	4.47	13.21	6.77	5.62	7.19	3.5	5.34	3.37	2.89	3.37	3.46	1.75

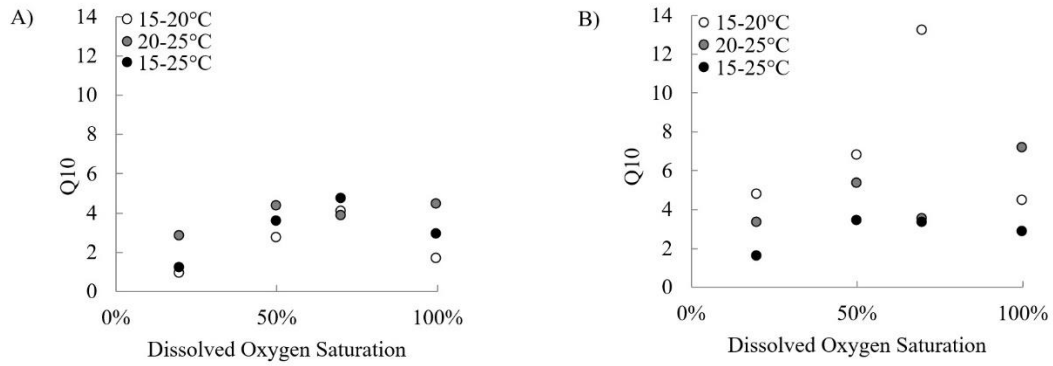


Figure 2.3 Interaction effects between dissolved oxygen and temperature on Q_{10} values for oxygen consumption rates in A) small and B) large *Capitella teleta*.

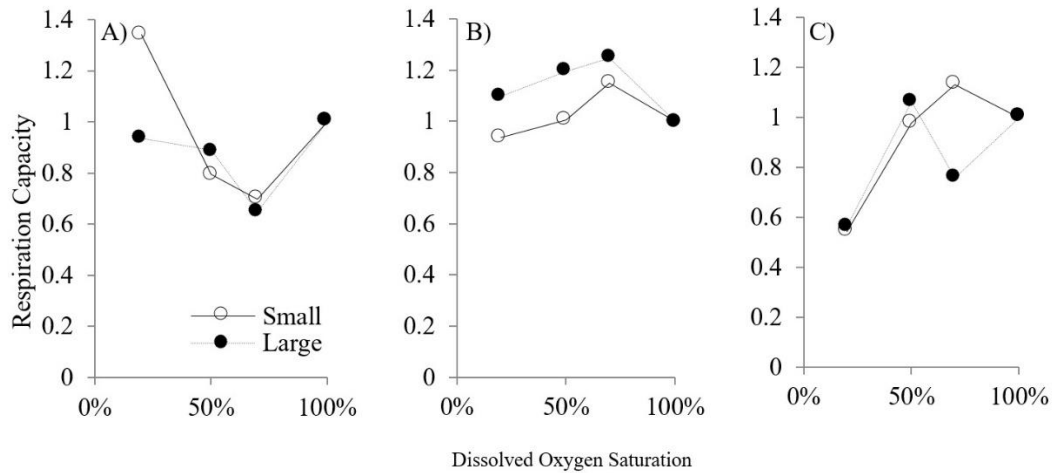


Figure 2.4 Respiration capacity ($VO_{2x}/VO_{2(100\%)}$) for small and large size categories of *Capitella teleta* at three temperatures (A = 15°C, B = 20°C, and C = 25°C) and four dissolved oxygen saturations.

Respiration capacity ($VO_{2x}/VO_{2(100\%)}$) was maintained at $\geq 90\%$ at hypoxia at 15°C and 20°C, but dropped to $\sim 55\%$ for both size classes at 25°C (Figure 2.4). At 25°C, respiration was maintained at $>80\%$ at DO levels higher than hypoxia (i.e., 20% saturation), suggesting a critical threshold between oxyregulation and oxyconforming strategies falls somewhere between 50-20% DO saturation. A body size effect for respiration capacity was not apparent.

2.3.2 Allometric Relationships

Exponents of allometric relationships varied among experimental treatments, but allometric relationships did not follow the $2/3^{\text{rd}}$ or $3/4^{\text{th}}$ scaling rules. Mass-specific scaling exponents (b') ranged from -1.01 to -0.42 (i.e., b range from 0 to 0.58), and constants (a) ranged from 0.038 to 0.002 (Table 2.3). Hypoxia (20% saturation) showed relatively lower constants and scaling exponents at all temperatures (Figure 2.5). Hypoxia relationships were approximately isometric, while scaling exponents for treatments at higher DOs were a mean of -0.56 ± 0.07 . Constants generally were >0.01 at high DO levels, and dropped to a mean of 0.0032 at 20% saturation. Variation in both the scaling exponents and constants suggest a reduced effect of body size on mass-specific respiration at hypoxia. A temperature-related trend was not apparent for the scaling exponent; however, variation in the constant was related to temperature; higher temperatures exhibited higher constants.

Table 2.3

Nonlinear regression equations relating VO_2 (mg O₂/g/hr-1) to body weight (g) in *Capitella teleta* exposed to multiple dissolved oxygen and temperature treatments. Regressions equations fit in the form of $\text{VO}_2 = aW^b$, where W is weight (mg) n= number of samples; r^2 = correlation coefficient. Non mass-specific allometric exponent b is calculated as $b = 1 + b'$.

	15°C						20°C						25°C					
	a	b	b'	n	r^2		a	b	b'	n	r^2		a	b	b'	n	r^2	
100%	0.005 ± 0.005	0.25	-0.75 ± 0.15	17	0.67		0.019 ± 0.009	0.44	-0.56 ± 0.07	19	0.77		0.025 ± 0.010	0.35	-0.65 ± 0.06	21	0.86	
70%	0.008 ± 0.004	0.39	-0.61 ± 0.07	15	0.82		0.018 ± 0.016	0.39	-0.61 ± 0.15	20	0.47		0.046 ± 0.031	0.45	-0.55 ± 0.08	15	0.78	
50%	0.003 ± 0.003	0.19	-0.81 ± 0.12	14	0.79		0.022 ± 0.022	0.45	-0.55 ± 0.17	16	0.42		0.010 ± 0.009	0.21	-0.79 ± 0.16	16	0.69	
20%	0.001 ± 0.001	-0.16	-1.16 ± 0.19	16	0.79		0.014 ± 0.0018	0.39	-0.61 ± 0.13	18	0.43		0.014 ± 0.016	0.33	-0.67 ± 0.17	21	0.45	

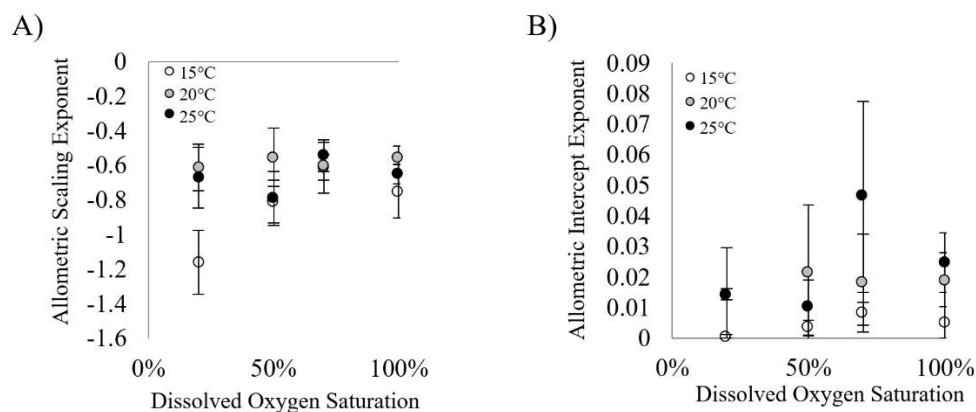


Figure 2.5 A) Allometric exponent, b , and B) constant, a , (of $VO_2 = aW^b$) for 12 (three temperature crossed with four dissolved oxygen saturation) treatments.

2.3.3 Critical Sizes of Ontogenetic Shifts in Allometric Mass-Specific Respiration Curves.

Statistically significant shifts in the allometric scaling exponent b occurred at higher DO levels (70% and 100%) at 15° C and 25° C (Table 2.4). All ontogenetic shifts occurred between 0.002-0.008 g, with the majority of shifts occurring between 0.002-0.004 g (Figure 2.6). For those relationships with recognizable shifts, mass-specific respiration exponents for small individuals approached negative isometric relationships; whereas, large individuals exhibited flatter slopes resembled the $3/4^{\text{th}}$ scaling rule (Figure 2.7). The scaling exponent of the larger body sizes appears to relate to DO; however, statistical significance shifts were only observed at high DO levels (Table 2.4)

Table 2.4

The critical sizes for ontogenetic breaks and scaling exponents for smaller and larger size ranges of *Capitella teleta* at four dissolved oxygen saturations and three temperatures.

Statistically significant breaks denoted by *.

Temperature		20%	50%	70%	100%
15°C	Size at Break	0.0029	0.0038	0.0083	0.0029
	p value	0.141	0.019*	<0.001*	<0.001*
	<i>b</i> before	-1.55	-0.96	-0.63	-0.96
	<i>b</i> after	-0.65	-0.56	0.06	-0.25
20°C	Size at Break		0.0032		
	p value	NO	0.030	NO	NO
	<i>b</i> before	BREAK	-1.11	BREAK	BREAK
	<i>b</i> after		0.042		
25°C	Size at Break	0.0042	0.0011	0.0020	0.0057
	p value	0.069	0.08	<0.001*	<0.001*
	<i>b</i> before	-0.56	-2.15	-0.800	-0.75
	<i>b</i> after	-3.19	-0.44	-0.46	2.55

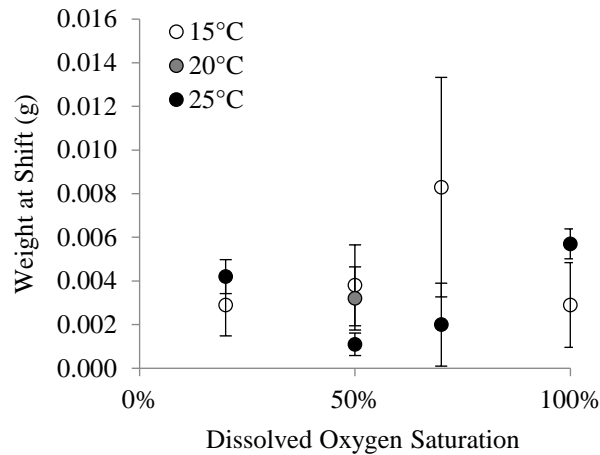


Figure 2.6 The body size of *Capitella teleta* where shifts in allometric weight exponent (*b*) occur when exposed to 12 treatments (three temperatures and four dissolved oxygen levels). Graph includes points that are statistically significant or marginally significant ($p < 0.1$).

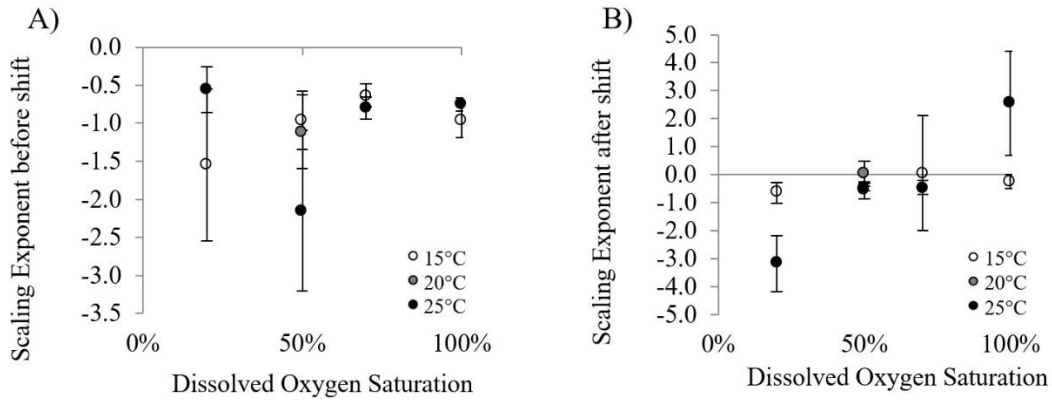


Figure 2.7 The allometric scaling exponent b (of $VO_2 = aW^b$) A) before and B) after body size shifts of *Capitella teleta* when exposed to 12 treatments (three temperatures and four dissolved oxygen levels). Graph includes data that is statistically significant or marginally significant ($p < 0.1$).

2.4 Discussion

2.4.1 Physiological Relationships

Capitella teleta showed synergistic ontogenetic respiration responses in relation to combined levels of DO and temperature, as evidenced by changing Q_{10} values in relation to changing DO level and body size. Notwithstanding DO level, large body sizes showed greater increases in mass-specific respiration rates than small sizes between 15-20°C; however large and small sizes showed equal rates of increase over higher temperature ranges (20-25°C). Similarly, Yong et al. (2009) observed a significant interaction between body size and temperature in the oxygen consumption, and Q_{10} values of the polychaete, *Neanthes japonica*. As seen in this study, the respiration of large sizes increased 3x faster than small individuals over a lower temperature range (18-21°C); whereas all sizes showed similar rates of change across higher temperature ranges. The bivalve, *Mulina lateralis*, also displayed higher Q_{10} values at 10-20°C versus 20-30°C; however, the observed effect of body size (1 mg vs 10 mg) was minimal (Shumway 1983). These trends suggest that effects of temperature on Q_{10} are greater for increases

within the endemic temperature range to which the organism has evolved to tolerate naturally occurring fluctuations, as opposed to more extreme temperatures, at which the organism is unable to compensate for further metabolic demands. Hypoxia tolerance has been shown to decrease with temperature due to a combination of rising metabolic demand in the face of decreasing oxygen availability (Alteri and Gedan 2015, Vanquers-Sunyer and Duarte 2011). Such an interaction between temperature and body size was observed in the survival of *Mulina lateralis* under hypoxia (Shumway et al. 1983). The survival of large bivalves was halved over an initial increase of 10°C; whereas the survival of small sizes was minimally affected. With an additional 10°C increase, both sizes converged at only 5% of the baseline survival rate.

The oxygen regulatory ability of polychaetes (Shumway 1979), bivalves (Shumway 1983), and crustaceans (Bridges and Brand 1980) has been shown to vary with body size and temperature; in general, mass-specific respiration of large organisms is relatively independent of oxygen compared to small organisms. Although, the range of body sizes in this study was not wide enough to show an effect of body size on oxygen independence; a 50% reduction in respiration capacity at 25°C under hypoxia suggested a reduced degree of independence under these conditions. Limitation of respiration capacity under temperature stress have been observed for multiple species, as a result of an inability to increase ventilation and circulation enough to meet oxygen demands in terms of oxygen uptake and delivery at high temperatures (Frederich and Pörtner 2001). Temperature can also affect the oxygen affinity and cooperativity (increased affinity with partial binding) of erythrocytes, with reduced oxygen affinity leading to a lower ability to meet oxygen demands at higher temperatures (Barclay 2013, Wells et al. 1980, Wood

1980). Such physiological limitations compounded with the physical reduction of oxygen availability at high temperatures should lead to an inability to meet metabolic demands through aerobic respiration and a consequent greater reliance on less efficient anaerobic metabolism, and eventually, mortality. Under hypoxia, *C. teleta* exhibited a reduced survival time of under 7 days at 25°C, and were unable to survive for even 24 h at 35°C (personal observation); suggesting this species experienced physiological limitations near its upper thermal tolerance.

2.4.2 Allometric Relationships

The mass-specific allometric relationships seen in this study did not adhere to any proposed metabolic theory ($2/3^{\text{rd}}$ or $3/4^{\text{th}}$ rule). However, exponents for the older mature large size class related better to the $2/3^{\text{rd}}$ scaling rule, as opposed to small young immature individuals which showed relatively isometric relationships. Such a dichotomy in the allometric scaling of young vs. adult animals has been noted before, with adults typically showing higher scaling exponents than young (Glazier 2006, Zeuthen, 1953). Adult organism may better adhere to metabolic theory due to the larger body sizes. A review of 18 polychaete species under similar normoxia conditions as this study showed all species adhered to one of the universal metabolic rules (Shumway 1979). However, 78% of the reviewed species in Shumway (1979) ranged from 0.5g DW to 8.5 g DW, which much larger than the range of body sizes in this study (maximum size of *C. teleta* was 0.0024 g DW). Thus, the narrow size range possibly precluded detection of this broad allometric rule (Mendez et al. 2013). However, low allometric scaling exponents have been noted for certain benthic bivalves, gastropods, anthozoa, and crustaceans (Glazier 2006).

Allometric mass-specific scaling exponents decreased with DO and values reflected near isometric relationships under hypoxia ($b = 0.00$ to 0.24). The Gulf Killifish, *Fundulus grandis*, also showed weak body-size effects at hypoxia ($b = 0.37$) owing to a reduction in overall metabolism, or a switch to anaerobic metabolism (Everett and Crawford 2010). At 20°C , adult *C. teleta* reduced their oxygen consumption under low DO, while significant increases in the levels of succinate (an anaerobic respiration indicator) suggested changes in the scaling exponent may reflect increased anaerobic respiration (Linke-Gamenick et al. 2000). Nevertheless, this does not explain the lack of change in respiration capacity at 15°C . Interestingly, Everett and Crawford (2010) also observed higher scaling exponents at 50% and 70% DO, a similar trend to what was seen in the allometric relationships at 20°C , and for overall Q_{10} values for $15\text{-}25^{\circ}\text{C}$. However, this trend does not lend itself to further explanation.

The a values in this study directly varied with temperature at high DO levels, suggesting a physiological activity response. Movement of the organisms was apparently limited by the mesh cages during respiration measurements; however, temperature is well known to increase with the metabolic activity of an organism, which should be expressed as higher a values for more metabolically active individuals. In the review by Shumway (1979), the allometric intercept constant (a) for polychaetes ranged from 0.05-0.62 and primarily related to physical activity of the species. Errant polychaetes showed a mean a value of 0.344 ± 0.024 , whereas sedentary polychaetes showed a mean a value of 0.144 ± 0.047 . Values of a within this study fell below the minimum reported in the review, but appropriately adhere to the sedentary polychaete category.

This study demonstrated ontogenetic shifts in the allometric b value for four of the 12 treatments. Breaks in respiration curves for *C. teleta* occurred at 0.002-0.003 g across the observed range of DO and temperature. This break in body size is similar to that shown by Forbes and Lopez (1990), who demonstrated a size break at 1.7 mm³ (comparable to 0.003 g) in the egestion of *C. teleta*. It is possible that segmented breaks in the regressions for respiration seen in this study could connote critical ontogenetic periods, or physiological shifts in the life history of *C. teleta*. Forbes and Lopez (1990) suggested that the observed size break in egestion signified the size at which sexual maturation occurred, based on “initial macroscopic appearance of the copulatory setae and onset of vitellogenesis in *Capitella* sp. I occur at about 1.00 mm³ (0.002 g) (males) and 3.00 mm³ (0.006 g) (females) respectively.” Forbes (1989) also reanalyzed respiration data of *Arenicola marina* (Kruger 1964) using a moving regression analysis and discovered a shift in the scaling exponent from 0.7 to >1.0 at 3.0 g. This shift also corresponded to the body size at which this species spawns. Overall, the mass-specific respiration rate of *Arenicola marina* decreased as a function of size until 3.0 g, after which the rate remained constant with growth; a similar trend to that seen in this study. Glazier (2005) proposed three models to explain different allometric phases within intraspecific relationships: 1) cellular models, where scaling may be due to changes in numbers and sizes of cells (i.e., changing total cell-surface area); 2) boundary approaches (i.e., where scaling exponents inversely related to metabolic intensity); 3) ontogenetic changes in energy-using processes (e.g. growth, reproduction, locomotion, and heat production); and 4) ontogenetic changes in body composition and tissue metabolic rates. The body size range where ontogenetic shifts occur for *C. teleta* suggests they may be

accounted for by the latter two models, in association with potential changes due to the onset of maturation and reproduction.

2.4.3 Conclusion

Capitella teleta showed synergistic ontogenetic respiration responses in relation to combined levels of DO, temperature, and body size, including changes in Q_{10} responses and respiration capacity. Further, findings of this study agree with Glazier (2006) who stated “metabolic scaling is not simply the result of physical or geometric constraints, but can be profoundly influenced by ecological circumstances.” Observed variability in the allometric coefficients in this study underscores the need to determine exponents under the specific conditions of interest rather than assuming the theoretical $2/3^{\text{rd}}$ or $3/4^{\text{th}}$ rules, or rather than assuming that the allometric relationship is maintained across varying levels of a factor. Many have argued against a universal metabolic based rule in view of significantly different scaling exponents between ectotherms and endotherms, between active versus resting states, and between intraspecific and interspecific relationships (Glazier 2005, Glazier 2006, White et al. 2007). This study further disputes the idea of a universal theory. Not only was variation seen in relation to environmental conditions, ontogenetic shifts illustrated changes in metabolic responses over different life stages.

CHAPTER III – ANAEROBIC ENZYMATIC ACTIVITY AND TOTAL CATABOLIC ENERGY PRODUCTION BY A MODEL TOLERANT POLYCHAETE, *CAPITELLA TELETA*, EXPOSED TO COMBINED LEVELS OF DISSOLVED OXYGEN AND TEMPERATURE IN RELATION TO BODY SIZE

3.1 Introduction

By 2100, the world's oceans are predicted to increase 4.8°C in sea-surface temperature, resulting in a 4-7% decline in dissolved oxygen (DO) in association with an increasing frequency, duration, and severity of eutrophication-induced hypoxic events (Field 2014, Matear and Hirst 2003, Diaz & Rosenberg 2008, Justic et al. 1996). In addition to environmental hypoxia (i.e., DO, 2 mg/l), functional hypoxia can occur when thermal stress elevates metabolic demands of the environment so high that they cannot be physiologically met by aerobic respiration (Alteri and Gedan 2015, Harcet et al. 2013, Vanquer-Sunyer and Duarte 2011). With the majority of current global hypoxic zones predicted to experience >2°C temperature increases by 2035, organisms may soon often face environmental hypoxia further exacerbated by functional hypoxia (Alteri and Gedan 2015). Under oxygen limitation, many organisms are capable of gradually resorting to anaerobic respiration (Cammen, 1987). While anaerobic metabolism is less efficient than aerobic respiration, it can enable metabolic efficiency to reach upwards of 60% of aerobic respiration potential (Cammen, 1987).

Anaerobic pathways can be generally classified into two categories: 1) glucose-succinate and aspartate-succinate pathways (end product succinate); and 2) glucose-lactate and -opine pathways (end products lactate and opine respectively) (González and Quiñones 2000, Harcet et al. 2013). The lactate and opine pathways (also known as

pyruvate oxidoreductases) produce energy at a faster, but less efficient rate than the succinate pathways, and are typically considered to be transitional pathways during times of functional and moderate environmental hypoxia (González and Quiñones 2000, Harcet et al. 2013). Conversely, succinate dehydrogenase is a component of the citric acid cycle that has been shown to be a sensitive indicator of mitochondrial anaerobic metabolism in polychaetes and serves as a pathway during longer hypoxia exposures. (Linke-Gamenick et al 2000, Schottler 1982). However, many marine invertebrates rely on the opine pathway, which produces a less acidic and more osmotically neutral end product than lactate (Zammit 1978, Plese et al. 2009). The five opine dehydrogenases include octopine dehydrogenase (ODH), alanopine dehydrogenase (ADH), strombine dehydrogenase (SDH), tauropine dehydrogenase, and β -alanopine dehydrogenase. Invertebrates can utilize only one, or all of the opine pathways. Typically, the more hypoxia-tolerant a species the more anaerobic pathways utilized (Gäde and Grieshaber 1986, González and Quiñones 2000).

Polychaetes are often subjected to low DO concentrations in nature due to living in depth in the sediment or due to hypoxic water conditions. With declining DO supply, many polychaetes have the ability to gradually switch to anaerobic respiration (Cammen, 1987). The main end products of anaerobic metabolism in marine invertebrates are succinate, acetate, and propionate, and also include alanine and opine (Muller et al. 2012). Quiruga et al. (2007) observed opine dehydrogenase as the most common anaerobic pathway in the polychaete, *Paraprionospio pinnata*, with the major end enzymes being ADH and SDH. ADH and SDH have also been shown to increase

significantly in response to anoxia in the brackish hard clam *Meretrix lusoria* (Lee and Lee 2012).

The polychaete species *Capitella teleta* (previously identified as *Capitella* sp. I) is an opportunistic, tolerant species often associated with disturbed and eutrophic habitats (Blake et al. 2009). Commonly occurring from the coastal northeastern US Atlantic, the native US habitat of *C. teleta* often ranges in sea surface temperature from ~5°C to 20°C annually. Further, with the exception of the Mississippi River region, the highest nitrogen loads into coastal system are observed in the mid-Atlantic region spanning Cape Cod to Chesapeake Bay and observes the largest concentration of highly eutrophic systems due to associations with high population densities (Bricker et al. 2008).

The extracellular hemoglobin of *C. teleta* has a moderate oxygen affinity ($P_{50} = 6.88 \pm 0.97$) and high cooperativity ($n_{50} 2.89 \pm 0.82$; Barclay 2013). Together these physiological traits confer on this species the capacity for high loading and unloading of oxygen as an adaptation to low DO environments; however, both affinity and cooperativity are suggested to reduce as temperature rise (Barclay 2013, Magnum et al. 1992, Weber 1980). NOAA recently issued an advisory report for the Northeast Atlantic Shelf citing the highest recorded sea-surface temperatures in 150 years during 2012, and temperatures above long-term means in 2013. As global climate changes, species must not only be able to adapt to increases in the mean water temperature, but must also cope with increased frequency and magnitude of interactions involving extreme thermal and hypoxia events (Sommer et al. 1997). During long-term exposures at 20°C, adult *C. teleta* reduce their oxygen consumption under low DO and observed significant increases in the levels of an anaerobic respiration indicator, succinate (Linke-Gamenick et al. 2000). The

presents of anaerobic respiration indicator suggest that the organism is experiencing pessimum physiological conditions, as defined by Pörtner (2002, 2010). Succinate is a part of the glucose-succinate pathway; whereas, this study will focus on the glucose-opine pathways.

As temperatures increase, it becomes ever more important to understand how organisms acclimate to functional and moderate hypoxia. In that regard, it is essential to understand the role anaerobic respiration plays in the physiological response. This study aims to quantify oxygen limitation of a tolerant polychaete species at multiple temperatures and DO levels by examining the rate of potential enzymatic activity of multiple pyruvate oxidoreductases. Further, the study will examine effects of body size on anaerobic enzymatic activity and connect enzymatic activity levels with aerobic respiration. I hypothesize that high temperatures will result in anaerobic enzymatic activity at higher DO levels due to functional hypoxia responses, and overall higher activity at high temperatures and low DO levels. Further, I hypothesize that different types of pyruvate oxidoreductases may be active during different stressor scenarios due to higher organismal anaerobic demand. I suggest this change in activity could occur as a result of maximum enzyme availability and enzymatic rate thresholds requiring the organism to capitalize on multiple, or different, opine dehydrogenases. Lastly, I hypothesize that smaller organisms will have overall higher enzymatic activities due to the high aerobic metabolic demands.

3.2 Materials and Methods

3.2.1 Experimental Setup

Experimental setup was identical to procedures described in Chapter II. After exposure and aerobic respiration was measured, the worm was wet weighed (Ohaus Analytical Plus, Model AP2500; ± 0.00001), frozen on dry ice, and stored at -80°C until analysis for anaerobic enzyme activity. In order to wet weigh the organisms, as much water as possible was removed by blotting the organisms on a plastic weight boat (kim wipes were not used as they often resulted in tearing the organism). While taking weight measurements, organisms were removed from experimental conditions for less than one minute, but otherwise always maintained under experimental conditions. Flash freezing of the whole organism took less than one minute due to the small sizes of experimental animals.

Table 3.1

Treatment levels of dissolved oxygen and temperature for anaerobic respiration measurements (mean \pm standard error).

Temperature ($^{\circ}\text{C}$)	Oxygen Saturation (%)	Dissolved Oxygen (mg/L)
15.4 ± 2.1	20	2.41 ± 0.30
	50	4.52 ± 0.91
	100	7.47 ± 0.32
24.2 ± 1.0	20	1.91 ± 0.24
	50	3.79 ± 0.37
	70	4.99 ± 0.60
	100	7.09 ± 0.38

3.2.2 Enzyme Activity Assays

In order to determine potential anaerobic pathways and assess the activity of pyruvate reductase enzymes under combined levels of DO, temperature, and body size,

the specific activities of LDH, ODH, ADH, and SDH were assayed. Enzymatic activity was measured following techniques modified from Schiedek (1997) and Dorgan et al. (2012). Briefly, individual worms were homogenized in 10-fold volume of an ice-cold phosphate buffer (0.1 mol l⁻¹, pH 7.4) with manual bullet pestles. Homogenate was centrifuged for 5 min at 5°C and 10,000 g. Assays were performed by adding 5 µl of supernatant to 195 µl of assay mixture (80 mmol l⁻¹ phosphate buffer (0.1 mol l⁻¹, pH 7.4) with 0.4 mmol l⁻¹ NADH). Reactions were initiated by 50 µl of substrate assays (total final volume = 250 µl). Assays included:

Lactate Dehydrogenase (LDH):	3.2 mmol l ⁻¹ pyruvate
Opine Dehydrogenase (ODH):	3.2 mmol l ⁻¹ pyruvate, 5.4 mmol l ⁻¹ arginine
Strombine Dehydrogenase (SDH):	3.2 mmol l ⁻¹ pyruvate, 250 mmol l ⁻¹ glycine
Alanopine Dehydrogenase (ADH):	3.2 mmol l ⁻¹ pyruvate, 250 mmol l ⁻¹ alanine

Enzyme activity was determined by measuring the decline in absorption at 340 nm using a spectrophotometer (Molecular Devices, SpectraMax M2). The decline in absorption (ΔA ; A min⁻¹) was measured for five minutes. Enzymatic activity (U) was calculated as: $\Delta A \times dil / \epsilon \times L$; where *dil* is the dilution factor (=550), ϵ is the extinction coefficient (6.22 mmol l⁻¹ cm⁻¹) for NADH at 340 nm, and L is the depth of the sample in a 96-well plate (0.67 cm). According to Dorgan et al. (2012), the decrease in NADH in opine dehydrogenase assays results from a combination of LDH and opines. Thus, the mean activity of LDH for each treatment was subtracted from that by the opine dehydrogenases. Data was lost for 70% and 100% DO at 15°C due to undergraduate labelling issues which combined both treatments together after enzymatic analysis and left no possible way to back calculate the identities of the samples.

3.2.3 Analysis

Effects of temperature on anaerobic enzymatic activity were examined by Q_{10} estimations where $Q_{10} = (R_2/R_1)^{10/(T_2-T_1)}$; where R_1 and R_2 are the rates of enzymatic activity at temperatures T_1 , and T_2 , respectively. The potential contribution of anaerobic enzymatic activity to the total catabolic energy production was estimated for small (≤ 0.0035 g) and large (> 0.0035 g) body sizes. Body size categories were determined based on pairwise regression segmentation breaks determined in Chapter II. Catabolic energy production (mmol ATP) was estimated for aerobic respiration (Chapter II) and anaerobic enzymatic activity based on the following relationships:

Aerobic: 1 ml O_2 / min consumed = 0.29 mmol ATP

(Burke 1979, Quiroga et al. 2007);

Anaerobic: 1 mole NADH = 1 mole ATP

(Quiroga et al. 2007).

3.3 Results

3.3.1 Anaerobic Pathways

The main anaerobic pathway of *C. teleta* was SDH, with weak activity by ADH, ODH, and LDH (Table 3.2). The activity of SDH and ADH increased with decreasing DO saturation at both temperatures (Figure 3.1). There was a minimal change in SDH activity and a 1.7x increase in ADH activity with increasing temperature at 20% DO. In contrast, both LDH and ODH activity levels were generally higher at 15°C than at 25°C (Table 3.3). Activity of both ODH and LDH was minimal at 25°C and 20% DO. Increasing temperatures at normoxia elicited ~8-fold increase in SDH and ADH, and a doubling of LDH and ODH activity. Overall, there was no large effect of temperature on

enzymatic activity at low DO saturation. Conversely, all four pyruvate reductases increased with temperature at higher DO saturations.

Table 3.2

Anaerobic enzymatic activity (mean \pm SD) of four pyruvate oxidoreductases (SDH = strombine dehydrogenase, ADH = alanopine dehydrogenase, ODH = opine dehydrogenase, and LDH = lactate dehydrogenase) at two temperature and four dissolved oxygen saturation levels (%).

	15°C				25°C			
	20%	50%	70%	100%	20%	50%	70%	100%
SDH	4.91	4.67	0.33	0.00	5.81	2.83	2.54	2.06
SD	5.81	3.42	0.53	0.00	7.95	2.17	2.47	2.70
n	14	8	9	4	11	8	9	7
ADH	0.63	0.21	0.09	0.00	1.05	1.10	0.70	0.41
SD	0.89	0.29	0.17	0.00	1.66	1.36	0.82	0.41
n	12	6	4	2	3	4	6	4
LDH	1.66	0.39	0.09	0.76	0.26	0.06	0.22	0.01
SD	1.58	-	0.13	-	0.43	0.08	0.42	0.02
n	9	1	2	1	4	4	4	5
ODH	0.66	1.04	0.50	0.95	0.08	2.30	0.94	1.49
SD	0.56	1.05	0.71	-	0.13	2.86	1.40	1.85
n	6	2	2	1	3	2	7	5

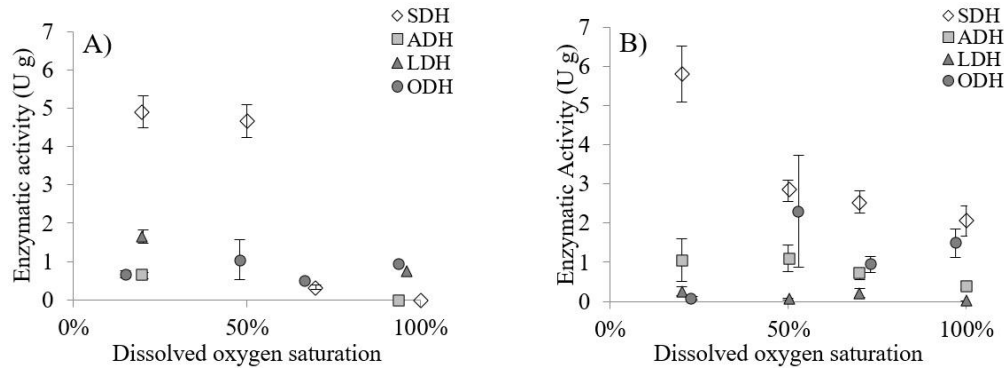


Figure 3.1 Anaerobic enzymatic activity of four pyruvate oxidoreductases (SDH = strombine dehydrogenase, ADH = alanopine dehydrogenase, ODH= opine dehydrogenase, and LDH = lactate dehydrogenase) at two temperatures (A = 15°C; B = 25°C) and four DO saturation levels (%) (\pm SE).

Table 3.3

Q_{10} values from 15° to 25° C for four pyruvate oxidoreductases (SDH = strombine dehydrogenase, ADH = alanopine dehydrogenase, ODH = opine dehydrogenase, and LDH = lactate dehydrogenase) at four dissolved oxygen saturations. No Q_{10} exists for SDH and ADH 100% due to no enzymatic activity measured at 15°C.

	20%	50%	70%	100%
SDH	1.18	0.61	7.67	-
ADH	1.66	5.31	8.05	-
LDH	0.16	0.16	2.36	0.01
ODH	0.12	2.20	1.89	1.58

3.3.2 Body Size Effects

Small body sizes maintained higher mass-specific enzymatic activity of SDH over all treatments (Table 3.4). Separation between small and large body sizes in enzymatic activity appeared at 50% saturation at 15 and 25°C (Figures 3.2 and 3.3). Body size correlated with enzymatic activity at lower DO saturation levels (i.e., 20% and 50%) at

15°C and at 70% saturation at 25°C (Table 3.5). Correlations could not be examined for high DO's at the low temperature, as most of the measured activity was zero. Allometric scaling exponents of mass-specific anaerobic activity curves ranged from 0.09 to 0.45.

Table 3.4

Enzymatic activity (mean \pm SE) of strombine dehydrogenase for two body size groups exposed to two temperatures and four dissolved oxygen saturation levels (%).

	15°C				25°C			
	20%	50%	70%	100%	20%	50%	70%	100%
Small	8.93	7.97	-	0.00	8.62	3.38	2.40	2.38
SE	0.71	2.05	-	0.00	1.26	0.60	0.91	0.98
n	8	3	-	2	7	4	3	3
Large	0.45	3.35	0.60	0.00	0.89	0.87	2.62	1.81
SE	0.11	0.48	0.09	0.00	0.45	0.26	0.43	0.73
n	6	5	9	2	4	4	6	4

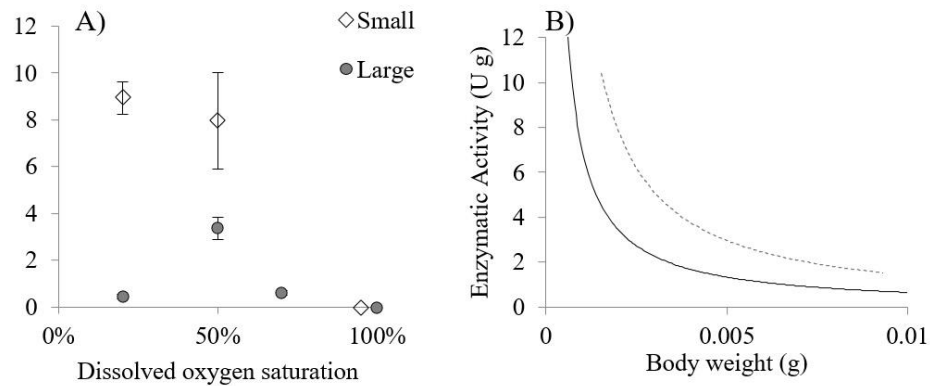


Figure 3.2 A) Allometric relationships for strombine dehydrogenase activity in *Capitella teleta* across four DO levels at 15°C (mean \pm SE); B) allometric mass-specific curves (20% = solid line and 50% = dashed line).

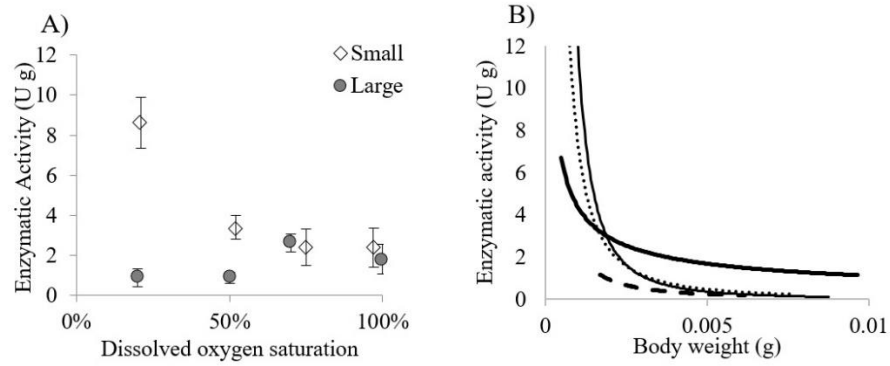


Figure 3.3 A) mass-specific allometric relationships for strombine dehydrogenase activity in *Capitella teleta* at 25°C (mean \pm SE); B) allometric curves (20% = solid line, 50% = dashed line, 70% = bold solid line, 100% = dotted bold line).

Table 3.5

Allometric relationships for anaerobic enzymatic activity of strombine dehydrogenase for *Capitella teleta* exposed to two temperature and four dissolved oxygen saturation levels (%). Equation in form of $y = aW^b$; n = number of samples; r^2 = correlation coefficient (mean \pm SE). Whole organism allometric exponent b is calculated as $b = 1 + b'$.

15°C						
	a	b'	r ²	n	F	P
20%	0.18 \pm 0.11	-0.53 \pm 0.08	0.77	15	44.02	<0.0001*
50%	0.031 \pm 0.031	-0.91 \pm 0.16	0.91	6	38.47	0.0034*
70%	-	-	-	8	-	-
100%	-	-	-	4	-	-
25°C						
20%	0.18 \pm 0.72	-0.59 \pm 0.64	0.12	11	1.22	0.30
50%	0.07 \pm 0.15	-0.60 \pm 0.32	0.49	8	4.75	0.08
70%	0.01 \pm 0.03	-0.85 \pm 0.36	0.55	9	8.55	0.02*
100%	0.008 \pm 0.06	-0.95 \pm 1.28	0.04	7	0.20	0.68

3.3.3 Catabolic Energy Production

Total catabolic energy produced from aerobic respiration averaged 1.24-3.95 mmol ATP/ min at 15°C and was 2.16-9.10 mmol ATP/min at 25°C (Figure 3.4). At normoxia, aerobic respiration accounted for most (60-100%) of the catabolic energy

production (Figure 3.5). Although aerobic respiration did not change drastically with DO at 15°C, potential anaerobic energy accounted for >45% of the total potential energy at 20% DO. Furthermore, anaerobic activity also contributed more to total potential energy (>35%) at 100% DO and 25°C, suggesting effects of functional hypoxia. The response to low DO was similar for both body sizes at 15°C and 25°C, with the contribution of anaerobic respiration ~50-70% of the total potential energy production. However, large worms maintained similar anaerobic respiration across DO levels at 25°C, thereby resulting in an energy reduction at 20% DO (i.e., 6.31 mmol ATP/min at 100% vs 3.96 mmol ATP/min at 20%) (Table 3.6).

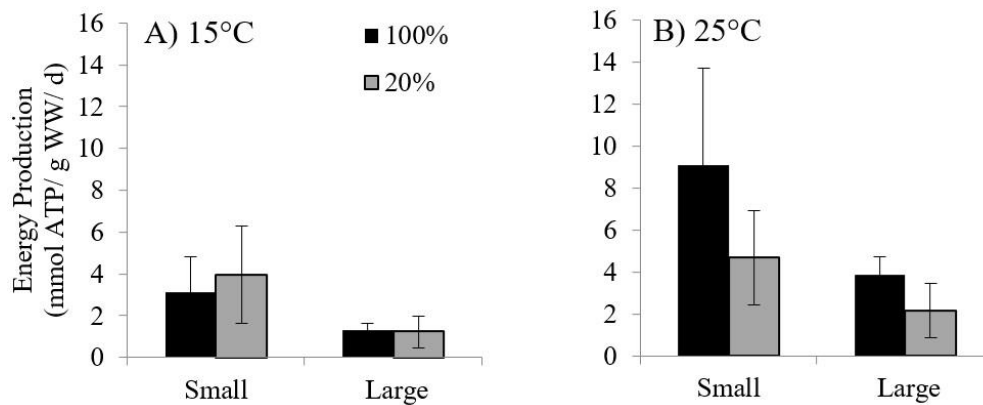


Figure 3.4 Catabolic energy produced by aerobic respiration for *Capitella teleta* exposed to two temperatures (A=15°C; B=25°C) and two dissolved oxygen saturations (20% and 100%) (WW= wet weight; mean \pm SE).

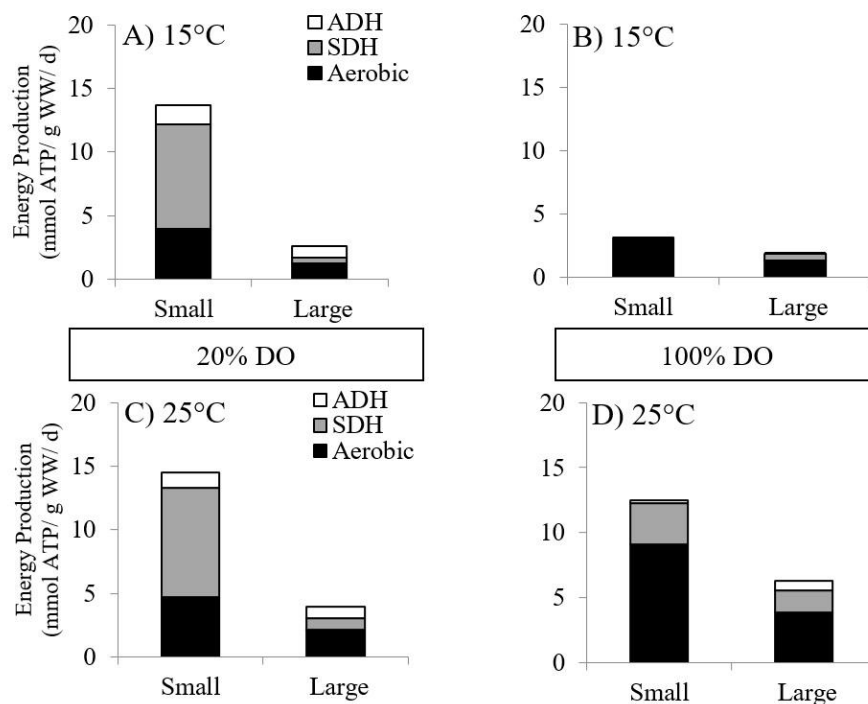


Figure 3.5 Relative contribution (mmol ATP/g WW/ d) of aerobic and anaerobic respiration to the total catabolic potential energy production of *Capitella teleta* exposed to 20% and 100% dissolved oxygen saturation and two temperature levels (A and B = 15°C; C and D = 25°C; WW= wet weight).

Table 3.6

Mass-specific catabolic energy (mmol ATP/ g WW/ d) produced by aerobic respiration vs. the two main anaerobic pyruvate oxidoreductases for *Capitella teleta* (mean \pm SE).

Total = mean energy available. WW = wet weight.

	15°C				25°C			
	20%		100%		20%		100%	
	Small	Large	Small	Large	Small	Large	Small	Large
Aerobic	3.95 \pm 2.33	1.24 \pm 0.76	3.10 \pm 1.70	1.30 \pm 0.35	4.67 \pm 2.24	2.16 \pm 1.30	9.10 \pm 4.60	3.84 \pm 0.90
SDH	8.26 \pm 5.70	0.45 \pm 0.65	0.00 \pm 0.00	0.58 \pm 0.68	8.62 \pm 8.85	0.89 \pm 1.79	3.16 \pm 3.10	1.68 \pm 1.84
ADH	1.44 \pm 0.88	0.87 \pm 0.14	0.00 \pm 0.01	0.11 \pm 0.19	1.22 \pm 1.78	0.91 \pm 0.39	0.24 \pm 0.48	0.79 \pm 0.74
Total	13.65	2.56	3.32	1.99	14.51	3.96	12.50	6.31

3.4 Discussion

3.4.1 Anaerobic Enzymatic Activity

While my study was limited by measuring enzymatic activity levels (as opposed to end product accumulation) and by 24h exposures, both ADH and SDH activities did increase over the 15 to 25°C exposures under normoxia. In invertebrates, the accumulation of SDH has been shown to be an indicator of metabolic stress (Zachariassen et al. 1991) or osmotic stress (Simpson et al. 1959). The increase in anaerobic enzymes observed in this study suggests a functional hypoxic response due to capacity limitation effects of thermal stress at 25°C, a temperature which the species does not experience under current natural conditions but probable to occur in the future. Metabolic demands of increasing temperature can lead to physical capacity limitations, for example, brought on by insufficient ability to further increase ventilation and circulation, and reduced oxygen affinity of blood cells, which can lead to unattainable oxygen demands even under normoxic conditions (Frederich and Pörtner 2001). Under these conditions, organisms could either rely to a greater degree on anaerobic respiration, or ultimately die off. This response has also been viewed in the polychaete, *Arenicola marina*, in which thermal stress by transfer from 12 to 25°C significantly increased strombine concentrations after 4h, and alanopine after 24h under normoxic conditions (Sommer and Pörtner 1999). Further, under normoxia, mortality rates of *C. teleta* increased sharply between 20°C and 25°C (~60% vs 20% mortality), further suggesting effects of capacity limitations of thermal stress (personal observations, see Chapter V). Further support for functional hypoxia at 25°C is seen in the estimated total catabolic

energy production under normoxia which revealed higher anaerobic contributions not seen at 20°C.

Functional hypoxias may be a particular issue for large individuals which appeared to show energy limitations at 20% DO. This study a significant correlation between body size and SDH activity at 15°C ($b' = -1.04$; $b = 1 + b'$) and 25°C ($b' = -2.31$); however, these values did not correspond to either the 2/3rd or 3/4th allometric rules, nor to the positive scaling values of various other polychaetes (Gonzalez and Quiñones 2000). The only other study of allometric anaerobic respiration for the polychaete, *Hyalinoecia artifex*, did not find allometric relationships for SDH or ADH; however, increased LDH activity was related to body size ($r^2 = 0.54$; $P = <0.001$) (Jessen et al. 2009). Additional research is needed on allometric relationships in the anaerobic activity of polychaetes, especially in order to understand the connection between potential anaerobic respiration as measured by anaerobic activity and true anaerobic respiration as measured by the accumulation of anaerobic end products.

3.4.2 Conclusion

In conclusion, *C. teleta* relied mainly on the SDH pathway for anaerobic respiration during environmental hypoxia, and all four pyruvate oxidoreductase pathways when temperature is high across all DO levels, suggesting functional anaerobiosis. Growth, mortality, and egestion of *C. teleta* indicate that the critical temperature for this species occurs between 20°C and 25°C, and the inability to survive at 30°C (personal observations). The utilization of all four pyruvate oxidoreductases reflects the tolerant nature of this species to environmental hypoxia. As Gonzalez and Quiñones (2000) note, organisms that possess more than one pyruvate oxidoreductase have a greater capacity to

cope with both environmental and functional hypoxia by regulating pyruvate consumption. However, this does not appear to be the case for *C. teleta*, as it cannot survive more than 24 h at 10°C above naturally experienced high temperatures.

In my study, enzymatic activities as measured at 24 h might have provided a biased estimate of maximum enzyme activity, due to the possibility of adaptive reversal, defined by a reduction in the accumulation of enzyme product with increasing duration of exposure. Adaptive reversal does occur after 10 h of exposure in *Arinicola marina* (Sommer and Pörtner 1999). Additional research is needed to determine a) whether a correlation exists between specific enzyme activity and end product accumulation for *C. teleta*, and b) whether this species can undergo adaptive reversal.

CHAPTER IV – THE EFFECT OF STARVATION ON GROWTH, EGESTION, AND
MORTALITY OF THE MODEL TOLERANT POLYCHAETE, *CAPITELLA*
TELETA, UNDER COMBINED LEVELS OF DISSOLVED OXYGEN,
TEMPERATURE, AND BODY SIZE.

4.1 Introduction

Benthic fauna face two potential bioenergetic limitations within sediments, the availability of food and dissolved oxygen (DO) (Forbes and Lopez, 1990). For example, under DO limitation deposit feeding worms partition time and energy between feeding and ventilation of their burrows, and often feeding occurs between exclusive ventilation intervals (Forbes 1989, Grassle and Grassle 1976, Forbes and Lopez 1990). In addition, many benthic organisms cease feeding in order to reduce metabolic demands and focus on ventilation during periods of DO limitation (Forbes and Lopez 1990, Sagstia et al. 2001). During periods of starvation many organisms can metabolize structural proteins while undergoing negative growth, or degrowth (Davey-Huggins 2001, Calow 1981). Furthermore, polychaete ingestion and growth rates have been shown to be sensitive to nitrogen concentrations within the sediment, leading to negative growth under low nitrogen levels (Tenore 1983, Horng 1999, Linton and Taghon 2000). Opportunistic species are particularly susceptible to degrowth due to their metabolic strategy to directly utilize external energy rather than build up internal energy reserves (Grassle and Grassle 1974, Davey-Huggins 2001).

The ability of an organism to withstand starvation is directly related to its metabolic rate, suggesting related effects should be influenced by the physical environment, including temperature, DO, pH, etc. In the current era of climate change

and anthropogenic stressors, many marine organisms are faced with increasing temperatures and/or increasing frequency and extent of hypoxic conditions. Thus, periods of starvation might become more prevalent (Justic et al. 1996, Alteri and Gedan 2015). Moreover, concurrent effects of increasing temperature and decreasing DO also have opposing effects on metabolism. Metabolic rate is directly related to temperature, as shown by Q_{10} effects on respiration and enzymatic reactions with increasing temperature as a reflection of increased metabolic demand; conversely, low DO can culminate in metabolic depression (Alteri and Gedan 2015, Brown et al. 2004, Pörtner 2001, Forbes 1989, Sagasti et al. 1991). Metabolic depression is a response to environmental stress allowing an organism to survive on minimal resources by reducing the basal metabolic rate (Guppy 2004, Storey and Storey 1990). When faced at the same time with these opposing constraints, physiological trade-offs must occur in order for optimal survival; however, the response will not necessarily be a simple linear, additive outcome.

In order to properly assess effects of climate change on marine ecosystems it is important to examine interactive effects of multiple stressors upon ecophysiological responses of individuals. This is especially important for sedimentary habitats, where the benthic fauna is confronted with multiple bioenergetic limitations within an environment in which the fauna also plays a crucial functional role in metabolizing and recycling nutrients (Forbes and Lopez 1990). The degrowth response affords a useful opportunity to understand bioenergetic consequences and acclimation to physiological stressors because it eliminates complicating circumstances surrounding consumption (such as influence of sediment particle size) while lending insights into the metabolic demands of

the organisms through the consumption of structural proteins (Callow 1977, Forbes and Lopez 1990).

In this chapter, I aim to examine degrowth, egestion, and mortality of a tolerant, opportunistic polychaete, *Capitella teleta*, in response to various levels of DO and temperature while under food limitation in order to gain insights into the metabolic responses of this species. I hypothesize degrowth rates will be highest at high temperatures and high DO levels due to a maximized metabolism, while degrowth will be minimal during low DO levels and low temperatures due to reduced metabolic demands. When the organisms are exposed to high temperatures and low DO levels, I predict the organism will experience rapid levels of degrowth due to the high temperatures, but will result in early mortality due to the combined effects of reduced DO. Concerning egestion, I propose egestion rates will cease earlier during low DO levels due to metabolic depression, while worms exposed to high DO levels will continue active egestion as the metabolism will not respond to reduced food levels as quickly as reduced DO levels.

4.2 Material and Methods

4.2.1 Model Species

The polychaete, *C. teleta* (previously identified as *Capitella* sp. I), is an opportunistic species often associated with disturbed and eutrophic habitats (Blake et al. 2009). Commonly found in the northeastern United States, Japan and the Mediterranean, *C. teleta* has been described as the most tolerant capitellid sibling species with the “most rapid response to disturbed habitats, the highest rate of increase, largest maximum population size, and highest mortality” (Blake et al. 2009). As a ‘head down’ deposit-feeding polychaete, *C. teleta* burrows through sediment to obtain nutrients from ingested

sediments. Ingestion occurs in the top few centimeters of the sediment surface, while egestion occurs at the sediment surface where the posterior end of the worm protrudes at the sediment-water interface (Grassle and Grassle 1974, Grassle and Grassle 1976).

The native U.S. habitat of *C. teleta* typically ranges seasonally from ~5°C to 20°C in sea surface temperature; however, NOAA recently issued an advisory report for the Northeast Atlantic Shelf citing the highest recorded sea-surface temperatures in 150 years during 2012, and above long-term means for 2013. These recent trends illustrate that species in general must not only be able to adapt to increases in the mean water temperature, but also cope with increased frequency and magnitude of extreme thermal events (Sommer et al. 1997).

4.2.2 Culture Maintenance

Stock cultures of *C. teleta* were obtained from Dr. Judy Grassle of Rutgers University and were reared at 15°C and 27 ppt (artificial seawater). Groups of ~50 polychaetes were maintained in 10.2 cm culture dishes with 15-30 mL of enriched sediment (For detailed culture maintenance see Appendix A). Sediment was collected from the Mississippi Sound, passed through a 1 mm sieve and frozen in 30 mL plastic, food safe containers. Before use for cultures, sediment was thawed and Tetramin© fish flakes added at a ratio of 2.5 g of flake to 54 g of mud. Every two weeks cultures were ‘cleaned’ by replacing sediment and water.

4.2.3 Experimental Treatments

In an attempt to standardize DO conditions, treatments were classified into four oxygen saturation categories (20%, 50%, 70%, and 100%), which were fully crossed with three temperatures (15°C, 20°C, and 25°C)(Table 4.1) (Figure 4.1). For all experiments,

salinity was held constant at 27 ppt. To ensure broad coverage, polychaetes were initially assigned to one of three size categories: small (<0.003g), medium (0.003-0.005g), and large (≥ 0.005 g), then ultimately indexed by their actual sizes. The experimental flow-through system was composed of four sections, each designated as one of the DO treatments, and further split into three replicates of each of the three temperature treatments (i.e., nine experimental chambers) (Figure 4.2). The nine chambers further represented the three body sizes, yielding a sample size of three for each treatment combination (DO \times Temperature \times Body Size)

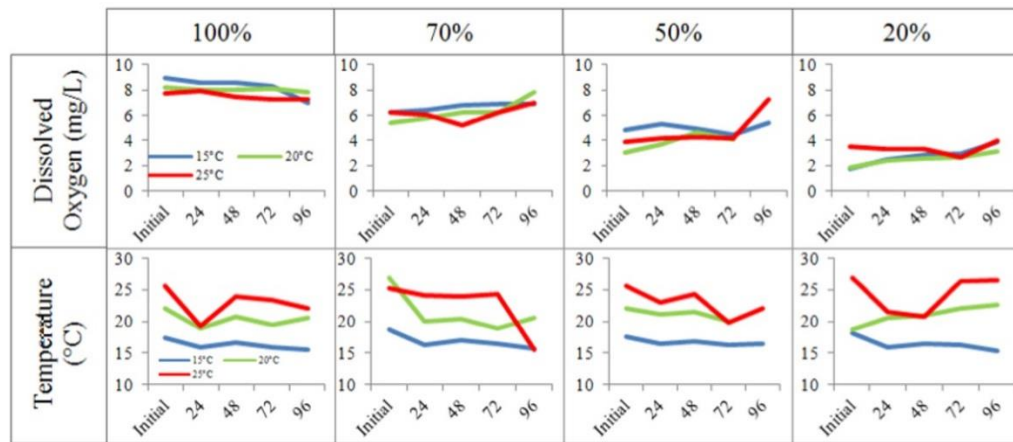


Figure 4.1 Variation in the twelve DO (mg/L) and temperature treatments over four days during starvation experiment (lines on bottom panel represent same temperature treatments as in upper panel).

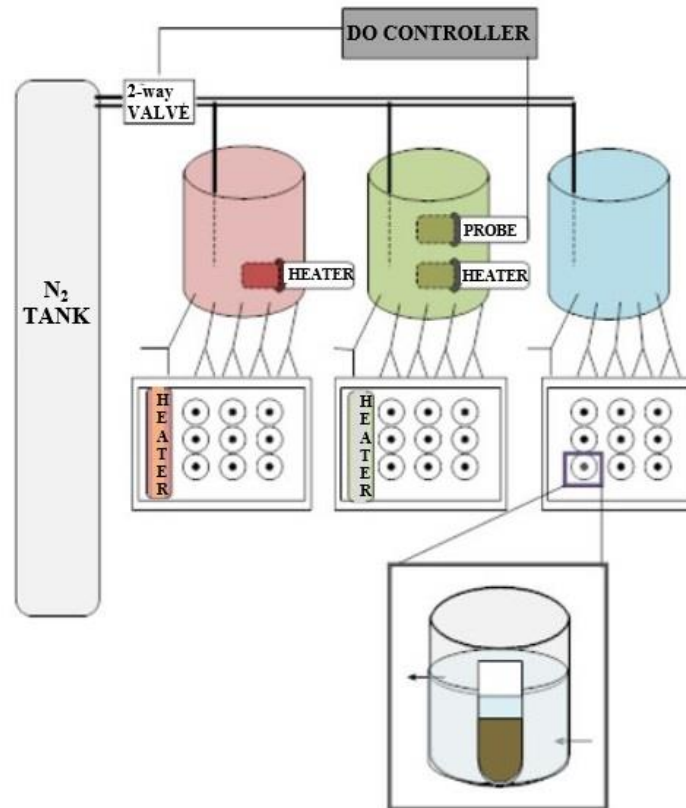


Figure 4.2 Flow-through experimental layout for one of the DO treatments comprising three replicates of each of three temperature treatments and body size categories. Inset illustrates a PVC experimental chamber containing a 5 mL centrifuge tube enclosure which housed one worm. Each of the four DO treatments was set up using the same layout. Red = 25°C, green = 20°C, and blue= 15°C.

4.2.4 Treatment Control

A DO control system (Profilux 3; GHL Systems) maintained the DO treatment designated for each section of the flow-through system. A DO probe threshold switch set for the target DO \pm 5% triggered a solenoid valve to pump nitrogen gas when the actual DO concentration was different than the target level. One DO probe kept within the 20°C treatment bucket was used for each section. For the 100% treatment, air pumps continuously bubbled in ambient air. A 3-piece airlock was fit to the top of each bucket lid via a rubber grommet port to allow for the relief of pressure without contamination by

ambient air. The flow-through system was housed in a 144 square foot controllable walk-in environmental chamber with a 2.4 m ceiling which was maintained at 15°C.

Temperatures of warmer treatments were controlled using aquarium heaters within the buckets, and within a water bath holding the experimental chambers. DO and temperature levels within chambers were measured twice daily using a fiber optic YSI meter.

Table 4.1

Mean DO and temperature conditions (\pm SE) for the twelve oxygen saturation \times temperature treatments.

Temperature (°C)	Oxygen Saturation (%)	Dissolved Oxygen (mg/L)
16.4 \pm 1.0	20	2.79 \pm 0.8
16.6 \pm 0.3	50	5.03 \pm 0.4
16.9 \pm 1.2	70	6.65 \pm 0.3
16.3 \pm 0.8	100	8.25 \pm 0.7
21.0 \pm 1.5	20	2.52 \pm 0.5
21.1 \pm 0.9	50	3.86 \pm 0.7
21.4 \pm 3.2	70	6.30 \pm 0.9
20.4 \pm 1.2	100	8.01 \pm 0.1
24.4 \pm 3.0	20	3.39 \pm 0.5
23.0 \pm 2.2	50	4.75 \pm 1.4
22.7 \pm 4.0	70	6.16 \pm 0.6
22.9 \pm 2.4	100	7.50 \pm 0.3

4.2.5 Flow-through System

The flow-through system was gravity driven by supply buckets elevated ~76 cm above the experimental chambers, through which water flowed into a waste water container ~90 cm below the buckets. Each DO treatment section consisted of three 25 L fermentation buckets representing the three temperature treatments (Figure 4.2). Each supply bucket had five 3.2 mm sealed male barbs secured 5 cm from the bottom of the bucket. A T-shaped valve was fixed to each barb and connected to two 100 ml PVC chambers using nylon aquarium tubing, thus allowing a total of nine chambers and one

drainage tap to be connected to each supply bucket. One of the three supply buckets representing a DO treatment level (i.e., 15°C bucket) had a 1.3 cm rubber grommet inserted into its side 5 cm from the bottom in order to hold the oxygen sensor probe. High temperature treatment buckets (i.e., 20° and 25°C) also employed ½” grommets to hold 100W titanium heaters (Azoo).

Experimental chambers were fashioned from 3” sections of 2” I.D. PVC tubing. Cut edges were sanded to smooth them. The bottom of each chamber was sealed with a 2” knock-out plug and silicone. Male barbs were silicone sealed 1” from the top and bottom edges of each chamber, thus allowing for the containment of ~100 ml of water in each chamber. Each temperature treatment comprised nine chambers within a 16 L Rubbermaid water bath (47.5 cm L x 33.8 cm W x 13.7 cm D) with a snap lid. Holes were drilled through the sides of water baths, through which aquarium tubing delivered to and drained water from chambers. Aquarium heaters covered with water controlled the temperatures of the water baths. The top open ends of chambers were secured with an oxygen impermeable sealing plastic film (DuraSeal (Electron Microscopy Sciences)), which formed a tight seal with the PVC chamber when held in place with a rubber band. The plastic film was changed daily to ensure proper sealing of chambers upon checking them.

A flow rate of 3-4 ml/min ensured the water in each chamber was completely replaced about every 30 minutes. Chamber flow rates were controlled by Homboldt compressor clamps on tubing located between the buckets and chambers. The flow-through rates were measured three times to ensure consistent rates of flow for each chamber.

Worm enclosures were fashioned from 5 ml centrifuge tubes. Nine 1.6 mm holes were drilled into the sides of tubes within the first 1.3 cm of the tops of the tubes and sanded to facilitate flow through them. To ensure that water was exchanged efficiently between chambers and enclosures, food coloring added to enclosures while inside chambers showed complete diffusion of the coloring from the enclosures to the chambers within seconds (<10 seconds).

4.2.6 Starvation Experiments

Polychaetes were initially measured and allocated to size categories before assigning them to DO/ temperature treatments. Subjects were allowed to acclimate for 24 h to the temperature treatment with food. However, once the experiment began organisms were kept in empty vials; this gives comparable degrowth results using combusted sediments as a medium while reducing handling damage (Davey-Huggins 2001). During the experiment, subjects were starved for 4 d following acclimation and measured every day to the nearest 0.00001 mg on a microscale. Water on the surface of the subject was removed by gently sliding it across a plastic weigh boat until no traces of water were observed coming off of the animal. Organisms were not blotted with paper materials as this often lead to damage of the organism, particularly smaller organisms. During daily measurements, subjects were out of the experimental chamber for less than 5 minutes, but organisms were always kept in petri dishes of the corresponding treatment conditions. If feces were present in the vial, it was collected with a pipette and preserved in 5% formalin. Organism mortality was recorded daily. Worms were only scored as dead if a body was found within the sample, otherwise it was noted as missing.

4.2.7 Quantifying Egestion

Fecal pellets were only produced during the first 24 hr (FP d⁻¹). The weight of each individual feces was estimated using a regression relationship with worm volume from Forbes (1989), which was modified to worm weight:

$$\text{Individual wet weight (g)} = 0.002 * \text{volume (mm}^3\text{)}$$

$$(n=81; r^2= 0.84; \text{personal observation})$$

$$\text{Individual fecal pellet weight (ug)} = 707.6 * \text{wet weight (g)} + 0.357$$

$$(n=15; r^2= 0.98; \text{Forbes 1989}).$$

Personal observations on fecal volume were determined through photographic analysis using MetaVue Version 7.1.7.0 software and a Nikon SMZ 1500 camera. A maximum of 10 fecal pellets per individual were measured from 84 worms over the full range of body sizes. Fecal volumes were estimated using the equation: $\text{Volume} = \Pi (\text{projected area})^2 / 4 (\text{length})$ (Davey-Huggins 2001, Forbes 1989, Forbes and Lopez 1990, Forbes et al. 1994). Estimates of the total weight of sediment egested versus total volume egested were highly correlated across treatments, indicating the correlation that was provided for weight of feces at 20°C 100% by Forbes (1989) was applicable to all treatment levels in this study (Appendix C). The weight of sediment egested (ug d⁻¹) was calculated by multiplying the daily number of fecal pellets produced by the estimated weight of an individual fecal pellet for each individual. Allometric trends were estimated using the geometric mean of the weight for each individual for the day of collection and the day before collection. Since worms in the starvation experiment were unable to ingest new sediment, the weights of egested pellets were included in the individual worm measurements; however, the total weight egested in 24 h was typically less than 0.0001g (86% of worms did not

see a change in weight) and only 14% of worms saw a minimal increase in weight in the first 24 h.

4.2.8 Data Analysis

Positive growth was observed for a minimal amount of observations and was assumed to reflect measurement error due to the small body sizes of subjects. Positive growth values were ‘corrected’ using two methods: (1) values that increased negligibly by 0.0001-0.0002 g were changed to reflect the value from the previous day, or (2) larger values were changed by interpolating across the preceding and the following days. Corrections accounted for 17% of the 449 measured values (11% using the first method and 6% using the second method). The fact that most of corrections were based on the first method reinforced the measurement error interpretation, especially in light of the use of measurements taken by multiple researchers. Past studies using wet weights for capitellids have also noted a $\leq 5\%$ error between weight measurements, further supporting the need to correct small positive changes in weight (Cammen 1985).

Gross production efficiency (GPE), defined as the % daily loss normalized by the μg sediment egested during a particular day, was analyzed using a 2-way ANCOVA in SPSS 23®. Analysis was conducted on cube root transformed data with the initial body size as the covariate and DO and temperature as the fixed factors, and all possible interactions. The covariate did not interact with any of the fixed factors, hence fulfilling the parallel slopes assumption (DO interaction p-value = 0.39, and temperature interaction p-value = 0.54). The cube root transformation was appropriate when dealing with negative data values (i.e., weight loss) (Cox 2011). Because the covariate was not significant, weight was pooled and reanalyzed as a 2-way ANOVA with temperature and

DO as fixed factors, and all possible interactions. Post-hoc comparisons among treatment levels were made using Tukey's tests. Normality was tested using Shapiro-Wilk test (W) in conjunction with Q-Q plots. Shapiro-Wilk failed for 2 of 12 treatments (100% DO and 25°C); however, the W statistic ranges from 0-1 (with W =1 being normal) and all treatment levels in this study had a $W > 0.89$ with visually normal Q-Q plots (Appendix D). Since the data passed the Levene's heterogeneity test, the ANOVA was regarded as acceptable in terms of assumptions.

Total specific growth rate was calculated as: $G (\% d) = [LN (\text{final wet weight}) - LN (\text{initial wet weight}) / \text{time}] * 100$. The specific growth rate was calculated from the initial wet weight and the final wet weight from either when the experiment ended (day 4), or the last weight taken before individual died. Only individuals having at least two daily measurements after taking the initial weight were included to ensure subjects were responding to experimental treatments rather than extraneous factors (e.g. unknown damage before the experiment, etc.). Total specific growth was analyzed in SPSS 23 as a 2-way ANCOVA using a cube root transformation with the initial body size as the covariate. Fixed factors included DO and temperature, and all possible interactions. The covariate did not interact with any of the fixed factors (DO interaction p-value = 0.67 and temperature interaction p-value = 0.71). Total weight loss was defined as: $\text{total \% loss} = (\text{end weight} / \text{initial weight} * 100) - 100$. Total weight loss was analyzed as a 2-way ANCOVA on untransformed data with the initial body size as the covariate. The covariate did not interact with any of the fixed factors, hence fulfilling the parallel slopes assumption (DO interaction p-value= 0.26 and temperature interaction p-value= 0.22). In both cases, the covariate was not significant and weight was pooled and reanalyzed as a

2-way ANOVA with temperature and DO as fixed factors and all possible interactions included. Post-hoc comparisons of treatment levels were made using Tukey's tests.

Daily growth was calculated as the percent body weight lost since the previous measurement: % daily lost = weight of day_x / weight the day_{x-1}. Analysis of daily growth was performed using a mixed model with day as a repeated measure and DO, temperature, and initial body size category as fixed factors. All possible interactions were also included. Mixed model was used in order to include a repeated measures analysis (i.e., time as factor) while also retaining the data for subjects that did not survive the entire 96 h experiment, which are excluded using traditional methods. Analysis was conducted using the autoregressive first order covariance structure (AR1 diagonal p-value = <0.001 and AR1 rho p-value = 0.01). The Q10 values for specific degrowth rates were calculated as $Q_{10} = (R_2/R_1)^{10/(T_2-T_1)}$; where $R_{1,2}$ are the rates of degrowth at temperatures $T_{1,2}$, respectively.

4.3 Results

4.3.1 Specific Growth Results

Body sizes covariate was non-significant ($F = 2.95$; $p = 0.09$), degrowth data were pooled across body sizes to further examine the effects of DO and temperature. Degrowth rates ranged from -2.34 to -69.31% d across all treatments (Table 4.2) (Figure 4.3). Although the 100% DO treatment showed relatively slower degrowth, the overall effect of DO on degrowth was non-significant ($F = 0.382$; $p = 0.77$) (Figure 4.4). Temperature had a significant effect on specific-growth ($F = 4.617$; $p < 0.05$), growth was significantly lower at 15°C compared to 20°C ($p < 0.05$) as shown by mean loss of -25.4 vs -35.9% d, respectively. Furthermore, Q_{10} values for specific growth rates were between 15-20°C

ranged from 1.6 to 2.8 fold, whereas the Q_{10} values between 20-25°C were minimal (0.2-1.1) (Table 4.3).

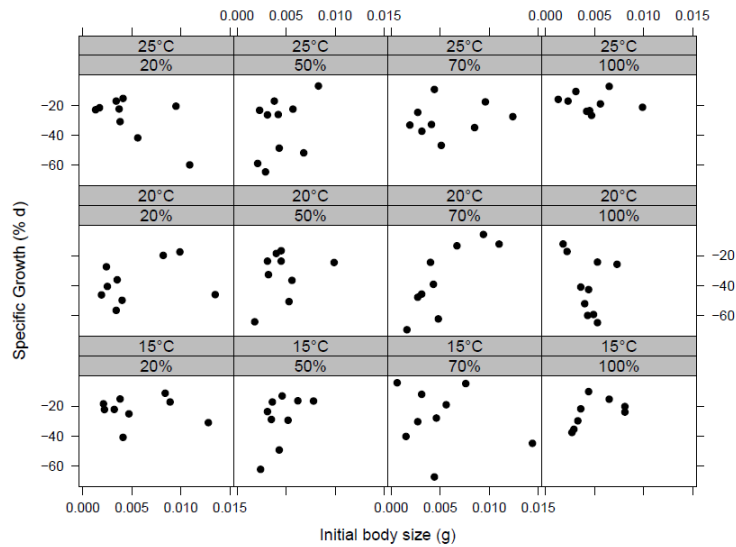


Figure 4.3 The specific growth rate (% d) by body size of *Capitella teleta* during starvation while exposed to 12 treatment combinations comprising four DO levels and three temperature levels.

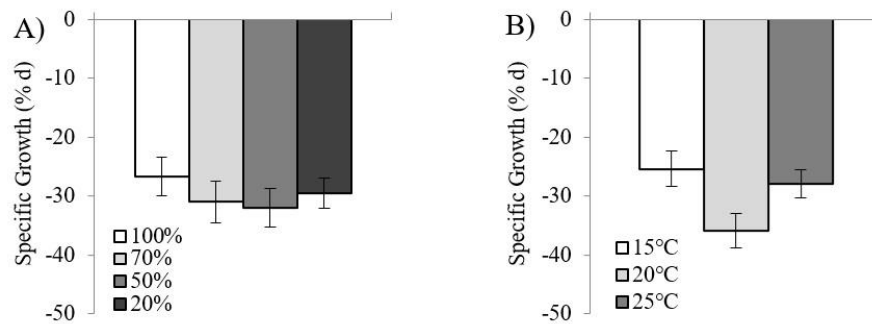


Figure 4.4 The specific growth rate (% d) of *Capitella teleta* under starvation pooled across (A) four DO saturation levels and (B) three temperature levels (\pm SE).

Table 4.2

Summary of the daily specific growth (SG % d⁻¹) and total weight loss of *Capitella teleta* during starvation while exposed to 12 treatment combinations comprising four DO saturation and three temperature levels (\pm SE).

	15°C			20°C			25°C		
	SG	Total Lost	n	SG	Total Lost	n	SG	Total Lost	n
100%	-24.4 \pm 9.5	-53.7 \pm 12.1	9	-39.9 \pm 18.9	-69.7 \pm 16.7	9	-18.6 \pm 6.3	-46.3 \pm 12.1	9
70%	-28.0 \pm 20.5	-58.0 \pm 28.0	8	-35.6 \pm 22.7	-65.8 \pm 25.7	9	-29.5 \pm 11.0	-62.5 \pm 14.1	10
50%	-24.4 \pm 11.7	-63.1 \pm 18.1	8	-32.4 \pm 15.5	-62.1 \pm 18.5	9	-34.7 \pm 19.5	-61.4 \pm 19.5	10
20%	-22.7 \pm 8.9	-54.9 \pm 14.2	9	-37.8 \pm 13.6	-64.8 \pm 12.3	9	-28.2 \pm 14.2	-54.1 \pm 17.7	9

Table 4.3

The Q₁₀ values of the specific degrowth rate (% d) of *Capitella teleta* during starvation while exposed to 12 treatment combinations comprising four DO saturation and three temperature levels

	15-20°C	20-25°C	15-25°C
100%	2.67	0.22	0.76
70%	1.62	0.69	1.05
50%	1.76	1.12	1.41
20%	2.77	0.56	1.24

The total weight lost after 4 d of starvation ranged from -16.67 to -95.24% of the initial weight (Figure 4.5). Body size did not have a significant effect on the total lost ($F=0.326$; $p=0.57$), so data were pooled across body sizes for further analysis. The effect of DO was also non-significant ($F=0.729$; $p=0.54$); however, the temperature effect was significant ($F=3.14$; $p<0.05$). Although post-hoc pair-wise tests did not identify any significant differences, 20°C appeared to be different from 15°C and 25°C (Figure 4.6). There was no interaction effect between DO and temperature ($F=0.88$; $p=0.51$).

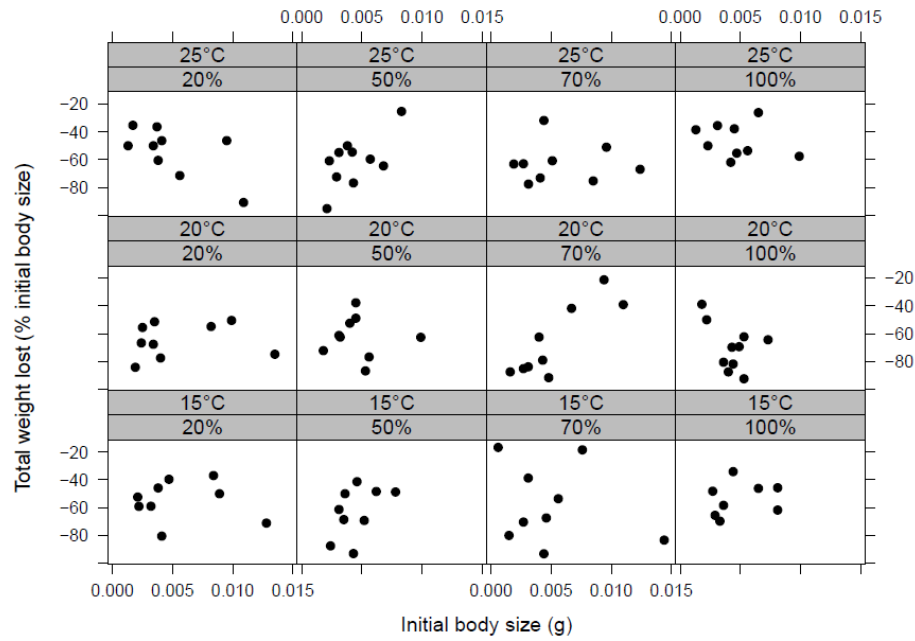


Figure 4.5 Total weight loss (%) based on size of *Capitella teleta* during starvation while exposed to 12 treatment combinations comprising four DO and three temperature levels.

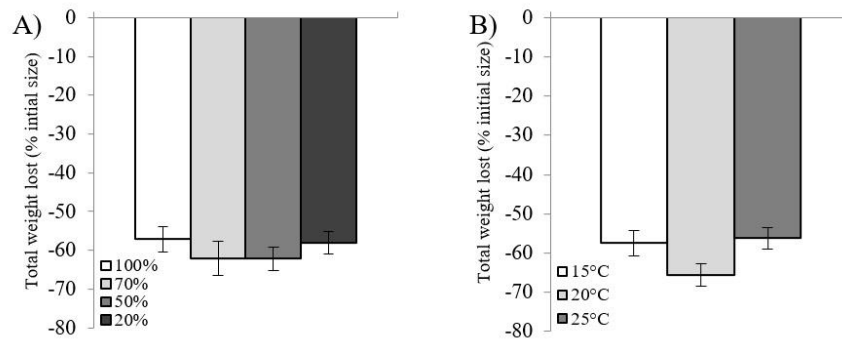


Figure 4.6 Total weight loss (% loss of initial size) of *Capitella teleta* under starvation pooled across (A) four DO saturations and (B) three temperatures (\pm SE).

4.3.2 Daily Weight Loss

Overall, weight loss was significantly greater at all temperatures during the first 24 h, after which loss decreased over the next 48 h; the rate of weight loss again increased between 72 and 96 h ($F = 4.58$; $p < 0.005$) (Figure 4.7A). Daily weight loss appeared faster up to 72 h at 20°C. All temperatures showed similar degrowth rates at 72

h. Overall, temperature effects on degrowth were only marginally significant ($F = 2.56$; $p = 0.08$) (Figure 4.7B). Although there was no significant effect of DO ($F = 0.483$; $p = 0.70$), it is worth noting all small individuals ($n=4$) at 25°C / 20% DO experienced 0% degrowth during the first 24 h, which was not observed in any other size or treatment.

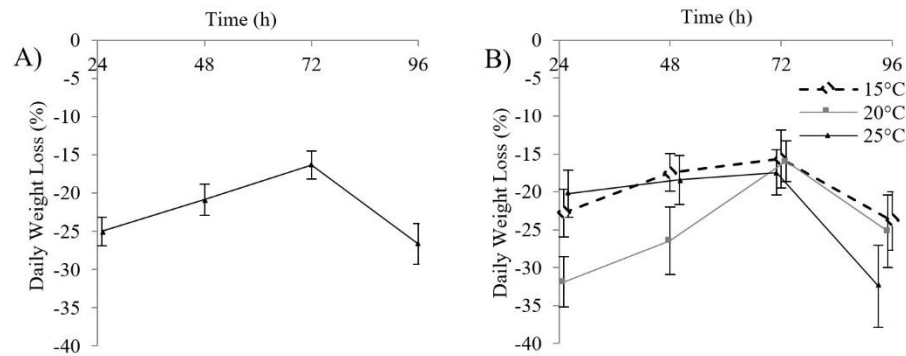


Figure 4.7 Daily weight loss (%) of *Capitella teleta* over 96 h of starvation. Statistical significance was observed for (A) pooled temperature treatments; (B) temperature-specific effects (\pm SE).

4.3.3 Fecal Counts and Egestion Rates

Most subjects continued to produce fecal pellets for 24 h following initiation of starvation, ranging from 0 - 35 pellets (Figure 4.8A). Only 33 of 113 individuals produced 0 pellets. The volume of individual fecal pellets correlated significantly with estimated individual fecal pellet weight (mean $r^2 = 0.74$; $p = 0.049$), indicating that the formation of feces did not change with DO or temperature, which validated the use of the Forbes fecal-pellet weight regression to calculate total sediment egested (Appendix C). The total sediment egested per individual during the starvation experiment was $<140 \mu\text{g d}^{-1}$ for all treatments and body sizes. Total sediment egested per individual during the first 24-hour period of starvation ranged from 0 - $131.86 \mu\text{g d}^{-1}$. One or more individuals failed to egest any sediment for all 12 treatment combinations. The maximum amount of sediment egested during the first 24 h period occurred within the 100% DO and 25°C

treatment combination. Generally, the egestion rate decreased with DO at 15°C, effectively reducing egestion by ½ from 100% to 70% and from 70% to 50% saturation, and suggesting metabolic depression with decreasing DO (Figure 4.8B).

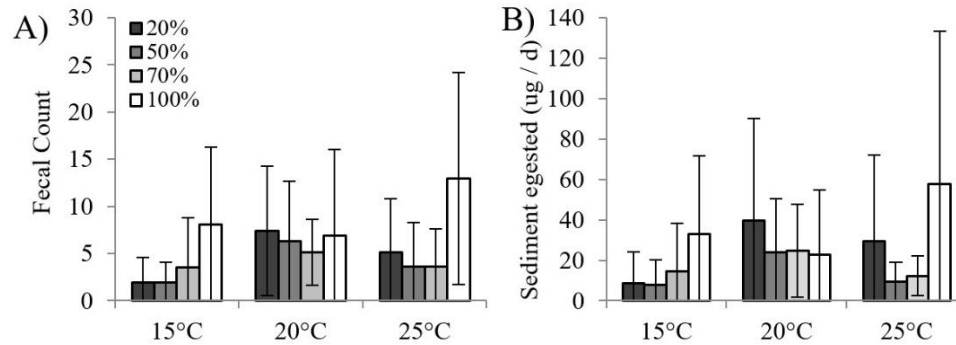


Figure 4.8 The (A) fecal count and corresponding (B) estimated sediment egested by *Capitella teleta* during the first 24 h of starvation under 12 treatment combinations of three temperature and four DO saturation levels (\pm SD).

Interestingly, at warmer treatments of 20°C and 25°C, some of the higher egestion rates were observed at 20% DO; however, mean egestion was still higher at 100% DO and 25°C, whereas egestion remained fairly consistent across DO levels at 20°C. The Q_{10} values for egestion showed very different responses depending on the increment of temperature change. Between 15-20°C, the rate of egestion increased from 0.48 to 20.3 fold as DO decreased (Table 4.4). The Q_{10} values for egestion between 20 and 25°C were lower than for all other treatments, except 100% DO. Similar to the Q_{10} trends in the specific growth rate, the rates of increase for 15-25°C were lower than for the rates of change from 15-20°C.

Table 4.4

The Q_{10} values for the egestion rate ($\mu\text{g d}^{-1}$) of *Capitella teleta* spanning three temperature intervals over four DO saturation levels.

	15-20°C	20-25°C	15-25°C
20%	20.25	0.55	3.35
50%	9.23	0.16	1.20
70%	2.86	0.25	0.84
100%	0.48	6.38	1.75

4.3.4 Body-Size Egestion Relationships

Total sediment egested did not generally relate to body size; however, significant body-size trends in egestion rates for roughly half of the treatment combinations illustrated how body-size responses varied with respect to the treatments (Figure 4.9) (Table 4.5). Egestion by small individuals appeared to decrease with DO at all temperatures, and increased slightly at 25°C (Figure 4.10A). The medium size class showed the highest egestion rate at 70% DO, and egestion subsequently decreased with DO (Figure 4.10B). Lastly, egestion by the large size class also decreased with DO up to hypoxia, where egestion by the large size class increased substantially, and was highest at 20% DO and 20C (Figure 4.10C).

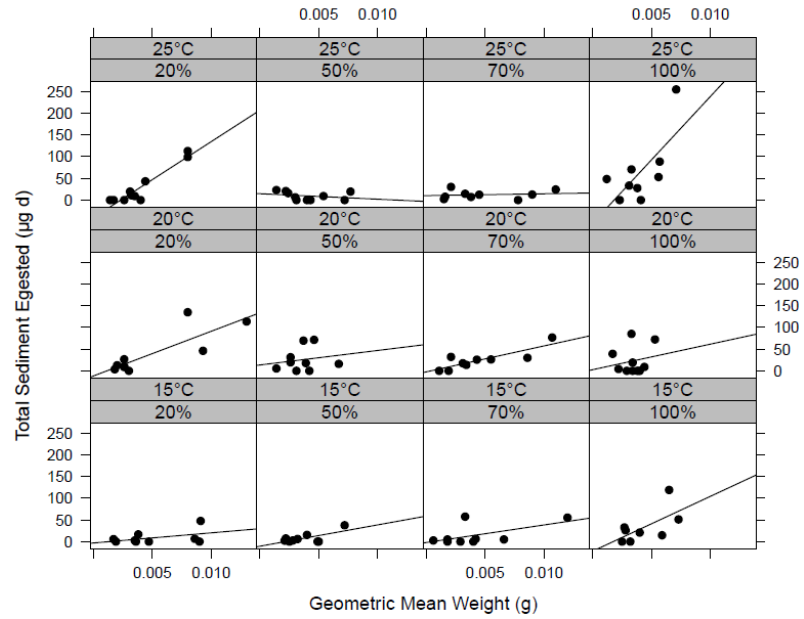


Figure 4.9 Relationships between body size and the total sediment egested (ug) during the first 24 hrs of starvation for *Capitella teleta* exposed to combinations of four DO (100%, =70%, =50%, =20%) and three temperature levels. Body size was calculated as the geometric mean of measurements for initial and 24hr later time points.

Table 4.5

Regressions between the geometric mean body size and sediment egested (ug) during the first 24 h of starvation of *Capitella teleta*. Regressions are fit as: $y = Mx + b$, where y is sediment egested and x is the geometric mean body size. Statistically significant regressions are denoted by *.

15°C						
	M	b	r²	n	F	P
20%	2,468.35 ± 1,760.17	-3.89 ± 10.29	0.22	9	1.97	0.20
50%	4,639.96 ± 1,809.23	-10.54 ± 7.41	0.48	9	6.57	0.04*
70%	3,369.51 ± 1,675.63	-1.73 ± 8.79	0.37	9	4.04	0.08
100%	12, 192.34 ± 6,605.07	-21.90 ± 31.26	0.36	8	3.41	0.11
20°C						
20%	9,995.64 ± 2,574	-11.93 ± 16.20	0.68	9	15.08	0.006*
50%	2,901.47 ± 4,232.77	7.85 ± 15.87	0.05	10	0.47	0.51
70%	6,108.57 ± 1,170.75	-5.98 ± 6.37	0.8	9	27.22	0.001*
100%	2,946.53 ± 7,874.34	7.65 ± 28.19	0.02	10	0.14	0.72
25°C						
20%	13,866.11 ± 1,602.53	-30.77 ± 7.31	0.9	10	75.08	<0.0001*
50%	12.44 ± 6.20	-788.31 ± 1,364.85	0.04	10	0.33	0.58
70%	535.86 ± 889.95	8.98 ± 5.27	0.05	9	0.36	0.57
100%	23,501.48 ± 6259.60	39.94 ± 26.25	0.64	10	14.1	0.006*

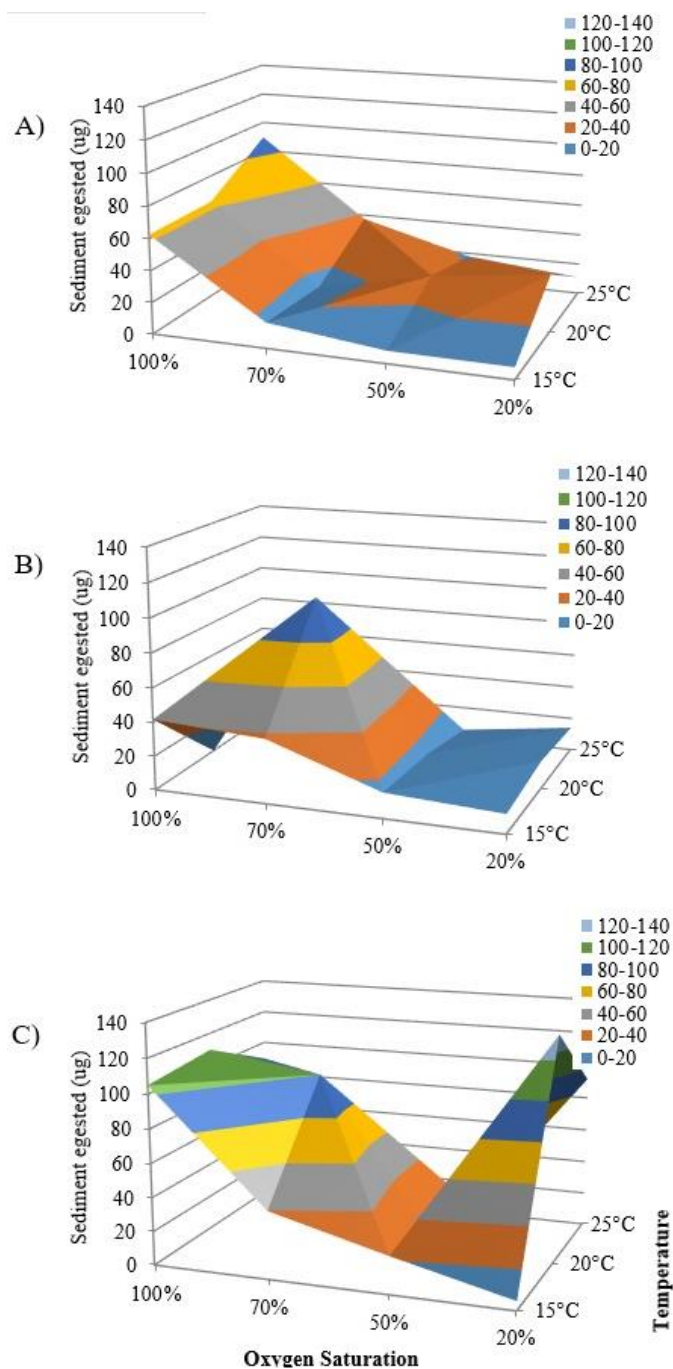


Figure 4.10 Body size trends in the sediment egested by *Capitella teleta* during the first 24 h of starvation at three temperatures and four DO saturations (A) small subjects; (B) medium subjects; and (C) large subjects.

4.3.5 Egestion vs. Degrowth

Overall, total sediment egested did not correspond with daily specific growth during the first 24 hours of starvation (i.e., $r^2 < 0.30$ for most treatments) (Table 4.6; Figure 4.11). However, gross production efficiency (GPE) was significantly less at 50% DO compared to other DO treatments ($F = 3.81$; $p < 0.05$) (Figure 4.12), suggesting more weight loss per μg sediment egested. The 50% DO level showed significantly more loss, $(-3.23 \pm 0.68\%)$ per μg sediment egested compared to the other DO treatments $(-1.29 \pm 0.69\%)$ ($p < 0.001$). There was no apparent effect of temperature on GPE ($F = 1.00$; $p = 0.372$). The initial body size approached significance relative to DO level ($F = 2.71$; $p = 0.053$), suggesting smaller body sizes may be less efficient at low DO; however, allometric power relationships between body size and GPE were non-significant ($r^2 < 0.10$ for all DO levels), as were linear relationships between body size and GPE ($r^2 < 0.3$) (Figure 4.13).

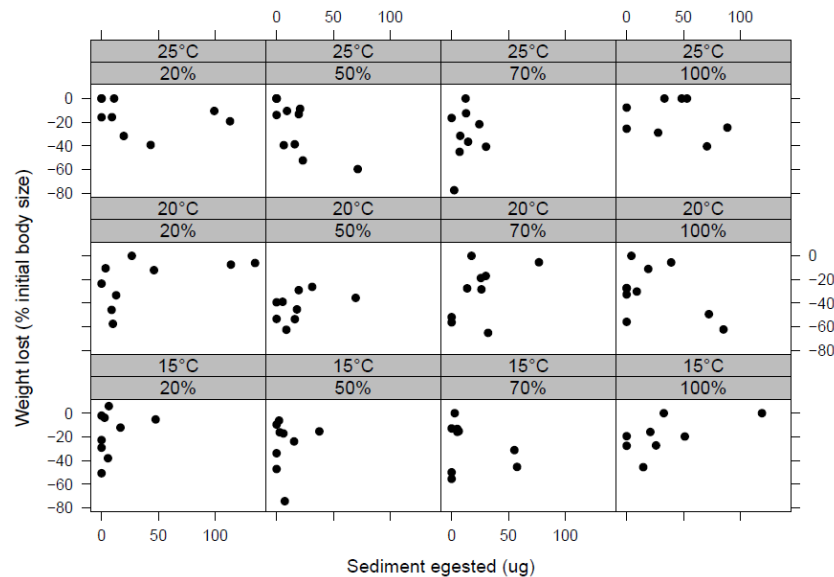


Figure 4.11 Weight loss (%) after 24 h of starvation in relation to total egested sediment (μg) for *Capitella teleta* when exposed to 12 treatment combinations of four dissolved oxygen and three temperature levels.

Table 4.6

Correlations between daily specific growth (%) and total sediment egested (ug) during the first 24 h of starvation for *Capitella teleta*. Statistically significant correlations are denoted by *.

15°C				
	r ²	n	F	P
20%	0.09	9	0.69	0.43
50%	0.06	9	0.42	0.54
70%	0.03	9	0.24	0.64
100%	0.39	8	4.56	0.07
20°C				
20%	0.25	9	2.29	0.17
50%	0.05	10	0.38	0.55
70%	0.22	9	1.94	0.21
100%	0.13	10	1.23	0.30
25°C				
20%	0.48	10	7.28	0.03*
50%	0.26	10	2.83	0.13
70%	0.11	9	0.89	0.38
100%	0.37	10	4.14	0.08

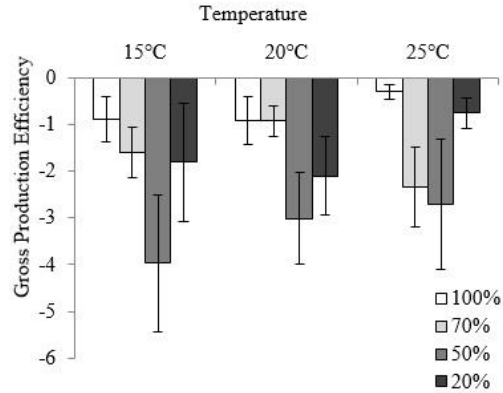


Figure 4.12 The gross production efficiency (GPE) (% weight lost per total µg sediment egested) for *Capitella teleta* after 24 h of starvation when exposed to 12 treatment combinations of four dissolved oxygen saturation and three temperature levels (\pm SE).

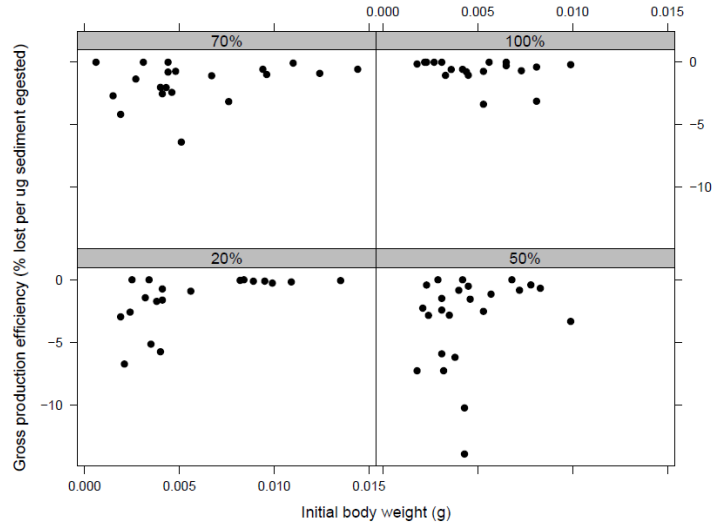


Figure 4.13 Relationship between body size (g) and gross production efficiency (% weight lost per μg sediment egested) of *Capitella teleta* after 24 h of starvation when exposed to four dissolved oxygen saturations (20%, 50%, 70%, and 100%).

4.3.6 Mortality

The highest mortality rate occurred at 25°C and 20% DO, in which 70% of the individuals died after 96 h of starvation (Figure 4.14). The 15°C treatment showed less than 20% mortality over all DO levels. Overall, 70% DO showed the lowest mortality across all temperatures and low DO levels showed higher mortality at higher temperatures. Temperature had less of an effect on mortality at high DO levels.

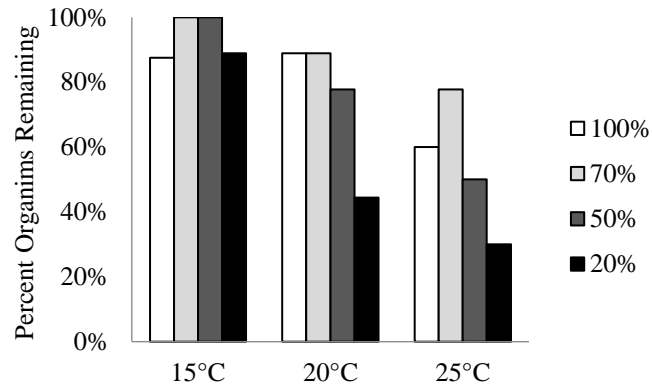


Figure 4.14 Total mortality over four days for *Capitella teleta* under starvation when exposed to combinations of three temperatures (15°C, 20°C, and 25°C) and four dissolved oxygen concentrations (100%, 70%, 50%, and 20%).

Consideration of mortality based on body size revealed larger subjects survived for longer periods than smaller ones (Figure 4.15). The medium size class exhibited complete mortality at 20% DO at 20°C. After 96 hr, all size classes showed 70-80% mortality at 20% DO and 25°C. Most mortality occurred at around 50-60% loss of initial body weight; however, deaths occurred at lower percent losses at 20% DO and higher temperatures (Figure 4.16).

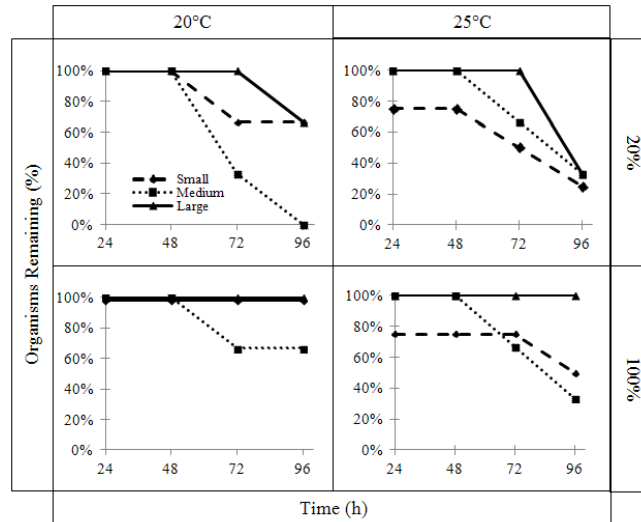


Figure 4.15 The mortality of three body sizes (small= diamond, medium= square, and large= triangle) of *Capitella teleta* after 4d of starvation at two temperatures (20°C and 25°C) and two oxygen saturations (20% and 100%).

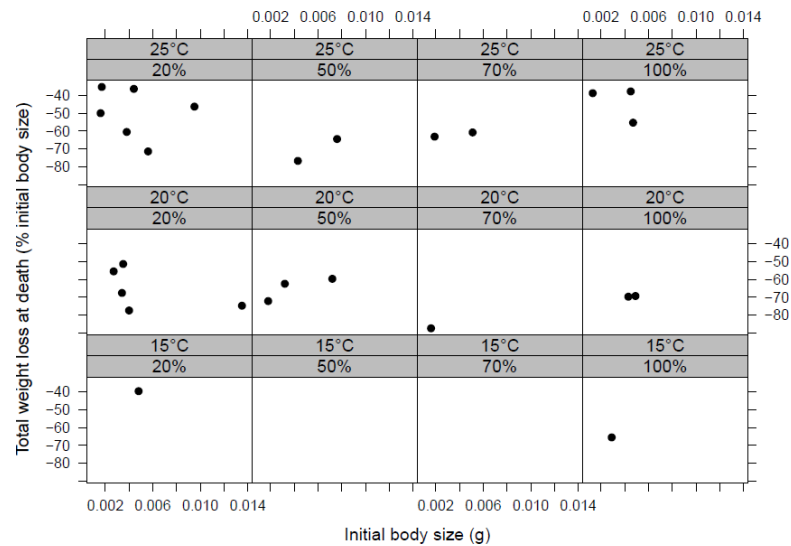


Figure 4.16 Total weight loss at mortality vs. body size for *Capitella teleta* under starvation at combined treatments comprising three temperatures (25°C, 20°C, and 15°C) and four dissolved oxygen saturations (100%, 70%, 50%, and 20%).

4.4 Discussion

Degrowth rates were significantly influenced by temperature with most weight lost occurring in the first 48 h. A reoccurring trend within the degrowth data involved a

biphasic response, involving maximum degrowth at the 20°C treatment. This suggests *C. teleta* may reach its optimum thermal limit between 20-25°C. A similar trend was observed in the aerobic metabolism of the polychaete, *Neanthes japonica*, which showed respiratory Q_{10} values ranging from a 1.5-3.0 fold increase up to 27° C, followed by a Q_{10} of less than 1.0 fold at 30°C (Liu et al. 2009). Survival of *N. japonica* is not possible at 31°C, which is only 4°C higher than the critical threshold. Organisms display oxygen-limited thermal tolerances due to a reduction in its capacity to fulfill the oxygen demand at extreme temperatures (Pörtner 2001). The onset of temperature-dependent aerobic limitation is defined as the pejus temperature, also known as the temperature at which physiological rate processes are maximized. Further increases in temperature are marked by the transition to anaerobic metabolism needed for organisms to survive short-term temperature extremes, also referred to as the critical temperature. The biphasic response observed within this study suggests that the pejus temperature for *C. teleta* under starvation most probably falls between 20-25°C. This interpretation is further confirmed by minimal anaerobic activity occurring at 25°C/ 100% DO (Chapter III). Personal observations have also shown that *C. teleta* cannot survive for 24 h at 30°C, further confirming that the critical temperatures fall within the 25-30°C range.

Temporal patterns of weight loss were similar to Davey-Huggins (2001), who observed that most of the weight loss by *C. teleta* under starvation and normoxia occurred during in the first 48 h. Active egestion was only observed for the first 24 h of this study. However, the fact that most worms visually had 50% or more of their guts filled with sediment for the duration of the experiment suggests decreased activity after 24 h. For normoxic conditions, the decrease in rate of weight loss after the first few days

reflect decreased activity in worms that have been given combusted sediments, including ceased feeding and tube building (Davey-Huggins 2001). Kristensen (1989) observed a decline in the metabolic rate during starvation over a 21 d period for the polychaete, *N. virens*. The presence of food in the gut during the first day likely helped maintain a high metabolic rate due to the biochemical and mechanical demands of specific dynamic action (SDA), which would be rapidly reduced within 2-3 d for *N. virens*. Compared to the opportunistic deposit feeding *C. teleta*, the scavenging *N. virens* most likely can rely on energy reserves lasting for 3-6 d. Without reserves, the SDA for *C. teleta* might decline even faster for *N. virens*. Pamatmat and Findlay (1983) found that heat production as a direct measure of metabolism decreased exponentially for *C. capitata* over a 20 h period of starvation at ambient DO and 20°C. Similarly, the significant decrease in growth after the first 24 h of this experiment was likely associated with a reduction in metabolism. This reduction also likely included some contribution from a depressed SDA, as suggested by reduced egestion after 24 h despite the continued presence of food in the gut. Though not significant, the higher rate of loss at 20°C during the first 24 h suggests elevated metabolic effects with temperature were not observed at 25°C, which is above current natural temperatures for this species. Elevated weight loss after 72 h may have been exacerbated by daily handling of subjects. They did show signs of distress by the fourth day, when more subjects were fleeing their experimental containers.

Although the overall effect of DO on daily weight loss was non-significant, the trend suggests that subjects exposed to 20% DO may have been metabolically depressed sooner within the first 24 h period. Within the first day, fecal counts were reduced to a

mean of 5 (vs. 13 at 100% DO), GPE was minimal ($< -2.0\%$ / μg), and weights of over 20% of the individuals changed negligibly during the first 24 h. Furthermore, mortality was also minimal under hypoxia during this early period of negligible weight loss, and mortality was not substantial until 72 h, as corresponded with notable losses in weight. Metabolic depression is a common physiological mechanism for surviving harsh conditions, especially oxygen limitation. It allows for energetic demands to be met by anaerobic pathways, and ultimately, for better tolerances of marine species (Storey and Storey 1990). The transition to a metabolically depressed state is often achieved through a reduction of physical activities, such as movement, feeding/digestion, and ventilation, and often relies on starvation as a means to reduce energy expenditure. Accordingly, the use of starvation as a coping mechanism during hypoxia may point to an initial benefit under starvation under low DO compared to high DO conditions in which organisms are not stressed. However, while starvation was not initially as detrimental under hypoxia, accelerated rates of degrowth and mortality after 48 h suggest this coping mechanism only works for short-term hypoxia.

Overall, mortality was highest after 96 h of starvation at 20° C and 25° C under 20% DO. Elevated mortality during starvation at low DO may reflect deficits in amino acids necessary for anaerobic respiration. For example, the main anaerobic enzymatic pathway for *C. teleta* (see Chapter III), strombine dehydrogenase, was also shown for the bivalve, *Ostrea chilensis*, by Dunphy et al. (2006). During starvation, *O. chilensis* showed decreased SDH activity over a 16-week period of starvation. This was attributed to a lack of the essential amino acid glycine which is sourced through the diet and needed for the strombine dehydrogenase reaction. Further research is necessary to determine if

starvation of *C. teleta* under hypoxic conditions results in a reduced ability to maintain anaerobic respiration due to reduced amino acid availability.

4.4.1 Conclusion

Increasing temperature often intensifies oxygen limitation due a combination of increasing physiological demand in the face of the decreasing oxygen saturation of overlying waters. These mechanisms suggest that increasing temperature should result in higher critical DO thresholds with warming. Although mortality was greater at high temperatures, the effect of DO on specific and daily degrowth was non-significant. This may reflect that metabolic depression due to starvation nullified the short-term DO physiological response under all DO levels. The availability of food may reveal more direct responses; as high DO levels should sustain an active metabolism. As daily changes in weight varied greatly within treatments, larger sample sizes are likely necessary to properly capture daily trends in degrowth and determine the possibility that hypoxia may initially benefit individuals by ameliorating degrowth for up to 48 h owing to a rapid metabolic depression response.

Lastly, although metabolic depression can greatly extend survival time for organisms with stored energy reserves; because the opportunistic life history *C. teleta* does not entail the allocation of energy to reserves, this species may not be able to survive starvation for very long compared to equilibrium species. Davey- Huggins (2001) observed that *C. teleta* survived starvation for 18 days at 100% DO/ 22°C, while maintaining the ability to recover from degrowth. Further research is needed to determine the ability of *C. teleta* to survive starvation under chronic exposure, how recovery from

starvation may differ relative to multiple stressors, and how responses observed in this study compare with those to additional stressors, such as pH.

CHAPTER V GROWTH, EGESTION, AND MORTALITY OF A MODEL
TOLERANT POLYCHAETE, *CAPITELLA TELETA*, TO VARYING
LEVELS OF DISSOLVED OXYGEN, TEMPERATURE,
AND BODY SIZE

5.1 Introduction

Although there is a strong consensus within the scientific community that coastal systems are threatened by anthropogenic climate change, only 2.2% of all climate change studies test for non-independent effects of more than one stressor variable directly related to climate change (Field 2014, Harley et al. 2006, Levin 2003). The dissolved oxygen (DO) levels of the ocean are currently affected by both global warming and eutrophication (Levin 2003). Sea surface temperature is also predicted to increase up to 4.8°C by 2100, subsequently causing an additional 4-7% decline in oceanic oxygen levels (Matear et al 2000). In addition, the occurrence of existing hypoxic zones is expected to increase in frequency, duration, and severity in conjunction with temperature increases up to 2°C by 2035 (Field 2014, Justic et al. 2007, Matear and Hirst 2003, Diaz & Rosenberg 2008, Justic et al. 1996). Understanding how marine organisms will respond to concurrently increasing temperature and DO stress cannot be fully comprehended by independently examining effects of these stressors. Environmental factors frequently interact to elicit complex nonlinear responses due to opposing trade-off effects. For example, low DO can affect the energy budget of an individual through behavioral effects, elevated anaerobic respiration, and metabolic depression, all of which can also increase sensitivity to other stressors and reduce the capacity for growth and/or ultimately cause mortality (Burnett and Sickle 2001, Forbes 1989). Conversely, temperature often

elicits results a bi-phasic metabolic response (Pörtner 2001), involving increasing physiological rates with temperature up to a critical threshold, marked by protein damage, increased membrane fluidity, and failure in organ function (Harley et al. 2006).

Understanding interactions between temperature and DO stressors can be especially important for marine organisms like deposit feeding polychaetes, which must allocate time between feeding and respiration when faced with low oxygen availability.

Polychaetes employ a wide range of feeding modes, including deposit feeding, as represented by species within 50 of the 78 polychaete families (Cammen 1987). Deposit feeding species feed on surface or buried particles, including organic matter, mineral grains, fecal pellets, microalgae, meiofauna, and detrital particles. Many studies have shown that deposit feeding worms allocate time and energy costs between feeding and ventilation of their burrows, with feeding occurring between ventilation intervals (Forbes 1989, Grassle and Grassle 1976, Forbes and Lopez 1990). As Forbes and Lopez (1990) suggest ‘the tradeoff between efficient metabolism and food intake may be especially important in infauna that must partition time between feeding and respiratory activities’. The literature suggests that deposit feeding diminishes with declining DO, and ceases when the hypoxia (2.0 mg/L) is reached (Forbes 1989, Sagasti et al. 2001); however, no studies critically examine whether feeding actually ceases under hypoxia, or if there is an allometric trend in terms of the critical DO where feeding ceases. Furthermore, little is known about how deposit feeding organisms respond to elevated metabolic demands at higher temperatures, while simultaneously dealing with metabolic depression due to reduced DO levels. Metabolic depression is a response to environmental stress allowing

an organism to survive on minimal resources by reducing the basal metabolic rate (Guppy 2004, Storey & Storey 1990).

The overall objective of this study is to examine the influence of temperature and DO stress on the growth, egestion, and mortality of a model tolerant, deposit-feeding polychaete, *Capitella teleta* across a range of body sizes. I hypothesize all worms will exhibit reduced growth rates under DO stress due to depressed metabolic rates. I also propose that both small and large individuals will be metabolically taxed to the point of hindered growth rates at high temperatures. Under low DO and high temperatures, I further hypothesize that positive growth rates will be absent due to reduced feeding as a result of low DO level and increased metabolic demands as a result of high temperatures.

5.2 Materials and Methods

5.2.1 Model Species

The polychaete species *C. teleta* (previously identified as *Capitella* sp. I) is an opportunistic species often associated with disturbed and eutrophic habitats (Blake et al., 2009). The small head-down deposit-feeding polychaete ranges in size from 20 to 40 mm (3-12 mg) (Grassle and Grassle 1976), and lives within mucus-lined burrows while feeding on surface and near-surface sediments (Levin 1984). Factors that can influence the ingestion rate of *C. teleta* include percent organic matter within sediments (Forbes et al. 1994, Ramskov and Forbes 2008) and sediment particle size (Taghon 1989, Horng and Taghon 1999). Commonly occurring in the northeastern United States, Japan and the Mediterranean, *C. teleta* has been described as the most opportunistic capitellid sibling species with the most rapid individual growth ($>20\% \text{ d}^{-1}$), short generation times (37-50 d at 15°C), and multiple broods per year allowing for explosive population growth (104

m²) (Grassle and Grassle 1974, Blake et al. 2009). *Capitella teleta* has red blood cells with a moderate oxygen affinity ($P_{50} = 6.88 \pm 0.97$) and high cooperativity ($n_{50} 2.89 \pm 0.82$) owing to tolerance to hypoxic conditions (Magnum et al. 1992). However, increasing temperatures reduce oxygen affinity and cooperativity suggesting possible reduced tolerance at higher temperatures (Barclay 2013, Wells et al. 1980). In Chapter III, I determined *C. teleta* relies heavily on anaerobic respiration during low DO and high temperature scenarios with the majority of available possible energy coming from the opine dehydrogenase pathway.

5.2.2 Culture Maintenance

Stock cultures of *C. teleta* were obtained from Dr. Judy Grassle of Rutgers University and reared at 15°C and 27 ppt (artificial seawater). Groups of ~50 polychaetes were maintained in 11 cm culture dishes with 15-30 mL of enriched sediment. Sediment was collected from Halstead Bayou in Ocean Springs, MS, passed through a 1 mm sieve and frozen in 30 mL plastic, food safe containers. Before using for worms, sediment was thawed and Tetramin© fish flakes added at a ratio of 2.5 g of flake to 54 g of mud. Cultures were cleaned every two weeks by replacing the sediment and water.

5.2.3 Experimental Treatments

In an attempt to standardize the effect of temperature on DO concentrations in water, experimental DO treatments were classified into four oxygen saturation treatments (20%, 50%, 70%, and 100%) and fully crossed with three temperatures (15°C, 20°C, and 25°C) (Table 5.1) (Figure 5.1). For all experiments, salinity was held constant at 27 ppt. Polychaetes were initially assigned to one of three size categories: small (<0.003g), medium (0.003-0.005g), and large (≥ 0.005 g), and ultimately indexed by their actual sizes

for some analyses. The experimental flow-through system comprised four sections, each of which was designated to one DO treatment, which was further split into three temperature levels replicated three-fold into nine sampling chambers (Figure 5.2). The nine sampling chambers further represented the three body sizes, thus yielding a sample size of three for each of the 36 body-size (3) by DO (4) by temperature (3) treatment combinations.

Table 5.1

Mean experimental temperature (°C) and DO levels (mg/L) for the 5 d growth experiment (\pm SE).

Temperature (°C)	Oxygen Saturation (%)	Dissolved Oxygen (mg/L)
17.1 \pm 0.7	20	2.51 \pm 0.5
17.5 \pm 0.9	50	4.57 \pm 0.6
16.8 \pm 0.5	70	5.59 \pm 0.5
17.6 \pm 0.7	100	7.98 \pm 0.5
21.1 \pm 0.6	20	2.41 \pm 0.5
20.8 \pm 2.1	50	4.03 \pm 0.6
20.9 \pm 0.8	70	5.47 \pm 0.6
21.1 \pm 0.8	100	7.23 \pm 0.6
24.8 \pm 1.1	20	2.55 \pm 0.3
24.6 \pm 0.9	50	4.10 \pm 0.2
22. 2 \pm 2.9	70	5.36 \pm 0.5
24.3 \pm 0.4	100	6.77 \pm 0.3

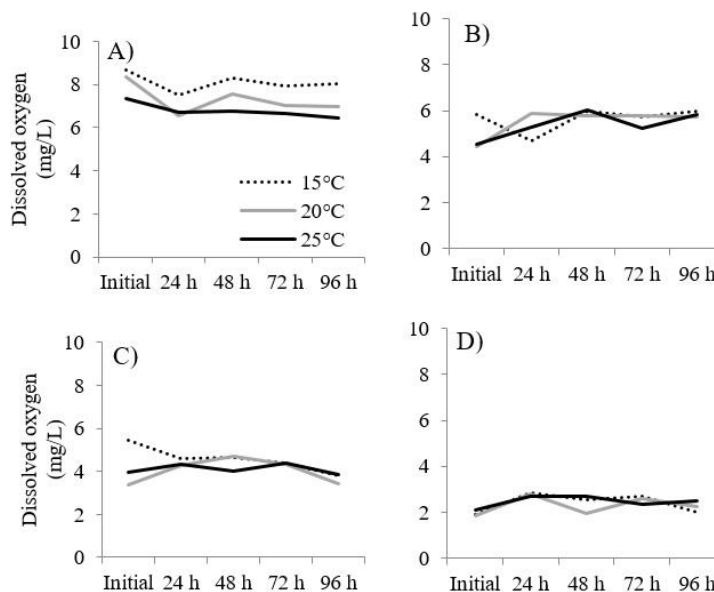


Figure 5.1 Variation in DO (mg/L) over 5 days for growth experiments at three temperature and four dissolved oxygen saturation levels (A = 100%, B = 70%, C = 50%, and D = 20%).

5.2.4 Regulation of Treatment Conditions and Flow-through System

Regulation of treatment conditions and the flow-through system were identical to the starvation experiments. See Chapter VI for details.

5.2.5 Growth Experiments

Polychaetes were initially measured and allocated to size categories before assigning them to DO/ temperature treatments. Subjects were allowed to acclimate for 12-24 h to the DO/temperature treatment with 2 ml of enriched mud to ensure worms were given unlimited food. Based on culturing instructions (Appendix A), 50 worms were kept in 30 mL of mud for 2 weeks. This was scaled down to give one worm ~ 5 mL mud for 1 day. Following the initial weight measurement, worms were subsequently weighed to the nearest 0.00001 mg on a microscale each day of the 4 d experiment. Subjects were blotted on the side of a plastic measuring dish in order to reduce excess

moisture. Wet weight measurements of capitellids have been shown to be reproducible to $\leq 5\%$ (Cammen 1985). Subjects were out of the sampling chamber for less than 5 minutes and always kept under treatment conditions during weighing. Missing or dead subjects were replaced during the first two days. Worms were only counted as dead when a body was present, otherwise they were noted to be missing. Less than 15% of worms were dead or missing during the 4 d period. Any damage to the worm during handling was noted for future reference. On the fourth day, subjects were measured and preserved in 5% formalin.

5.2.6 Growth Data Analysis

Wet-weight specific growth rate was calculated as $G (\%d^{-1}) = [LN (\text{final wet-weight}) - LN (\text{initial wet weight}) / \text{time (days)}] * 100$. The gross production efficiency (GPE) was used as an indicator of assimilation and estimated as the change in worm weight over the experimental duration normalized by the total amount of sediment egested over the experimental period (Forbes et al. 1994).

Specific growth rate was calculated as $G (\% d) = [LN (\text{final wet-weight}) - LN (\text{initial wet-weight}) / \text{time}] * 100$. The specific growth rate was calculated for the period starting from the initial wet weight to either (a) the final wet-weight when the experiment ended (day 4) or (b) the final wet-weight before individual died. Only individuals having at least two weight measurements (survived past 24 h) were included in the specific growth analysis to ensure that worms were responding to desired treatments and not extraneous factors (i.e. unknown damage before experiment began). Only two worms were excluded from the specific growth analysis due to having died within the first 24 h. Overall growth was analyzed using raw data with a 3-way ANOVA with DO ($n = 4$),

temperature ($n = 3$), and body size ($n = 3$) as fixed factors, and all possible interaction effects. Body size was accorded three levels (small, medium, and large), based on the initial body size categories. The ANOVA was reduced as a 2-way ANOVA when temperature was deemed to be non-significant as a main effect or in any interaction term.

Daily growth was calculated as the % weight gained or lost each day from the previous daily measurement. Analysis of daily growth was conducted using a mixed model ANOVA on raw data, with DO and temperature as fixed factors, body size as a covariate, and time as a repeated measure. Mixed model was used in order to include a repeated measures analysis (i.e., time as subject factor) while also retaining the data for subjects that did not survive the entire 96 h experiment, which would have been excluded using traditional methods. The covariate did not have interactions with any of the fixed factors (temperature interaction $p = 0.34$, DO interaction $p = 0.66$, and day interaction $p = 0.42$). Analysis was conducted using the autoregressive first order covariance structure (AR1 diagonal p -value = <0.0001 , AR1 rho. p -value = 0.035). The Shapiro-Wilk test (W (Razalia and Wah 2011) was used in conjunction with Q-Q plots to test normality of daily growth data. In 3 out of 12 cases (at 70% DO, 25°C, and day 4) W showed that normality was not met (W statistic ranges from 0-1, with $W = 1$ being normal); however, all treatment levels in this study showed $W > 0.96$ (Appendix E). Thus, the mixed model analysis was used based on these high W values and visual confirmation of normality through Q-Q plots.

5.2.7 Egestion Analysis

The top 0.5 mm of the sediment layer was removed from the worm containers every day before recovering the subject for measurement. This sediment was fixed in 5%

formalin until feces could be counted. Counts were made by spreading the sediment on a gridded petri dish and removing individual pellets with a pipette. Count extrapolation from split samples was not attempted due to the tendency of feces to clump within mucous excretions. To account for changes in time between collections, fecal pellet production rates (pellets per hr.) were scaled up to daily fecal pellet production rates (pellets per d). The weight of individual pellet was estimated using a known correlation with worm volume described for *C. tellata* by Forbes (1989), which was modified to worm weight:

$$\text{Individual worm weight (g)} = 0.002 \times \text{volume (mm}^3\text{)}$$

$$(n=81; r^2= 0.84; \text{personal observation})$$

$$\text{Individual fecal pellet weight (}\mu\text{g)} = 707.6 \times \text{worm weight (g)} + 0.357$$

$$(n=15; r^2= 0.98; \text{Forbes 1989}).$$

Personal observations on fecal volume were determined through photographic analysis using MetaVue Version 7.1.7.0 software and a Nikon SMZ 1500 camera. A maximum of 10 fecal pellets per individual were measured from 84 worms over the full range of body sizes. Fecal weights were collected from organisms at 20°C and 100% DO. Fecal volumes were estimated using the equation: $\text{Volume} = \Pi (\text{projected area})^2/4 (\text{length})$ (Davey-Huggins 2001, Forbes 1989, Forbes and Lopez 1990, Forbes et al. 1994).

Sediment egested ($\mu\text{g d}^{-1}$) was calculated by multiplying the daily fecal pellet production by the estimated weight of an individual fecal pellet for each individual based on its size to pellet weight estimate. Allometric trends were examined based on the geometric mean of the weight on the day of collection and that from the previous day for each individual. In order to reduce physical stress and minimize the time out of the

experimental chamber, worms were not subjected to daily counts of fecal pellets within the digestive tract. Further, studies have shown fecal weight is dependent on the size of the worm (Forbes 1989). As such, it was assumed that the weight and number of pellets inside the gut remained constant from day to day and depended on the weight of the organism during that day. Daily egestion was analyzed using a mixed model analysis with fixed factors of temperature, DO, time, size category, and all possible interactions. Time was modeled as a repeated measure and within subject factor. Size categories were based on the geometric mean between the days surrounding the egestion measurement and further broken into small and large body sizes categories based on size breaks estimated in Chapter II. Analysis was conducted using the autoregressive first order covariance structure (AR1 diagn. p-value = <0.0001 and AR1 rho. p-value = 0.052).

Egestion was further examined through the gross production efficiency (GPE) which is defined as the change in worm volume over the experimental duration normalized by the total sediment egested over the experimental period (Forbes et al., 1994). This analysis will give insight into the assimilation efficiency of the polychaetes. Egestion capacity will also be examined, where $\text{capacity} = \text{Egestion}_{\text{DOx}} / \text{Egestion}_{(100\%)}$; where $\text{Egestion}_{\text{DOx}}$ is the mean egestion at DO treatment X and $\text{Egestion}_{(100\%)}$ is the mean egestion at 100% DO for any given body size x temperature treatment. Lastly, the Q10 values for egestion were calculated as $Q_{10} = (R_2/R_1)^{10/(T_2-T_1)}$; where R_1 and R_2 are the rates of egestion at temperatures T_1 and T_2 , respectively. The egestion capacity, or the change of egestion rate over time, was estimated for each body size and each treatment combination as the ratio: $\text{egestion capacity} = \text{mean sediment egested on hour 96} / \text{mean sediment egested on hour 24}$.

5.3 Results

5.3.1 Growth Rates

5.3.1.1 Specific Growth Rates

Overall, specific growth rates of individuals ranged from -50.58 to 30.76% d across all treatments. There was a significant interaction between DO and body size ($F = 2.49$; $p < 0.05$) (Figure 5.3). Medium and large size classes maintained minimal negative growth rates across DO levels. Conversely, small body sizes maintained positive or near positive growth rates at low DO; and growth dropped to -9.48 % d at 100% DO (Table 5.2). Although the growth rate became less negative with temperature, there was no significant difference among treatments ($F = 0.271$; $p = 0.76$) (Figure 5.4).

Table 5.2

Mean specific growth rates (% d) of *Capitella teleta* under four dissolved (\pm SE).

	100%	70%	50%	20%
Small	-6.41 \pm 15.20	2.12 \pm 4.33	-2.93 \pm 10.57	6.79 \pm 9.40
Medium	2.09 \pm 8.33	-5.87 \pm 10.52	-10.46 \pm 10.78	-6.87 \pm 11.84
Large	-11.95 \pm 9.11	-16.48 \pm 5.48	- 9.46 \pm 10.82	-15.67 \pm 11.02

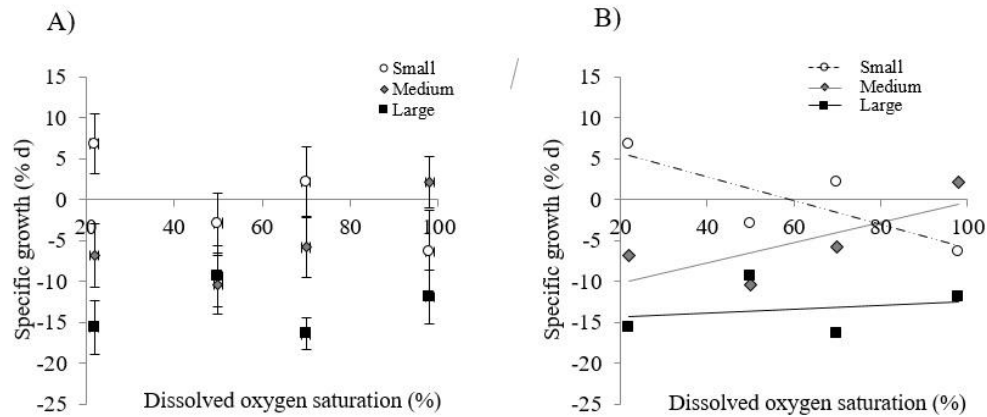


Figure 5.2 Specific growth rates for three body size classes of *Capitella teleta* under four dissolved oxygen saturations (20%, 50%, 70%, and 100%). (A) mean \pm SE; (B) body size trend lines.

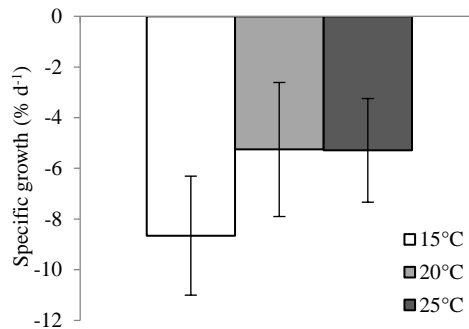


Figure 5.3 Specific growth rates of *Capitella teleta* exposed to three temperatures (\pm SE).

Because temperature the temperature effect on specific growth rate was non-significant, data were pooled across temperature levels to strengthen the DO interpretation. At 20% and 70% DO, the specific growth rate was moderately correlated with the initial body size ($r^2 > 0.4$), in that smaller initial sizes showed higher specific growth rates (Figure 5.5; Table 5.3). Similar but non-significant body size trends in specific growth were also apparent for the other two DO exposure levels (Figure 5.5).

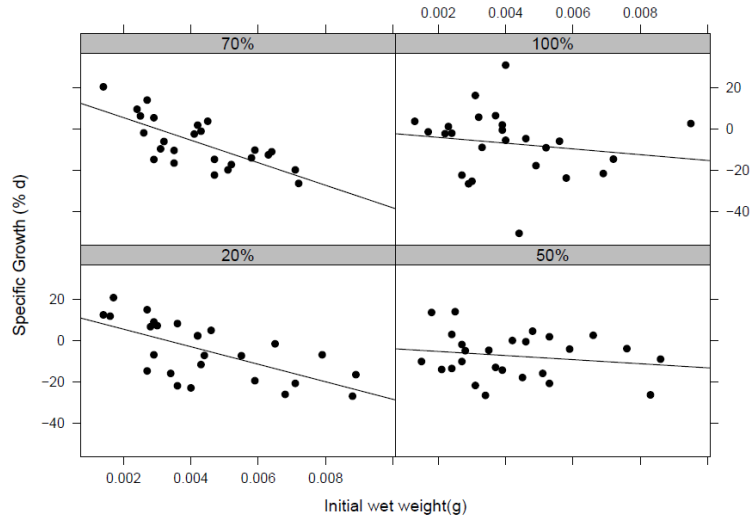


Figure 5.4 Relationships between the initial wet weight (g) and specific growth rate (% d) of *Capitella teleta* at four dissolved oxygen saturations.

Table 5.3

Linear regressions between the initial wet weight (g) and specific growth rate (% d) for *Capitella teleta* at four dissolved oxygen saturations. Relationships are in linear form: $y = Mx + b$ where y = specific growth and x = initial wet weight.

Dissolved Oxygen	M	b	r ²	n	F	p-value
20%	-4237.7	13.96	0.42	26	17.25	<0.001
50%	-990.7	-3.29	0.05	27	1.39	0.25
70%	-5452.3	16.27	0.52	28	24.58	<0.0001
100%	-3369.3	6.51	0.06	23	1.44	0.24

5.3.1.2 Daily Percent Growth

Total daily growth of individuals ranged from -62.3 to 69.2%. There was a significant interaction between DO and time, reflecting a decrease in % growth to negative rates at lower DO levels during the first 48 h, while positive % growth was maintained at high DO levels ($F=2.46$; $p<0.01$) (Figure 5.6). Mean % growth returned to

negative values for all treatments by 72 h. There was no significant effect of temperature ($F=0.33$; $p=0.72$) or body size ($F=0.20$; $p=0.65$) on total % daily growth.

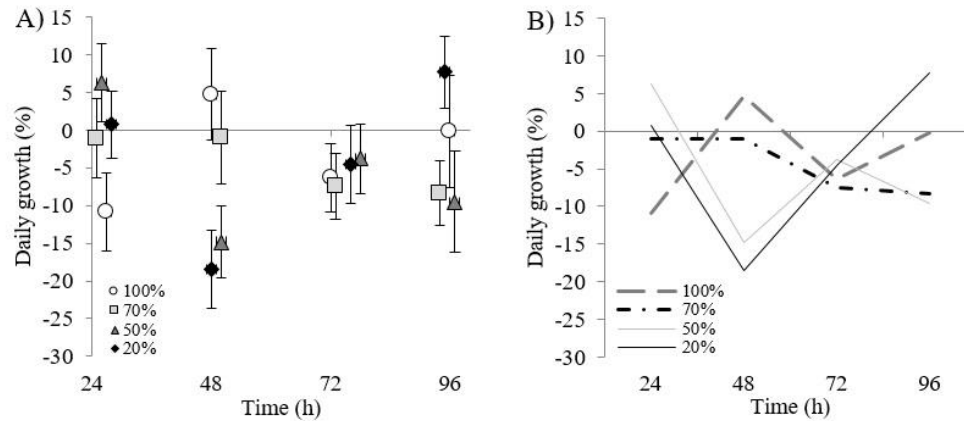


Figure 5.5 Daily growth (%) of *Capitella teleta* exposed to four dissolved oxygen saturations (20%, 50%, 70%, and 100%) for four days. (A) mean \pm SE; (B) mean DO % growth trend lines.

5.3.2 Egestion Rates

Egestion rates of individuals ranged from 0.00 to 5,077.67 $\mu\text{g d}$ (Figure 5.7). The interaction between DO, temperature, and day was significant for egestion rates ($F = 3.86$; $p < 0.001$). For the low DO treatments, egestion rate increased with temperature, as shown by Q_{10} values of ~ 1.5 fold for 50% DO and ~ 3 fold for 20% DO (Figure 5.8); however, egestion rate decreased over time for all low DO treatments, resulting in an overall egestion capacity of < 1 for all DO treatments (Figure 5.9). The 50% DO treatment exhibited an increasing egestion capacity with temperature; whereas the 70% DO treatment exhibited little change in egestion with temperature. However, egestion capacity decreased by 50- 60% with temperature for most DO treatments. Interestingly, the 100% DO treatment showed apparent detrimental effects of early oxygen super-saturation, including mortality and almost no egestion during the first 24 hr of the

experiment, which skewed ratios. This was especially apparent at 15°C, where egestion rates at 100 % DO were comparable to hypoxic (20% DO) treatments. Egestion capacities were mostly high at 100% DO due to minimal feeding during the first 24 h.

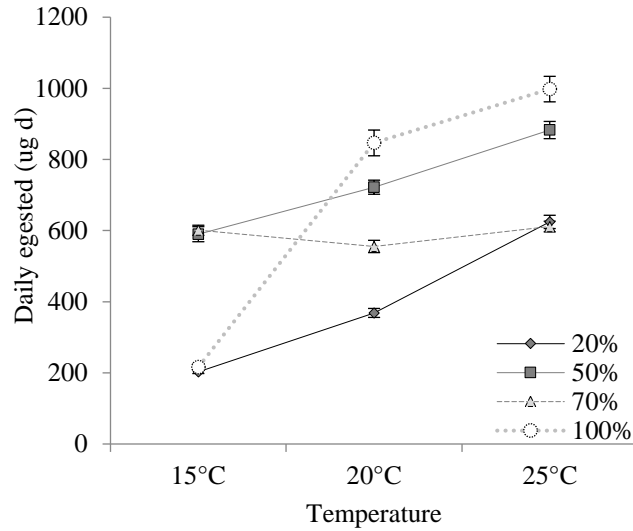


Figure 5.6 The mean daily egestion rate ($\mu\text{g d}^{-1}$) of *Capitella teleta* under four dissolved oxygen saturation and three temperature levels (\pm SE).

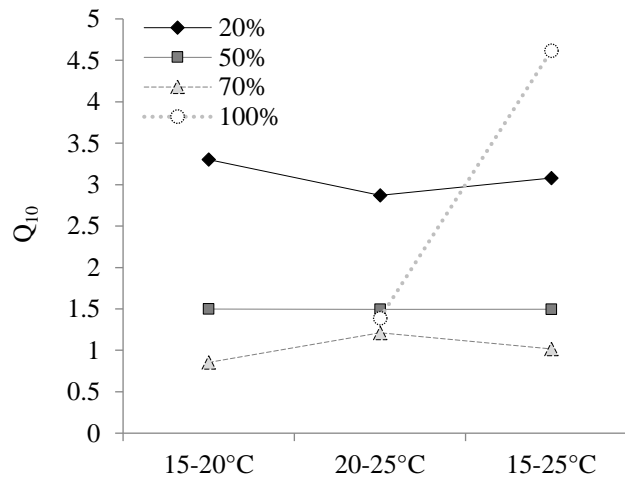


Figure 5.7 The Q_{10} value of the mean daily egestion rate ($\mu\text{g d}^{-1}$) of *Capitella teleta* under four dissolved oxygen saturations (A=20%, B=50%, C=70%, D=100%) crossed with three temperatures. The 15-20°C 100% DO is missing due to supersaturated conditions resulting in no feeding and high mortality ($Q_{10}=15.3$).

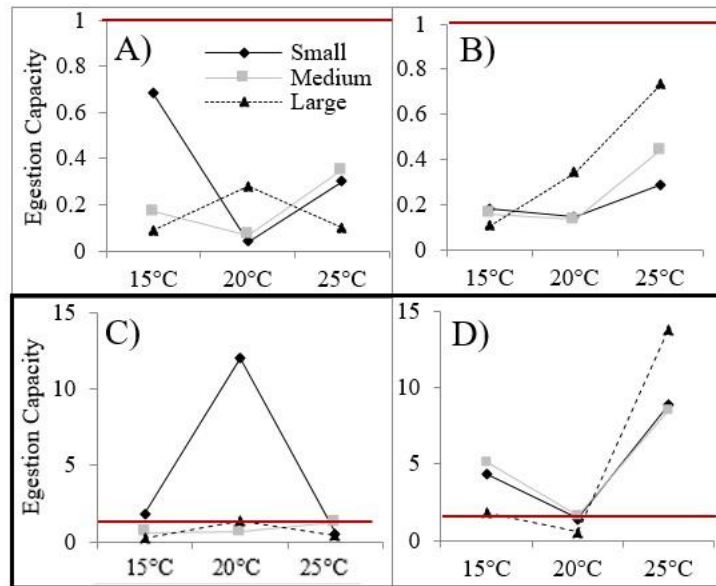


Figure 5.8 The egestion rate capacity of *Capitella teleta* at 24 and 96 hours under four dissolved oxygen saturations crossed with three temperatures. (A) 20% DO; (B) 50% DO; (C) 70% DO; (D) 100% DO. The 70% and 100% treatments (bold box) have a different Y-axis relative to lower DO treatments. Red lines mark a ratio of 1, or no change in egestion.

A three-way interaction was significant for egestion between DO, day, and temperature ($F = 4.13$, $p < 0.0001$) and DO, day, and size ($F = 2.26$, $p = 0.04$). The four-way interaction was not significant ($F = 1.58$, $p = 0.07$). In the first interaction, all temperatures saw a decrease in egestion under 20% DO by day 4, while only 15°C and 20°C appear to be significantly different (Figure 5.10). The same temperatures also appear to see a reduction in feeding by the 4th day under 50% DO, while 25°C does not see any change. Under high DO saturations, no temperature appeared to significantly change over time, except for 100% which observed an anomaly during the first 24 hr. Concerning the second interaction, larger worms had higher egestion rates overall; however, only certain circumstances appear to be statistically significant (Figure 5.11). Particularly days 2 and 3 appear to show the greatest differences at all temperatures

between the two body sizes. At 15°C and 20°C, egestion rates was more affected by body size as shown by high allometric scaling exponents suggesting a 1.5 – 2x increase in egestion rate as body size increases, particularly during the first 24 hr. (Table 5.4).

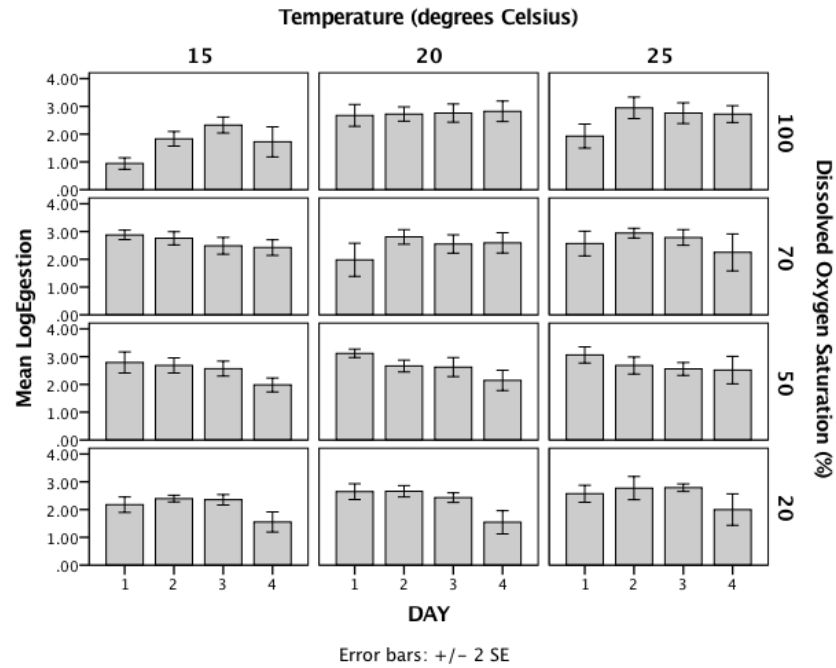


Figure 5.9 Log transformed-egestion ($\mu\text{g d}^{-1}$) of *Capitella teleta* over four days under three temperatures and four dissolved oxygen saturations.

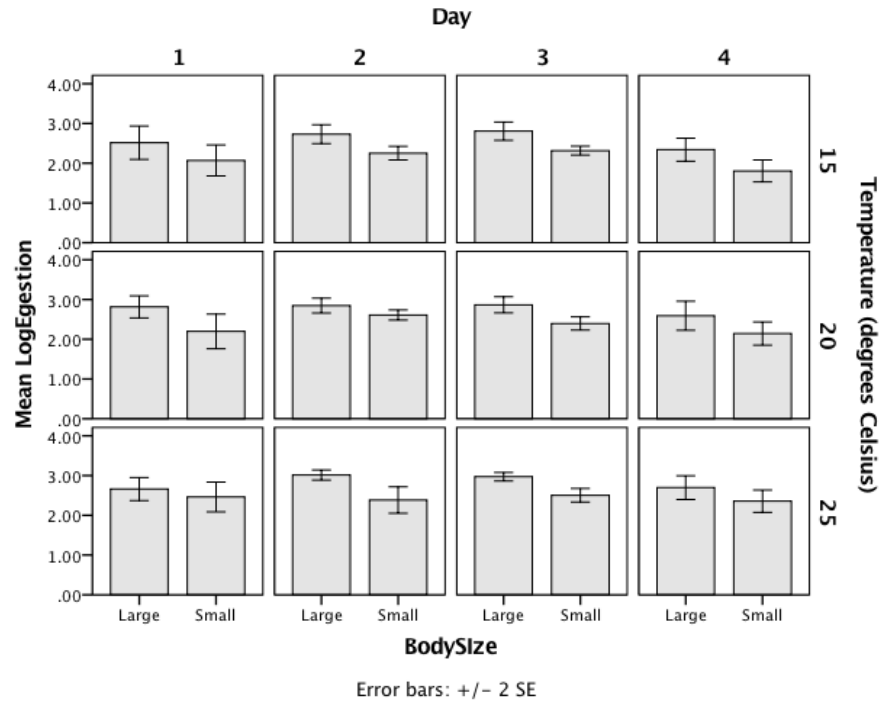


Figure 5.10 Log transformed-egestion ($\mu\text{g d}^{-1}$) of *Capitella teleta* over four days under three temperatures and two body sizes (small ≤ 0.003 , large > 0.003).

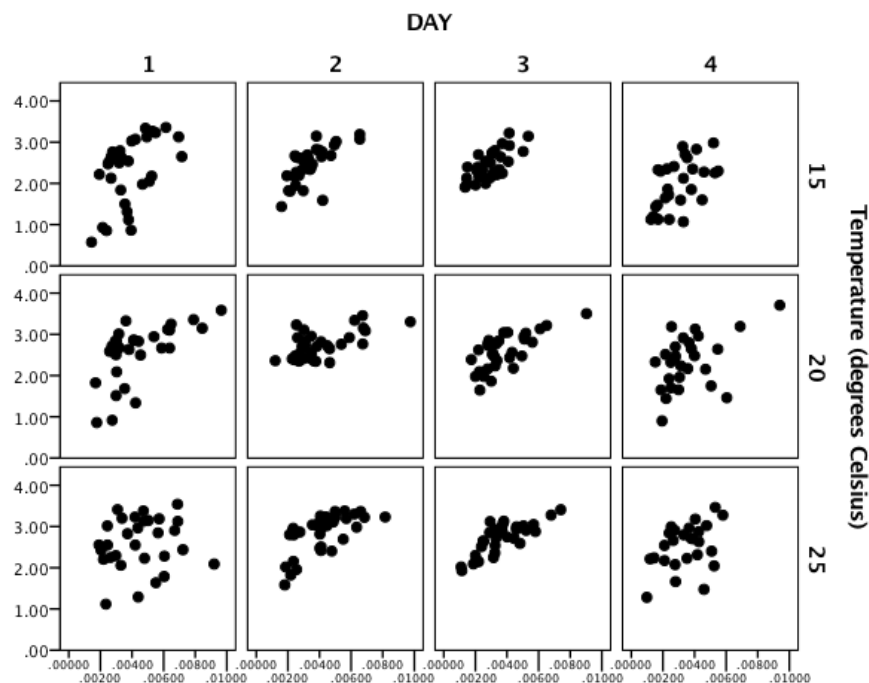


Figure 5.11 Relationships between the body size (g) and log-transformed egestion rate ($\mu\text{g d}^{-1}$) for *Capitella teleta* when exposed to three temperatures (i.e., pooled over 4 DO levels) over four days.

Table 5.4

Allometric relationships between body size (g) and egestion rate ($\mu\text{g d}^{-1}$) for *Capitella teleta* across three temperatures (i.e., pooled over 4 DO levels) spanning four days.

Regressions in the form: $y = aX^b$ where y = egestion rate ($\mu\text{g d}^{-1}$) and X = wet weight (g).

	15°C					20°C					25°C				
Time (h)	a	b	r ²	n	p	a	b	r ²	n	p	a	b	r ²	n	p
24	1.0E+09	2.77	0.32	31	<0.001	3.0E+08	2.46	0.56	29	<0.001	6.9E+03	0.53	0.05	31	0.24
48	1.0E+08	2.24	0.59	31	<0.001	2.3E+05	1.08	0.37	31	0.001	2.0E+07	1.87	0.46	34	<0.001
72	2.0E+06	1.53	0.36	31	0.004	1.0E+07	1.83	0.69	32	<0.001	6.0E+06	1.64	0.54	33	<0.001
94	4.0E+06	1.81	0.17	28	0.08	3.0E+06	1.65	0.41	28	<0.001	3.9E+05	1.23	0.20	28	0.01

5.3.3 Gross Production Efficiency

The mean gross production efficiency (GPE), change in daily volume normalized to amount egestion, for individuals across all treatments ranged from -63.19 to 50.37 % growth/ μg egested (Figure 5.13). Overall, the 100% DO at 15°C treatment exhibited the greatest loss of weight per μg egested, averaging -14.62% / μg ; however, this is also the DO treatment that showed anomalies (high mortality rates and little to no in egestion during the first 24-48 hrs of the experiment. All other treatments mean ~ -1 to -6 % / μg . Interestingly, near zero GPE values occurred across the entire range of growth rates. There were no strong trends in GPE over time or relative to body size; however, smaller body sizes displayed greater variability in GPE (Figure 5.14). The 50% DO treatment showed the lowest occurrence of positive GPE compared to all other DO treatments.

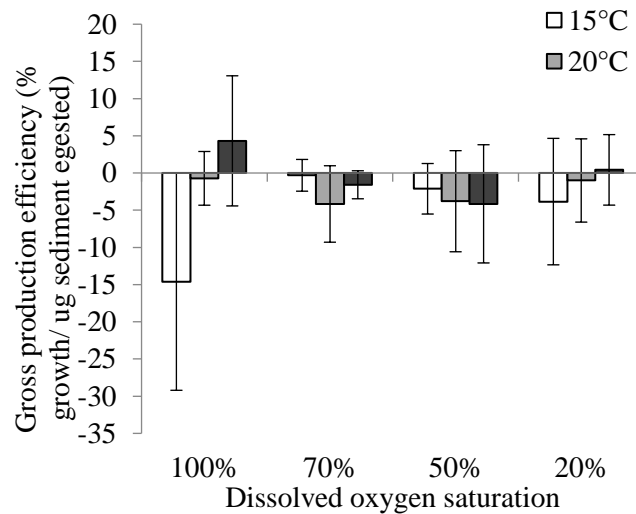


Figure 5.12 Mean gross production efficiency for *Capitella teleta* exposed to four dissolved oxygen saturation levels at three temperatures (\pm SD).

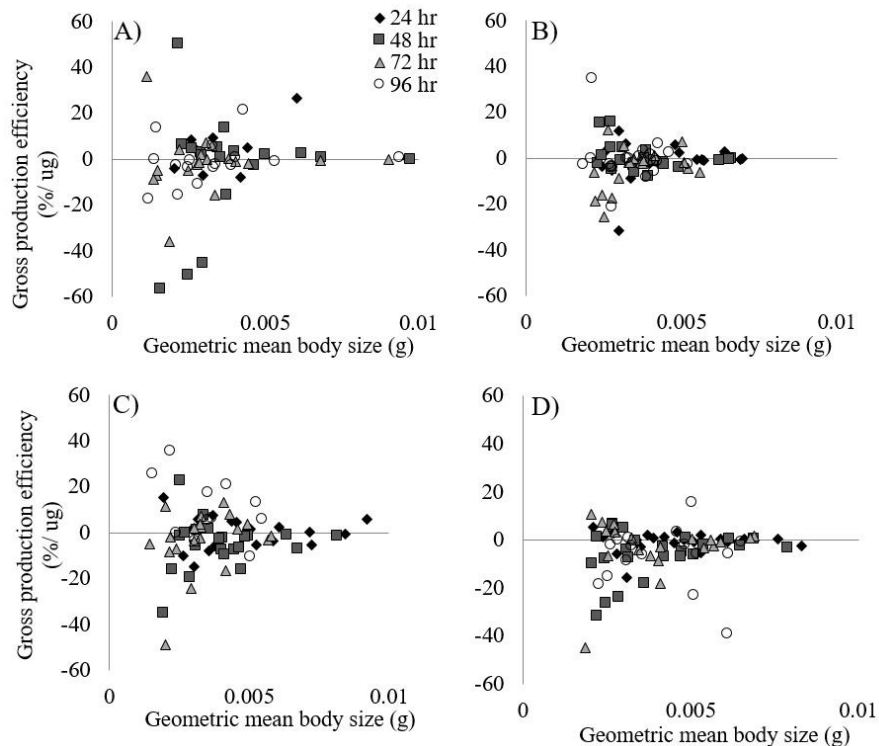


Figure 5.13 Gross production efficiency versus body size for *Capitella teleta* exposed to four dissolved oxygen saturation levels over four days. (A) 100% DO; (B) 70% DO; (C) 50% DO; and (D) 20% DO.

5.3.4 Mortality

Total mortality remained below 50% for all treatment combinations (Figure 5.15).

Most treatments (11 of 12) did not exhibit more than 30% mortality over the 4 days.

Mortality for the 25°C treatment was highest, averaging 78% survival in comparison to the other two treatments, which averaged 85% survivorship. The 100% DO at 25°C treatment showed notably high mortality during the first 24 h (4 of the 6 deaths for 100% 25°C), which corresponded with initial DO super-saturation of ~110% (Figure 5.16).

Furthermore, high mortality for the 100% DO at 15°C treatment also corresponded with relatively higher DO levels (averaging 98.6% DO vs. 95.2 % DO for other temperatures).

Small and medium size classes often showed higher mortality compared to large sizes for the three 100% DO treatments (Figure 5.17).

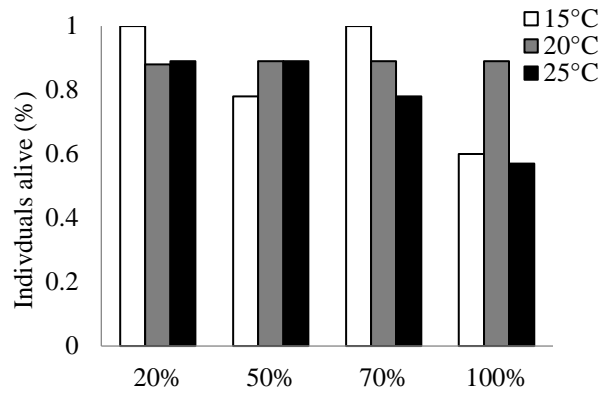


Figure 5.14 Survivorship (% alive) of *Capitella teleta* after four days of exposure to 12 treatment combinations of three temperatures and four dissolved oxygen saturations.

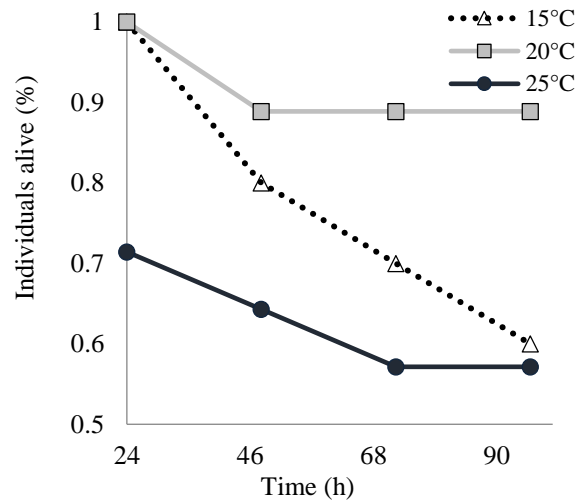


Figure 5.15 Survivorship (% alive) of *Capitella teleta* over four days while exposed to 100% DO at three temperatures.

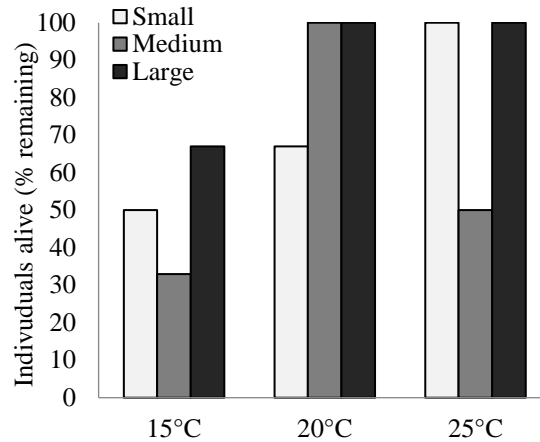


Figure 5.16 Survivorship (% alive) of three size classes of *Capitella teleta* after four days of exposure to 100% DO at three temperatures.

5.4 Discussion

5.4.1 Specific Growth and Egestion Rate

Small *C. teleta* exhibit significantly faster growth rate than larger individuals when under oxygen limitation. Strong ontogenetic effects in growth have been shown for *C. teleta* under normoxia at 21°C (Ramskov and Forbes 2008). In agreement with this experiment, Forbes (1989) observed higher specific growth rates in small worms than for large worms at low pO₂. Growth and ingestion are inextricably linked, as is egestion and assimilation. Furthermore, egestion rates directly reflect sediment ingestion rates; and the assimilation efficiency of deposit feeders has been estimated to be <15% (Hargraves 1972). Assuming a direct relationship between ingestion and egestion for *C. teleta*, ingestion was significantly reduced for all body size classes at 20% DO; however, small worms generally showed relatively higher ingestion rates than large individuals. While body size did not significantly influence egestion in this study, it may be the underlying parameter for the trend in faster growth rates of small individuals. Forbes (1989) observed higher gut turnover times for small *C. teleta* than larger counterparts which

would agree with the higher egestion rates observed in this study. Ingesting at near capacity under normal conditions is an adaptation of *C. teleta* for exploiting available food resources opportunistically; however, under suboptimal conditions many invertebrates are capable of transitioning to a metabolically depressed state, often achieved through a reduction of physical activities, such as movement, feeding/digestion, and ventilation (Storey and Storey 1990). Egestion capacity was < 1 at 20 and 50% DO suggesting metabolic depression may explain reduced specific growth rates at $< 50\%$ DO levels for larger worms.

Further, inability to adjust metabolism to temperature is indicative of an exploitative strategy (Forbes et al. 1994, Forbes and Lopez 1978, Newell 1980). Although a generally increasing trend in specific growth with temperature was seen in this study, the effect of temperature on both specific and daily growth was non-significant. In this study, egestion increased more markedly with temperature at 20 % DO (~3 fold) than $> 20\%$ DO treatments (~1.5 fold). This suggests *C. teleta* is consuming near its maximum capacity at DO saturations $> 20\%$, and is physiologically incapable of continually increasing ingestion with temperature at the higher DO saturation levels. Forbes and Lopez (1987) noted that *Capitella* spp. is not capable of a compensatory response in metabolic rate with increasing temperature. The rate of metabolic carbon loss was exponential with temperature, even for worms acclimated to experimental treatments for up to 16 days. They further calculated that temperature had a greater effect on the rate of metabolic carbon loss for small animals than for large ones. Lastly, when food was absent, starvation specific growth rates were significantly different across temperatures, suggesting the metabolism of *C. teleta* was influenced by temperature (Chapter VI).

Lastly, positive growth was not observed often in this study, but growth was not as negative as starving worms (Chapter VI). Specific growth rates for *C. teleta* reported by other studies range between ~15 to 23% d under normoxic conditions (Forbes 1989, Linton and Taghon 2000). Differences in observed specific growth rates may be a result of a short experimental time for this study; however, it is also possible worms were food limited. Food content of sediment used for this study emulated sediment typically used to culture these animals, and which is known to promote fast growth rates and to encourage reproduction. However, sediment prepared for this study was mixed at much larger quantities than amounts mixed for cultures. While effort was made to ensure sediment was homogeneously mixed after fish flake augmentation according to culturing protocol. However, in light of the small amounts of sediment in experimental tubes, the scale at which subjects interacted with sediments might explain a lot of the temporal variability in growth seen in this study. But, the sediment was renewed frequently. Comparison of egestion rates with Forbes and Lopez (1987) suggests that egestion rates of subjects were not as high as they should have been for the 100% DO treatment at all three temperatures. However, small individuals at 70% DO generally showed slightly higher than expected egestion rates as well as positive growth in this study. Finally, negative effects on growth could also have been caused as an artifact by the daily extraction of worms from the sediment. Extraction did appear to affect some organisms, and rates of escapement from chambers as well as animals splitting during removal increased as the experimental continued. However, an analysis using only the first 48 h of data gave results similar to the full duration. Given mean total specific growth was almost identical for individuals in

the 100% and 70% DO treatments, it appeared detrimental effects of handling over time were not substantial.

5.4.2 Conclusion

The specific growth rate of *C. teleta* (0.1 – 2% d) is much higher than for other benthic polychaetes, including nereids and *Glycerca* sp. (Cammen 1987). In contrast to *C. teleta*, these other polychaetes are much larger, show carnivorous or omnivorous life histories, and accumulate energy reserves. However, *Pectinaria californensis* is comparable in body size and shows corresponding high specific growth rates ranging from ~4-5.5% d (Nichols 1975, Cammen 1987). The opportunistic life style of *C. teleta*, which allows rapid exploitation of available food, is the main factor accounting for the rapid growth and egestion responses of this species. And this was particularly evident in its responses to DO and temperature within this study. Previous studies with this species done under normoxia did not detect any effect of body size on the growth rate of *C. teleta*; however, this study demonstrated that small individuals may exhibit faster growth rate than larger individuals when under oxygen limitation, and that this effect becomes less apparent as DO saturations increases.

CHAPTER VI MAKING THE CONNECTIONS: HOW DO COMPLEMENTARY
PHYSIOLOGICAL RESPONSES PRODUCE A STRESS RESPONSE
IN THE POLYCHAETE, *CAPITELLA TELETA*, UNDER
DISSOLVED OXYGEN AND THERMAL STRESS

6.1 Introduction

6.1.1 Stress Bioenergetic Framework

Living organisms can be defined as “non-equilibrium, thermodynamically open systems relying on external energy sources and constant energy flow” (Sokolova et al. 2012). The growth rate of an organism reflects many bioenergetic costs and benefits, including energy derived from, spent on, and allocated to consumption, egestion, assimilation, reproduction, etc. In 1960, Winberg described the energy flow through living open systems as:

$$\begin{aligned} \text{Consumption} = & \text{Production} + \text{Respiration} + \text{Excretion of protein metabolism byproducts} \\ & + \text{Excretion of unassimilated food.} \end{aligned}$$

Production is often described as the energy required for daily organismal maintenance and growth. Under optimal conditions, an organism is able to exceed baseline energetic costs of maintenance, thus allowing it to attain positive growth. In most cases, energy allocated to maintenance is given higher priority than energy provided for growth, reproduction, or storage (Koojiman 2010, Sokolova et al. 2012). Thus, during times of stress, organisms often redirect and reorganize energy flow and budgets into maintaining homeostasis. Energy is diverted from growth into maintenance, such as like heightened ventilation rates (Kristensen 1983) and active pumping of burrows (Mills 1978). In opposition, some stressors may induce overall metabolic reduction (also known as

metabolic depression), as evidenced by the cessation or reduction in feeding (Sagasti et al. 2001). Potentially conflicting physiological demands by concurrent multiple stressors likely will affect the bioenergetics of organisms in unexpected ways.

Sokolova et al. (2012) proposed a bioenergetic framework for examining stress on organismal physiology through combination of the dynamic energy budget (DEB) and the oxygen- and capacity-limited thermal tolerance concept (OCLTT) (Figure 6.1) (Koojiman 2010, Pörtner 2002, 2010). The DEB is a bioenergetics framework, often used in toxicology, to assess the influence of toxins on multiple bioenergetics parameters. Within this model, energy procured through consumption is placed in a storage reserve and then allocated to varying biological parameters, such as maintenance, activity, growth, and reproduction/development. The OCLTT model is used to outline levels of physiological stress, particularly as they relate to four physiological ranges: 1) optimum is defined as the range where energy balance is positive and maximum aerobic metabolism occurs, 2) pejus range is defined as reduced aerobic metabolism and increased maintenance energetic demands, 3) pessimum range is defined as diminished aerobic scope and emerging anaerobic metabolism used to cover baseline maintenance, and lastly 4) lethal range where energy demands cannot be met (Pörtner 2002). Under this concept, the ability to maintain aerobic respiration is viewed as a main indicator of stress, and used to distinguish between varying levels of physiological stress (Pörtner 2002).

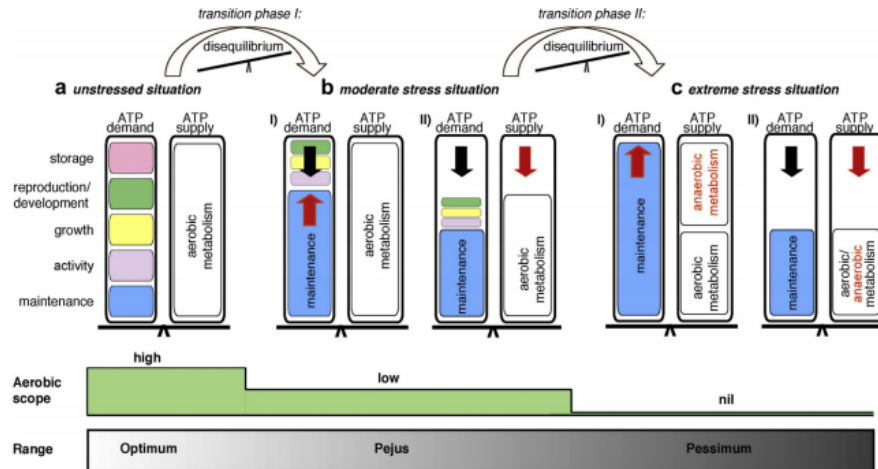


Figure 6.1 Bioenergetic framework combining the Dynamic Energy Budget (DEB) and oxygen- and capacity-limited thermal tolerance concept (OCLTT) for assessing stress based on organismal physiology (Sokolova et al. 2012).

6.1.2 Physiological Stress of Dissolved Oxygen and Temperature

Only 2.2% of all climate-change related studies focus on more than one abiotic factor and most studies overlook that ecosystems experience multiple stressors (Harley et al. 2006). There is a consensus in the scientific community that coastal systems are threatened by anthropogenic climate change, including multiple stressors like increasing sea surface temperatures and the frequency and magnitude of hypoxia (Field 2014, Levin 2003). Each stressor uniquely affects the physiology of organisms in potentially contrasting ways: hypoxia ultimately reduces respiration, ingestion, and overall metabolism; conversely, increasing temperature elevates vital rates and metabolic demands, and may cause physiological or functional hypoxia even under non-hypoxic conditions. Thus, multiple stressors may affect physiology in unexpected ways when occurring simultaneously, and so their effects need to be studied concurrently.

Accordingly, this chapter will integrate the proceeding chapters into the DEB/OCLTT framework for closer inspection of the stress response of *Capitella teleta* under

DO and thermal stress. The framework will be used to visualize the changes in overall physiology as DO and temperature stress increases and used to classify the level of physiological stress. I hypothesize *C. teleta* experienced optimal conditions only at high DO and low temperatures, followed by pejus ranges at low DO and low temperatures, and finally pessimum conditions during all high temperature scenarios. Further, this chapter aims to examine the relative importance of physiological responses, particularly respiration and egestion, in an effort to consider their contributions to the complete organismal response under a multi-stressor scenario, involving DO and thermal stressors. It is hypothesized that respiration will be more important to the growth response under low DO conditions, while ingestion will be of greater importance under high DO conditions. When DO stress is combined with thermal stress, I hypothesize that respiration will be further heightened and of greater importance in the contribution to growth as environmental DO will be limited but metabolic demand will be high.

6.2 Materials and Methods

6.2.1 Surface Plots and OCLTT Analysis

Surface planes were composed in R of growth, respiration, and egestion using the ‘scatterplot3D’ package. Data comparison for OCLTT was separated into two categories: ATP supply and maintenance and growth. ATP supply data was constructed in the same manner as discussed in Chapter III; such that, catabolic energy production (mmol ATP) was estimated for aerobic respiration (Chapter II) and anaerobic enzymatic activity (Chapter III) based on the following relationships:

$$\text{Aerobic: } 1 \text{ ml O}_2 / \text{min consumed} = 0.29 \text{ mmol ATP}$$

(Burke 1979, Quiroga et al. 2007);

Anaerobic: 1 mole NADH = 1 mole ATP

(Quiroga et al. 2007).

Anaerobic respiration is the sum of the mean of strombine dehydrogenase enzymatic activity and mean alanopine dehydrogenase enzymatic activity which were found to be the two main pathways of *Capitella teleta*. Data for 50% and 70% anaerobic respiration were calculated; however, it was based on very small sample sizes ($n < 3$). However, results should be interpreted cautiously as true anaerobic ATP output was not estimated in Chapter III, but rather an estimate of the possible ATP output through enzyme availability (i.e., anaerobic end products were not measured). Maintenance was represented through mean specific growth starvation data while growth data was represented as the mean specific growth of the fed experiments. Starvation data was used for maintenance as it reflects the metabolism of the organisms without possible constraints of food availability or particle size.

6.2.2 Contribution Analysis

The relative importance of respiration versus egestion versus body size upon specific growth was determined in R using the package ‘relaimpo’. This package was developed to decompose the model-explained variance into the contributions of each factor, essentially compartmentalizing the percentage of the model’s r^2 explained by each factor. Confidence intervals for the relative importance are estimated using a bootstrap of 1,000 samples. The purpose of the analysis was less in deriving regressions for specific growth, but rather in comparing the variability that was explained by the given parameters within each treatment. Data for the analysis consisted of raw specific-growth ($\% d^{-1}$), initial body size (g), and mean egestion rate ($ug d$) data from the fed-growth

experiments (Chapter V). As respiration was not taken during this experiment, respiration was estimated using allometric equations developed in Chapter II. The allometric equations calculate mass-specific respiration which was then calculated up to whole-organismal respiration in order to maintain consistent units between all of the parameters.

6.3 Results

6.3.1 General Comparisons

The surface plane for the 100% DO treatment suggests growth increases with egestion across all levels of temperature under normoxia (Figure 6.1). Conversely, although egestion still increases with the specific growth rate for the 20% DO treatment, growth clearly decreases with higher oxygen consumption under hypoxia. The 50% and 70% DO treatments both appear to maintain similar mean planes. Data are generally grouped by temperature at all DO levels, except for the 20% DO treatment. Body size trends were observed for all physiological parameters, except starvation growth rates and gross production efficiency (Table 6.1). In general, physiological rates for small individuals were higher than for larger organisms, which also appeared to result in higher mortality rates.

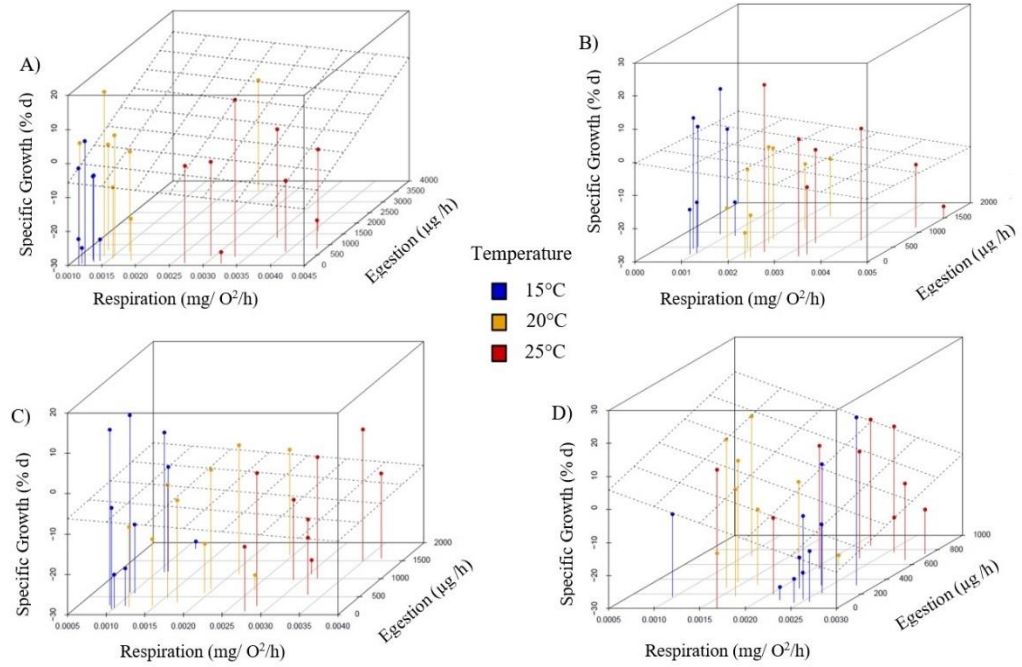


Figure 6.2 Surface plots of relationships between observed growth, respiration, and egestion for *Capitella teleta* at three temperatures and four dissolved oxygen saturations. (A) 100% DO; (B) 70% DO; (C) 50% DO; and (D) 20% DO).

Table 6.1

Summary of body size effects on the physiology of *Capitella teleta*.

	Small Body Sizes	Large Body Sizes
Mass-specific Respiration	<ul style="list-style-type: none"> • High VO₂ rates • Mean effects of temperature (Q₁₀= 2-4) • Maintained respiration at low temperatures • 40% reduction at high temperature 	<ul style="list-style-type: none"> • Low VO₂ rates • Larger effects of temperature (Q₁₀= 2-8) • Maintained respiration at low temperatures • 40% reduction at high temperature
Mass-Specific Anaerobic Respiration	<ul style="list-style-type: none"> • High enzymatic activity at low DO • Increased enzymatic activity at high temperatures • Increased activity at low DO levels for all temperatures 	<ul style="list-style-type: none"> • Low enzymatic activity at all DO levels • Increased enzymatic activity at high temperatures • No change in enzymatic activity at high temperature and low DO
Starvation Growth Rate	<ul style="list-style-type: none"> • No significant effect of body size • Specific growth rates averaged -25 to -36% d • Significant effects of temperature with increased loss at 20°C • Temporal effects with reduction in rate of loss at 72 h 	
Starvation Mortality	<ul style="list-style-type: none"> • Higher mortality rates, particularly under hypoxia 	<ul style="list-style-type: none"> • Longer survivorship during first 72 h
Fed Growth Rates	<ul style="list-style-type: none"> • Maintained positive, or closer to positive growth (mean= -0.11 % d) • Growth rate declined with decreasing DO 	<ul style="list-style-type: none"> • Maintained negative growth rates (mean = -9.33% d) • Growth rates were maintained or slightly increased with increasing DO
Fed Mortality	<ul style="list-style-type: none"> • Some mortality at 15°C and 20°C 	<ul style="list-style-type: none"> • Some mortality at 15°C
Egestion Rate	<ul style="list-style-type: none"> • Low egestion rates • Influenced by temperature 	<ul style="list-style-type: none"> • Higher egestion rates • Influenced by temperature
Gross Production Efficiency	<ul style="list-style-type: none"> • No apparent trend in body size (mean= -1 to -6%) • Small body sizes observed greater variability overall 	

6.3.2 ATP Supply and Demand

Small organisms maintained $\geq 60\%$ ATP supplied through aerobic respiration until 20% DO for both temperatures (Figure 6.2). Aerobic respiration only made up 20%

of ATP production at 20% DO. Large organisms supplied ~60% ATP through aerobic respiration across DO and temperature level. While larger organisms mostly rely on aerobic respiration for ATP supply as DO decreases, the total ATP produced becomes reduced at 20% DO 25°C while smaller organisms see no drop in ATP supplied (Figure 6.3). Conversely, smaller organisms see an increase in possible ATP supplied during 20% DO due to increase in anaerobic enzymes larger reliance on anaerobic respiration. According to the ideology of OCLTT, smaller organisms enter pejus conditions at 20% DO at both temperatures; however, pessimum conditions were not observed during this experiment as some level of aerobic respiration is maintained. Conversely, the ratio of aerobic to anaerobic ATP supply for larger organisms suggests the organisms are still within the optimum range; however, the reduction in overall ATP supply suggests the organism may be entering a pejus condition, particularly at 25°C.

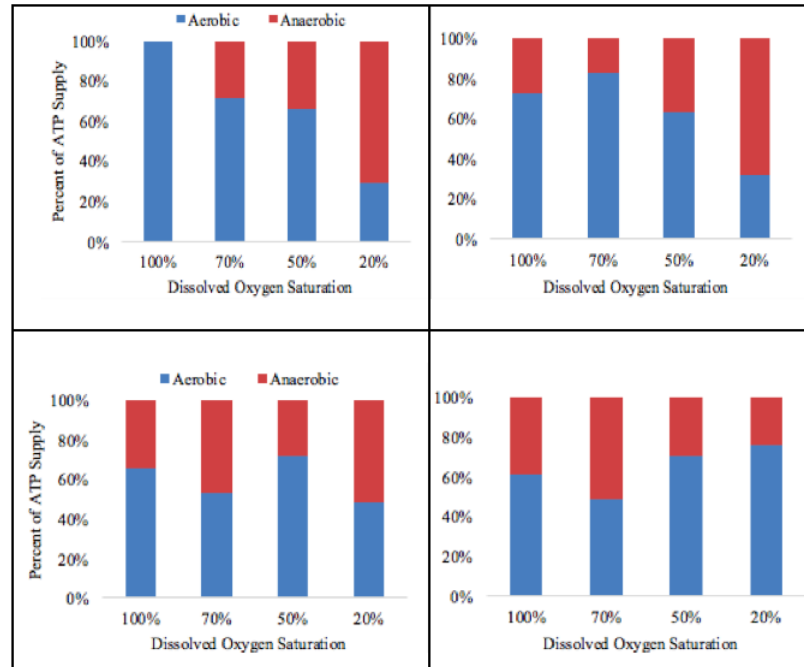


Figure 6.3 Percent ATP contribution from aerobic and anaerobic respiration for *Capitella teleta*. A) 15°C small body size, B) 25°C small body size, C) 15°C large body size, and D) 25°C large body size.

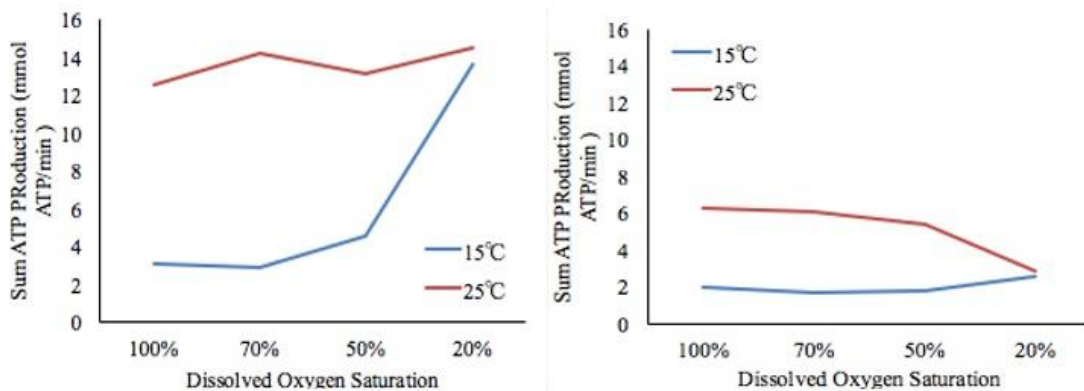


Figure 6.4 Sum ATP production (mmol ATP/min) from aerobic and anaerobic respiration for *Capitella teleta*.

For small individuals, higher metabolic rates resulted in reduced growth rates, except at 15°C; however, 100% DO at this temperature did have a high mortality anomaly during the first 24 hr which could be skewing the results (discussed in Chapter V) (Figure 6.4). Metabolism appears to increase at 50% DO at all temperatures, but

particularly at 15°C and 25°C, and drops again at 20% DO. This could suggest small polychaetes are increasing maintenance which is characteristic of entering the pejus range, and beginning to enter pessimum ranges during 20% DO where metabolism reduces. Conversely, for larger organisms, lower metabolic rates appear to result in reduced growth rates. At 15°C, metabolism reduces with DO resulting in increased degrowth rates. Conversely, maintenance appears to be held overall during 25°C with no apparent effect on the mean degrowth rate.

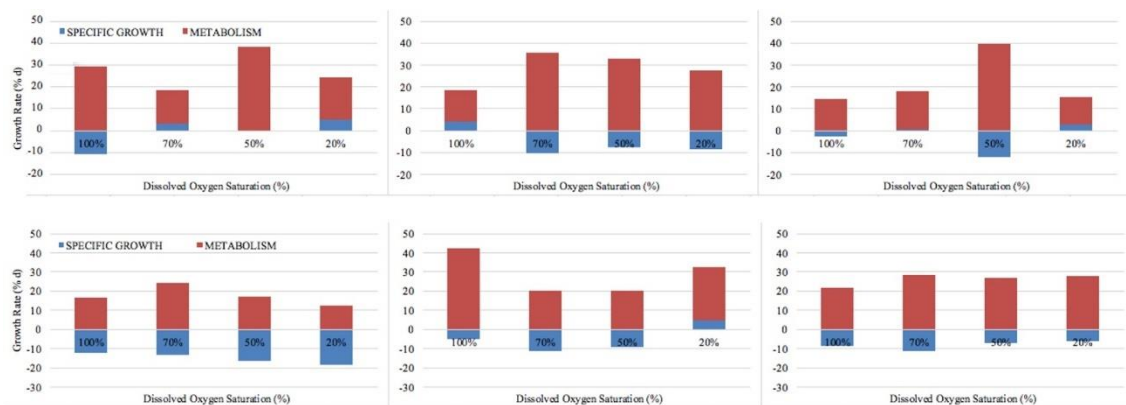


Figure 6.5 Percent contribution of maintenance and specific growth to the total ATP demand *Capitella teleta*.

6.3.3 Relative Importance of Independent Variables

Respiration, egestion, and initial size explained >40% of the specific growth variability for all treatments except 100% 15°C and 50% 15°C and 25°C (Table 6.2). Models were statistically significant for 70% 15°C and 25°C and 20% 15°C and 25°C. At 100% DO, >80% of variability explained by respiration and body size at lower temperatures, but egestion, body size, and respiration accounted equally for the explained variability at 25°C (Figure 6.5). Both 70% and 50% DO, observed an increase in explained variability by egestion at 20°C. At 20% DO, egestion contributed minimally to explained variability.

Table 6.2

Relative importance of egestion, respiration, and body size on specific growth models for *Capitella teleta* at four DO saturations. Model form: Specific growth (% d) = Egestion (ug d⁻¹) + Respiration (mg O₂ d) + initial wet weight (g).

		Egestion	Respiration	Body Size
100%	15°C $r^2 = 0.19$ $p = 0.86$	0.11	0.47	0.52
	20°C $r^2 = 0.61$ $p = 0.36$	0.11	0.39	0.49
	25°C $r^2 = 0.36$ $p = 0.57$	0.35	0.29	0.36
70%	15°C $r^2 = 0.94$ $p = 0.03^*$	0.23	0.4	0.37
	20°C $r^2 = 0.82$ $p = 0.05^*$	0.56	0.2	0.24
	25°C $r^2 = 0.71$ $p = 0.24$	0.25	0.39	0.36
50%	15°C $r^2 = 0.32$ $p = 0.47$	0.14	0.46	0.4
	20°C $r^2 = 0.72$ $p = 0.08$	0.5	0.2	0.29
	25°C $r^2 = 0.05$ $p = 0.96$	0.12	0.35	0.53
20%	15°C $r^2 = 0.83$ $p = 0.02^*$	0.34	0.39	0.27
	20°C $r^2 = 0.70$ $p = 0.15$	0.06	0.45	0.49
	25°C $r^2 = 0.76$ $p = 0.05^*$	0.14	0.45	0.4

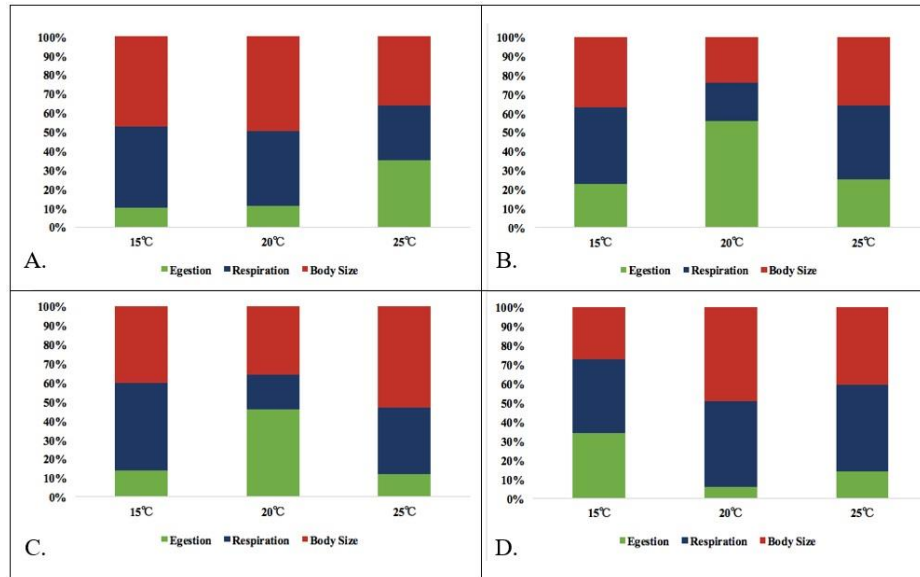


Figure 6.6 Contribution of egestion, respiration, and initial body size to the explained variability of specific growth rate models of *Capitella teleta* under four DO saturation levels. A) 100% DO, B) 70% DO, C) 50% DO, and D) 20% DO.

6.4 Discussion

6.4.1 Ecophysiological Connections

As presented in Chapter II, *C. teleta* was capable of holding $\geq 60\%$ of the baseline respiration rate at all DO and temperature treatment levels; however, when examining aerobic: anaerobic respiration ATP supply, it became apparent smaller organisms entered pejus physiological ranges. Further, aerobic respiration and body size accounted for the majority of explained variability of specific growth models. When given the opportunity to feed ad libitum, egestion accounted for a minimal amount of explained variability for the majority of the specific growth models. This seems to agree with the ecology of this species, as inferred by Forbes et al. (1994) “the highest population densities of *Capitella* sp. I, as well as other enrichment opportunists, occur in environments in which oxygen, rather than food, is in short supply”. Indeed, *Capitella* sp. I, is a tolerant species, exhibiting several special adaptations to low DO. For example, the extracellular

hemoglobin of *C. teleta* has a moderate oxygen affinity ($P_{50} = 6.88 \pm 0.97$) and high cooperativity ($n_{50} 2.89 \pm 0.82$), which together confer on this species the capacity for high loading and unloading of oxygen as an adaptation to low DO environments (Barclay 2013, Magnum et al. 1992, Weber 1980). However, much of this adaptation is for native, cold water conditions typically under 15°C, the minimal temperature examined in this dissertation. *Capitella teleta* possess relatively higher quantities of heme b, the protein responsible for the attachment/release of oxygen, at colder temperatures (4°C vs. 21°C) (Barclay 2013). Consequently, reduced oxygen affinity and cooperativity at higher temperatures mean that hemoglobin saturation is higher and DO uptake more efficient at colder temperatures (Barclay 2013, Wells et al. 1980). Barclay (2013) also noted that *C. teleta* was 6.2 fold larger at cold temperatures; and, they further suggested the ability to unload oxygen to deeper tissues due to higher oxygen saturation might contribute to their ability to attain such large sizes. Although differences in specific growth were non-significant relative to temperature, observed maximum sizes at low temperatures (4°C) suggest the existence of a temperature related metabolic effect that could be driven by lower heme quantity as well as lower affinity and cooperativity at higher temperatures. However, based on OCLTT aerobic: anaerobic ATP supply ratio, *C. teleta* did not appear to enter the range of pessimum even at 10°C over native temperatures.

Finally, adaptations related to the potential for anaerobic respiration undoubtedly play a role in explaining specific growth. Enzymatic activities of four pyruvate oxidoreductases permit anaerobic respiration during times of environmental or functional oxygen limitation in *C. teleta*. At 100% DO and 15°C, catabolic energy production occurred exclusively via aerobic respiration, whereas at 25°C, contributions by anaerobic

catabolic production suggest functional anaerobiosis can emerge at high temperatures. The inability to obtain the necessary oxygen at high temperatures may reflect reduced oxygen affinity and cooperativity in the face of increased metabolic demands. At low DO levels, some degree of aerobic respiration is maintained at both high and low temperatures, but anaerobic respiration plays a relatively greater role at high temperatures, as seen by the fact that >45% of the catabolic energy production occurred through alanopine or strombine dehydrogenase pathways under these conditions.

The exploitative strategy of an opportunistic species, such as *C. teleta*, requires a continuous input of energy in order to maintain positive specific growth, especially in light of the lack of energetic reserves. Other studies have shown that deposit feeding worms partition their time between feeding and ventilation, such that feeding typically occurs between ventilation intervals (Forbes 1989, Grassle and Grassle 1976, Lopez and Forbes 1990). Thus, the need to spend more time ventilating may explain the greater contribution of respiration to the specific growth model with decreasing DO saturation, particularly at 20% DO. For *C. teleta*, Forbes (1992) observed the lack of any compensatory ability to adjust feeding rates, as well as overall metabolism in the face of increasing temperatures (even when organisms were acclimated for 16 d). Furthermore, metabolic carbon loss rates were similar between starved and fed individuals, suggesting *C. teleta* lacks the ability to compensate for food level. However, estimates from their experiments were based on the first 2 h of starvation (Cammen 1986), whereas reduced metabolism occurred over the much more extended period of 72 h in this study. Though a greater amount of model variability was explained by egestion as temperature increased at 100% DO.

An interaction between DO level and food quality might have influenced the outcome of the growth experiment in this study. Forbes et al. (1994) observed, “the relationship between feeding rate and growth was influenced by the level of available oxygen such that when the nitrogen content of food was low, greater growth occurred at the lower oxygen level.” This effect might also explain the minimal observed values for my growth experiments (Chapter V). While comparisons between specific growth during starvation (-25.4 to -35.9% d) and fed (-0.11 to -9% d) experiments within this dissertation suggest that worms were not starving during the fed experiment, the low growth rates compared to the literature suggest that worms were not feeding without limit. Variable nitrogen levels may have occurred within the sediments due to inconsistent mixing of flake food into large volumes of mud. While pilot studies were run to ensure all feeding issues were considered (mud: flake food, preparation timing, mud depth, etc.), pilot studies were run on a smaller scale. The proper ratio of mud to flake food (7 mL food per 15 mud) was correct for the experiment; however, very large batches of mud were prepared for the experiment ahead of the experiment. It is possible the flake food was not consistently and homogeneously mixed throughout the larger quantities of substrate resulting in variable results. If this was indeed the case, I would expect to see higher variability within growth rates as some worms would be given plentiful nutrition, while others did not. It is also possible that handling the organisms as frequently as this study did also resulted in reduced feeding. Most studies in the literature do not handle organisms on a daily basis; however, feces were collected every single day suggesting this may not be the case. At any rate, the more frequent occurrence of positive growth at low DO levels likely reflected effects of metabolic depression under hypoxia; whereas,

higher metabolic demands under high DO conditions precluded positive growth under food limited conditions. Indeed, Forbes et al. (1994) suggested that degrowth reflects the breakdown of internal proteins due to the necessity to maintain metabolic demands under high oxygen availability and food limited conditions. Starvation experiments in this study (Chapter VI) showed degrowth had a mean of -25 to -35% d, thus supporting Forbes' degrowth hypothesis. However, the degrowth response could ameliorate with time. An observed temporal effect in this study suggested that metabolic acclimation to reduced food levels may occur after 72 h of starvation. Reduced egestion and minimal weight loss suggested lower metabolic demands at the outset of the experiment. However, high variability and small sample sizes precluded statistical detection of these differences.

In spite of the importance of bioenergetic parameters, body size accounted for a large percentage of explained specific growth variance (>40%) across most treatments. Body size played a prominent role in every physiological response examined throughout this study, except for starvation degrowth and gross production efficiency (GPE). Under normoxia and 20°C, smaller individuals show higher total carbon turnover rates and red blood cell oxygen affinity (Forbes 1992, Magnum et al. 1992). Accordingly, small individuals also exhibited higher-mass specific respiration (both aerobic and anaerobic) and overall growth rates within this dissertation.

6.4.2 Overall Outlook and Conclusions

Physiologically, *C. teleta* maintained aerobic respiration at low DO levels under its natural temperatures, but aerobic respiration was reduced by 40% at 25°C. The anaerobic respiration response at 25°C suggested functional anaerobiosis, even under normoxic conditions, perhaps because species was near its critical temperature limit.

Magnum et al. (1992) observed a correlation between temperature and red blood cell oxygen affinity among six species within the capitellid sibling species complex, for which species from warmer habitats had the highest affinities. Among the species examined, *C. teleta* had a medium affinity for oxygen; some sibling species displayed an affinity more than a 2 fold greater, indicating that adaptation to warmer temperatures may be feasible for this species if warming occurs gradually over an extended period of time. Egestion/ingestion have been shown to increase with temperature for *C. teleta*; however, a plateau for ingestion is inevitable due to physiological constraints, including a maximum feeding and gut turnover rates. However, such maximum rates have not been revealed within the literature, suggesting the critical limit for feeding has not yet been observed.

When under thermal and oxygen stress in these short-term studies, *C. teleta* appeared capable of surviving concurrent low DO and high temperature levels; however, this species is near its critical thermal limit at 25° C. Additional long-term studies are necessary to understand the full acclimation potential and adaptability of *C. teleta*. Finally, further research needs to address other climate-change related stressors on *C. teleta*, in particular effects of decreasing pH. Increasing acidity can affect blood cell physiology, feeding rates, feeding efficiency, tolerance to other stressors, and lead to an overall reduction in growth that is exacerbated by high temperatures (Zhang et al. 2015).

APPENDIX A – INSTRUCTIONS FOR CULTURING *CAPITELLA TELETA*

PER CAROLA NOJI FROM RUTGERS UNIVERSITY

- 1) The *Capitella teleta* cultures are kept at 15 degrees Celsius in natural, filtered seawater with a salinity of about 27 ppt.
- 2) Worms are kept in glass finger bowls that contain about 200 ml of filtered seawater (approximately 50 worms/bowl). The dimensions of the bowl are 1.3 cm depth and 10.2 cm diameter. Cultures are not aerated due to number because we have so many, but it is recommended if at all possible. Cultures are stacked about two or three bowls and the top bowl covered loosely with Saran-wrap and a rubber band (attach a small note telling the due date for next maintenance (every 14 days)).
- 3) Worms are fed highly organic mud that is collected from Wood's Hole or Tuckerton, frozen thoroughly, thawed, and sieved over a 1mm sieve and then frozen again into smaller containers and defrosted as needed. (About 2 weeks before I start using the mud I defrost it (and add dried kelp or tropical fish food flakes (Tetramin) (7 mL per 1l mud (only if natural organic content of the mud isn't high enough). Mix well. (Mud is kept at 4 degrees Celsius).
- 4) Every two weeks I sieve each bowl of adult worms over a 1 mm sieve to remove any debris, eggcases (you don't want several generations in your bowl), clean the bowl (no detergents are used in our lab under any circumstances!) and add fresh filtered (1µm) seawater (15 degrees Celsius) and about 15-30 mL of mud.
- 5) The juveniles are also fed every two weeks with about 15-30 mL of mud; however, they are sieved over a 300-micron sieve until they are about 8-10 weeks old. Once they are mature, you can use a 1 mm sieve.

6) To start a new culture, separate any females with egg cases and put them in individual Stender's dishes with only seawater. They can live without mud for the two weeks' time that it will take for their eggs to hatch. Eggcases are checked daily for any hatches. Once the eggs hatch and the larvae are released, gently pipette out the larvae and put about 50 per bowl. Fill the bowl about 2/3 with seawater and then gently add 15 mL of mud. Try not to disperse the mud when you are adding it. (It is only important to not disperse the mud when you have larvae, all other times are OK). A bowl with larvae is left undisturbed for the first 3 weeks after hatching. Then you exchange the seawater and add new mud and from then on the bowl has to be "serviced" every two weeks like the other bowls. Your larvae will mature in about 8-10 weeks and begin producing egg cases soon after that, if all goes well.

APPENDIX B COMPARISONS OF 24H AND 168 MASS-SPECIFIC
RESPIRATION OF *CAPITELLA TELETA*

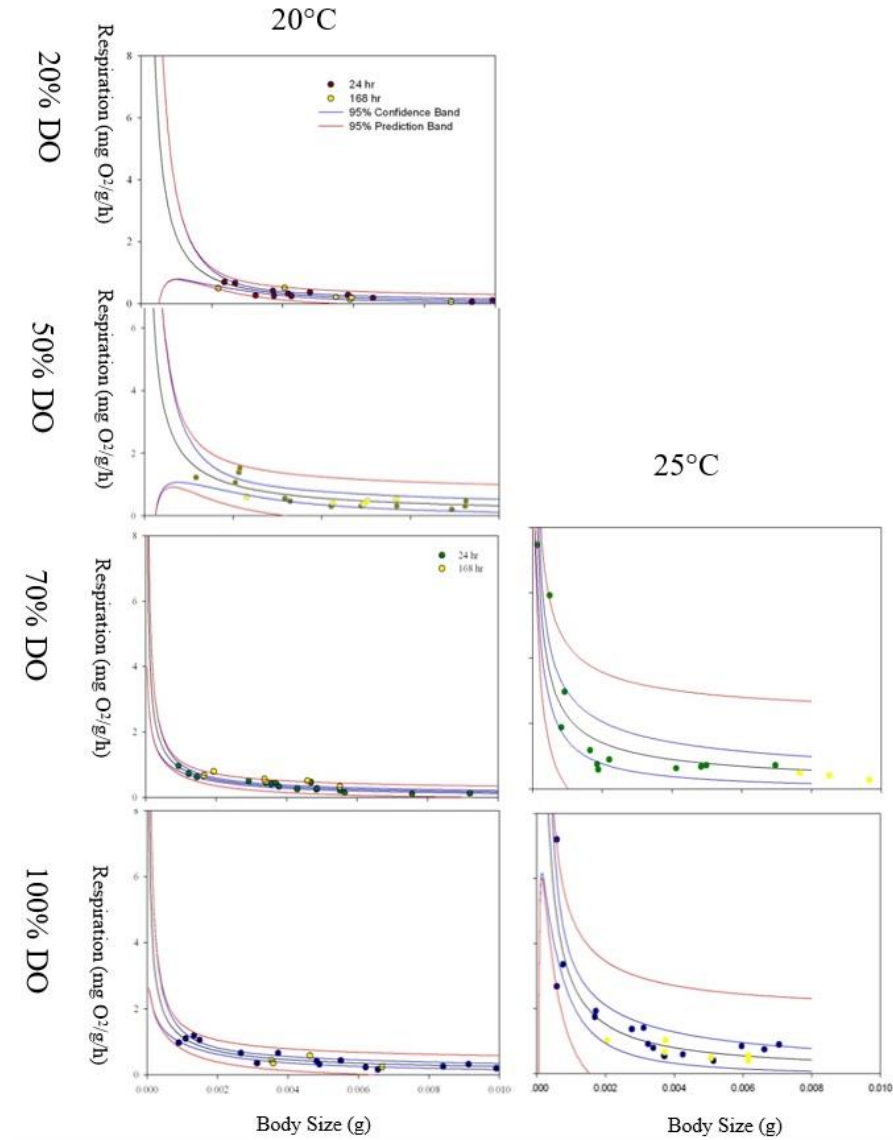


Figure B.1 Comparison of 24h and 168h mass-specific respiration for *Capitella teleta* at 20°C and 25°C and multiple levels of dissolved oxygen saturations. Confidence levels were constructed with 24h data only.

APPENDIX C – RELATIONSHIPS BETWEEN TOTAL VOLUME EGESTED
AND THE TOTAL WEIGHT EGESTED OF *CAPITELLA TELETA*

Table C.1

Correlations between the total volume egested ($\text{mm}^3 \text{d}^{-1}$) and total weight egested ($\mu\text{g d}^{-1}$) for *Capitella teleta* after 24 hours of starvation when exposed to three temperatures and four dissolved oxygen saturations.

	15°C		20°C		25°C	
	r^2	n	r^2	n	r^2	n
100%	0.76	9	0.93	10	0.78	9
70%	0.98	9	0.84	9	0.86	9
50%	0.81	8	0.33	7	0.52	8
20%	0.8	9	0.99	8	0.89	10

APPENDIX D Q-Q PLOTS OF GROSS PRODUCTION EFFICIENCY
OF *CAPITELLA TELETA*

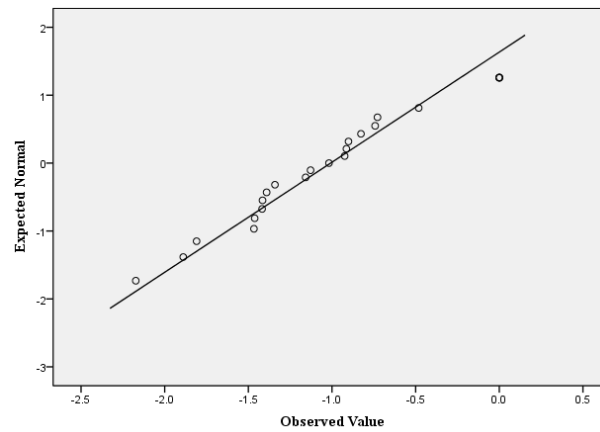


Figure D.1 Q-Q plot for cube root transformed gross production efficiency data from the 100% dissolved oxygen treatment. Data failed the Shapiro-Wilk normality test ($W = 0.88$; $p = 0.024$).

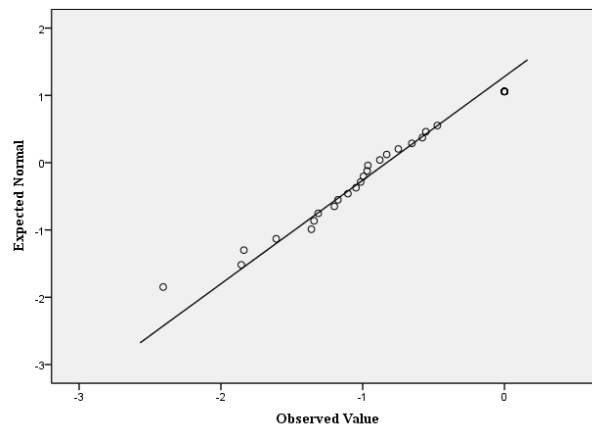


Figure D.2 Q-Q plot for cube root transformed gross production efficiency data from the 25°C treatment. Data failed the Shapiro-Wilk normality test ($W = 0.928$; $p = 0.042$).

APPENDIX E SHAPIRO-WILK TEST AND Q-Q PLOT FOR
DAILY GROWTH OF *CAPITELLA TELETA*

Table E.1

The Shapiro-Wilk test of normality for daily growth data from four dissolved oxygen saturation levels, three temperatures, and four time intervals. * = statistically significant at $p = 0.05$.

		Statistic	df	Sig.
Dissolved Oxygen Saturation	100%	0.98	90	0.274
	70%	0.96	98	0.005*
	50%	0.98	97	0.196
	20%	0.99	91	0.704
Temperature	15°C	0.99	127	0.812
	20°C	0.99	121	0.251
	25°C	0.96	128	0.001*
Time	Day 1	0.99	107	0.410
	Day 2	0.98	97	0.241
	Day 3	0.98	91	0.093
	Day 4	0.96	81	0.01*

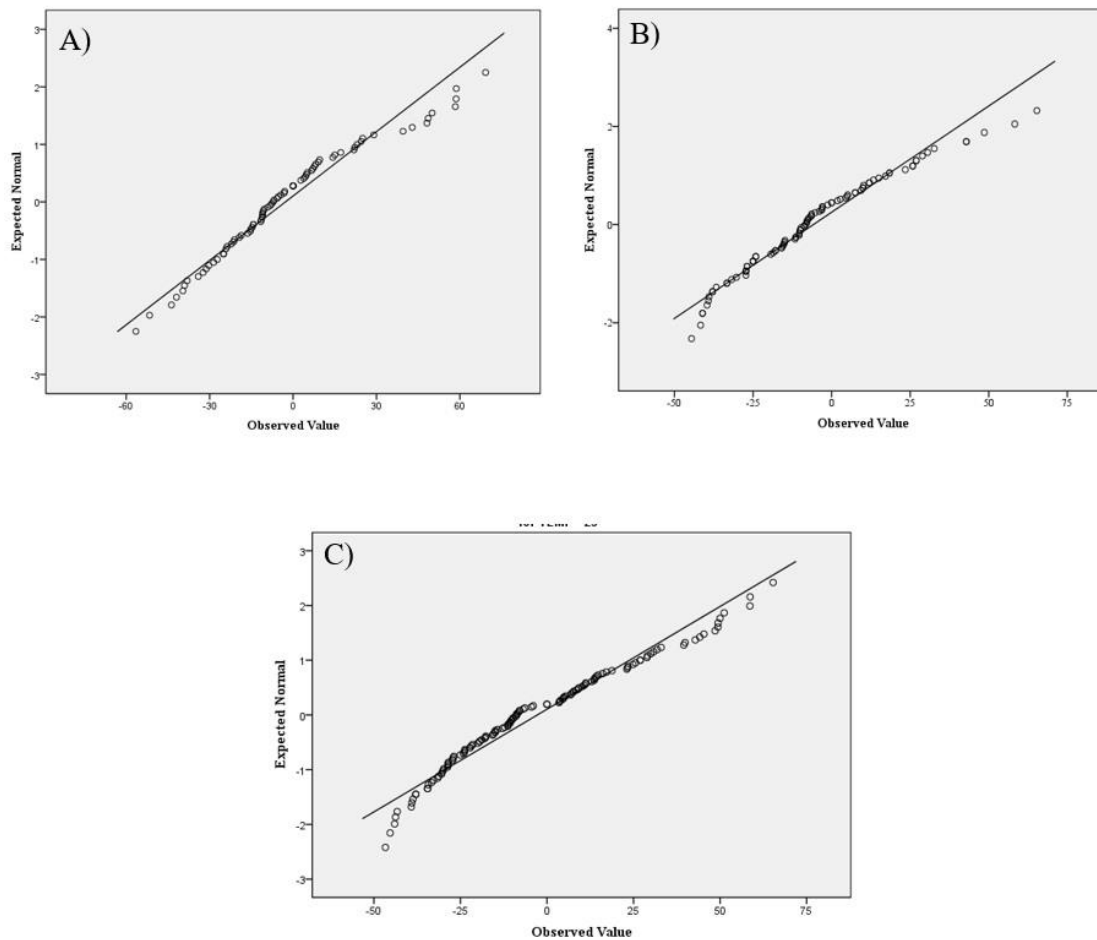


Figure E.1 Q-Q plots of treatments that failed the Shapiro-Wilk normality test. Plots include the treatments A) 70% dissolved oxygen, B) 25°C, and C) day 4.

REFERENCES

- Altieri, A. H. and Gedan, K. B. (2015).** Climate change and dead zones. *Global Change Biology* **21**, 1395-1406.
- Blake, J.A, Grassle, J.P., and Eckelbarger, K.J. (2009).** *Capitella teleta*, a new species designation for the opportunistic and experimental *Capitella* sp. I, with a review of the literature for confirmed records. *Zoosymposia* **2**, 25-53.
- Brey, T., Jarre-Teichmann, A., and Borlich, O. (1996).** Artificial neural network versus multiple linear regression: predicting P/B ratios from empirical data. *Marine Ecology Progress Series* **140**, 251-142.
- Bricker, S. B., Longstaff, B., Dennison, W., Jones, A., Boicourt, K., Wicks, C., and Woerner, J. (2008).** Effects of nutrient enrichment in the nation's estuaries: a decade of change. *Harmful Algae* **8**, 21-32.
- Bridges, C. R. and Brand, A. R. (1980).** Oxygen consumption and oxygen-independence in marine crustaceans. *Marine Ecology Progress Series* **2**, 133-141.
- Brown, J., Gillooly, J., Allen, A., Savage, V., and West, G. (2004).** Toward a metabolic theory of ecology. *Ecology* **85**, 1771-1789.
- Burnett, L. and Stickle, W. (2001).** Physiological responses to hypoxia. In: *Coastal Hypoxia: Consequences for Living Resources and Ecosystems* (ed. N.N Rabalais and R.E. Turner). pp. 101-114. Washington D.C: American Geophysical Union.
- Calow, P. (1977).** The joint effect of temperature and starvation on the metabolism of triclads. *Oikos* **29**, 87-92.
- Cammen, L. (1985).** Metabolic loss of organic carbon by the polychaete *Capitella capitata* (Fabricius) estimated from initial weight decrease during starvation,

- oxygen uptake, and release of ^{14}C by uniformly-labeled animals. *Marine Ecology Progress Series* **21**, 163-167.
- Cammen, L.** (1987). Polychaeta. In: *Animal Energetics* (ed. T.J. Pandian and F. Vernberg). pp. 217-260. San Diego: Academic Press Inc.
- Cloern, J.** (2001). Our evolving conceptual model of the coastal eutrophication problem. *Marine Ecology Progress Series* **9**, 191-202.
- Conley, D. J., Carstensen, J., Vaquer-Sunyer, R., and Duarte, C. M.** (2009). Ecosystem thresholds with hypoxia. *Hydrobiologia* **629**, 21-29.
- Cox, N.J.** (2011). Stata tip 96: Cube Roots. *Stata Journal* **11**, 149-154.
- Dales, R.P. and Warren, L.M.** (1980). Survival of hypoxic conditions by the polychaete *Cirriformia tentaculata*. *Journal of Marine Biology Association U.K.* **60**, 509-516.
- Davey-Huggins, P.** (2001). Individual and population level response to starvation and regrowth in the opportunistic polychaete *Capitella* sp. I. Dissertation, State University of New York at Stony Brook. Retrieved from ProQuest Dissertations and Theses. (Accession Order No. 3051068).
- Dawicki, S.** (2013). Sea Surface Temperatures Reach Highest Level in 150 Years on Northeast Continental Shelf, *Northeast Fisheries Science Center, Science Spotlight*. http://www.nefsc.noaa.gov/press_release/2013/SciSpot/SS1304/.
- Diaz, R. J. and Rosenberg, R.** (1995). Marine benthic hypoxia: a review of its ecological effects and the behavioural responses of benthic macrofauna. *Oceanography and Marine Biology* **33**, 245-03.
- Diaz, R. J. and Rosenberg, R.** (2008). Spreading dead zones and consequences for marine ecosystems. *Science* **321**, 926-929.

- Dunphy, B.J., Wells, R.M.G., and Jeffs, A.G.** (2006). Oxygen consumption and enzyme activity of the subtidal flat oyster (*Ostrea chilensis*) and intertidal Pacific oyster (*Crassostrea gigas*), response to temperature and starvation. *New Zealand Journal of Marine and Freshwater Research* **40**, 149-158.
- Dorgan, K.M., Lefebvre, S., Stillman, J.H., and Koehl, M.A.R.** (2011). Energetics of burrowing by a cirratulid polychaete *Cirrifomia moorei*. *Journal of Experimental Biology* **214**, 2202-2214.
- Everett, M. V. and Crawford, D. L.** (2010). Adaptation versus allometry: population and body mass effects on hypoxic metabolism in *Fundulus grandis*. *Physiological and Biochemical Zoology* **83**, 182-190
- Edgar, G.** (1990). The use of size structure of benthic macrofaunal communities to estimate faunal biomass and secondary production. *Journal of Experimental Marine Biology and Ecology* **137**, 195-214.
- Field, C. B. (2014).** *Climate change 2014: impacts, adaptation, and vulnerability*. In *Climate Change 2014–Impacts, Adaptation and Vulnerability: Regional Aspects* (ed. V.R Barros and C.B. Fields). New York: Cambridge University Press.
- Forbes, T.L. (1989).** The importance of size-dependent processes in the ecology of deposit-feeding benthos. In *Ecology of Marine Deposit Feeders*, pp. 171-200. New York: Springer.
- Forbes, T. and Lopez, G.** (1990). The effect of food concentration, body size, and environmental oxygen tension on the growth of the deposit-feeding polychaete, *Capitella* species I. *Limnology and Oceanography* **35**, 1535-1544.
- Forbes, T.L., Forbes, V.E., and Depledge, M.H.** (1994). Individual physiological

responses to environmental hypoxia and organic enrichment: Implications for early soft-bottom community succession. *Journal of Marine Research* **52**, 1081-1100.

Frederich, M., and Pörtner, H. O. (2000). Oxygen limitation of thermal tolerance defined by cardiac and ventilatory performance in spider crab, *Maja squinado*. *American Journal of Physiology-Regulatory, Integrative and Comparative Physiology* **279**, R1531-R1538.

Gäde, G., and Grieshaber, M. K. (1986). Pyruvate reductases catalyze the formation of lactate and opines in anaerobic invertebrates. *Comparative Biochemistry and Physiology Part B, Comparative Biochemistry* **83**, 255-272.

Glazier, D. S. (2005). Beyond the '3/4-power law': variation in the intra-and interspecific scaling of metabolic rate in animals. *Biological Reviews* **80**, 611-662.

Glazier, D. S. (2006). The 3/4-power law is not universal: evolution of isometric, ontogenetic metabolic scaling in pelagic animals. *BioScience* **56**, 325-332.

González, R.R. and Quiñones, R.A. (2000). Pyruvate oxidoreductases involved in glycolytic anaerobic metabolism of polychaetes from the continental shelf off central-south Chile. *Estuarine, Coastal and Shelf Sciences* **51**, 507-519.

Gonzalez, R.R. and Quiñones, R.A. (2002). Ldh activity in *Euphausia mucronata* and *Calanus chilensis*: implications for vertical migration behaviour. *Journal of Plankton Research* **24**, 1349-1356.

Grassle, J.F. and Grassle, J.P. (1974). Opportunistic life histories and genetic systems in marine benthic polychaetes. *Journal of Marine Resources* **32**, 253-284.

Grassle, J.P. and Grassle, J.F. (1976). Sibling species in the marine population

- indicator *Capitella* (Polychaeta). *Science* **192**, 567-569.
- Gray, J.S., Wu, R.S. and Or, Y.Y.** (2002). Effects of hypoxia and organic enrichment on the coastal marine environment. *Marine Ecology Progress Series* **238**, 249-279.
- Grieshaber, M.K., Hardewig, I., Kreutzer, U., and Pörtner, H. O.** (1994). Physiological and metabolic responses to hypoxia in invertebrates. *Reviews of Physiology, Biochemistry and Pharmacology* **125**, 43-147
- Guppy, M.** (2004). The biochemistry of metabolic depression: a history of perceptions. *Comparative Biochemistry and Physiology, Part B* **139**, 435-442.
- Harcet, M., Perina, D., and Plese, B.** (2013). Opine dehydrogenases in marine invertebrates. *Biochemical Genetics* **51**, 95-96.
- Hargrave, B. T.** (1972). Prediction of egestion by the deposit-feeding amphipod *Hyalella azteca*. *Oikos* **23**, 116-124.
- Harley, C. D., Hughes, R.A., Hultgren, K. M., Miner, B. G., Sorte, C. J., Thornber, C. S., Rodriguez, L.F., Tomanek, L., and Williams, S. L.** (2006). The impacts of climate change in coastal marine systems. *Ecology letters* **9**, 228-241.
- Horng, C. Y., and Taghon, G. L.** (1999). Effects of contaminated sediments on particle size selection by the polychaete *Capitella* sp. I. *Journal of Experimental Marine Biology and Ecology* **242**, 41-57.
- Jager, T., and Selck, H.** (2011). Interpreting toxicity data in a DEB framework: A case study for nonylphenol in the marine polychaete *Capitella teleta*. *Journal of Sea Research* **66**, 456-462.
- Jessen, G. L., Quiñones, R. A., and González, R. R.** (2009). Aerobic and anaerobic

- enzymatic activity and allometric scaling of the deep benthic polychaete *Hyalinoecia artifex* (Polychaeta: Onuphidae). *Journal of the Marine Biological Association of the United Kingdom* **89**, 1171-1175
- Justic, D., Rabalais, N., and Turner, R.** (1996). Effects of climate change on hypoxia in coastal waters: A doubled CO₂ scenario for the northern Gulf of Mexico. *Limnology and Oceanography* **41**, 992-1003.
- Justić, D., Bierman, V. J., Scavia, D., and Hetland, R. D.** (2007). Forecasting Gulf's hypoxia: The next 50 years? *Estuaries and Coasts* **30**, 791-801.
- Jorgensen, B. B.** (1996). Case study- Aarhus Bay. In *Eutrophication in Coastal Marine Ecosystems* (ed. B.B. Jorgenson and K. Richardson). pp. 137-154. Washington D.C.: American Geophysical Union.
- Kauffmann, K.** (1981). Fitting and using growth curves. *Oecologia* **49**, 293-299.
- Kooijman, S.A.L.M., Sousa, T., Pecquerie, L., van der Meer, J., and Jager, T.** (2008). From food-dependent statistics to metabolic parameters, a practical guide to the use of dynamic energy budget theory. *Biological Review* **83**, 533-552.
- Kristensen, E.** (1989). Oxygen and carbon dioxide exchange in the polychaete *Nereis virens*: influence of ventilation activity and starvation. *Marine Biology* **101**, 381-388.
- Levin, L.A.** (1984). Life-history and dispersal patterns in a dense infaunal polychaete assemblage: community structure and response to disturbance. *Ecology* **65**, 1185-1200.
- Levin, L.A.** (2003). Oxygen minimum zone benthos: adaptation and community response to hypoxia. *Oceanography and Marine Biology: Annual Review* **41**, 1-45.

- Linke-Gamenick, I., Forbes, V. E., and Sibly, R. M.** (1999). Density-dependent effects of a toxicant on life-history traits and population dynamics of a capitellid polychaete. *Marine Ecology Progress Series* **184**, 139-148.
- Linke-Gamenick, I., Vismann, B., and Forbes, V.** (2000). Effects of fluoranthene and ambient oxygen levels on survival and metabolism in three sibling species of *Capitella* (Polychaeta). *Marine Ecology Progress Series* **194**, 169-177.
- Linton, D.L. and Taghon, G.L.** (2000). Feeding, growth, and fecundity of *Capitella* sp. I in relation to sediment organic concentration. *Marine Ecology Progress Series* **205**, 229-240.
- Liu, Y., Xian, W., and Sun, S.** (2009). Metabolism of polychaete *Neanthes japonica* Izuka: relations to temperature, salinity and body weight. *Chinese Journal of Oceanology and Limnology* **27**, 356-364.
- Llanos, R. and Diaz, R.** (1994). Tolerance to low dissolved oxygen by the tubicolous polychaete, *Loimia medua*. *Journal of Marine Biology Association, U.K.* **74**, 143-148.
- Mangum, C. P., Woodin, B. R., Bonaventura, C., Sullivan, B., and Bonaventura, J.** (1975). The role of coelomic and vascular hemoglobin in the annelid family Terebellidae. *Comparative Biochemistry and Physiology Part A: Physiology* **51**, 281-294.
- Magnum, C., Colacino, J.M., and Grassle, J.P.** (1992). Red blood cell oxygen binding in Capitellid Polychaetes. *Biological Bulletin* **182**, 129-134.

- Matear, R. J. Hirst, A. C., and McNeil, B. I.** (2000). Changes in dissolved oxygen in the Southern Ocean with climate change. *Geochemistry, Geophysics, Geosystems* **1**, 11.
- Matear, R. J. and Hirst, A. C. (2003).** Long- term changes in dissolved oxygen concentrations in the ocean caused by protracted global warming. *Global Biogeochemical Cycle* **17**, 1125.
- Mendelsohn, B.** (Jan 2013). Personal communication
- Mendez, N. Lacorte, S. and Barata, C.** (2013) Effects of the pharmaceutical fluoxetine in spiked-sediments on feeding activity and growth of the polychaete *Capitella teleta*. *Marine Environmental Research* **29**, 76-82
- Meyer, N. P. and Seaver, E. C.** (2010). Cell lineage and fate map of the primary somatoblast of the polychaete annelid *Capitella teleta*. *Integrative and Comparative Biology* **50**, 756-767.
- Miller, J. R. and Russell, G. L.** (1992). The impact of global warming on river runoff. *Journal of Geophysical Research: Atmospheres* **97**, 2757-2764.
- Mill, P. J.** (1978). *Physiology of annelids*. London: Academic Press.
- Neuhoff, H. G.** (1979). Influence of temperature and salinity on food conversion and growth of different *Nereis* species (Polychaeta, Annelida). *Marine Ecology Progress Series* **1**, 255-262.
- Nichols, F. H.** (1975). Dynamics and energetics of three deposit-feeding benthic invertebrate populations in Puget Sound, Washington. *Ecological Monographs* **45**, 57-82.

- Pamatmat, M. and Findlay, S.** (1983). Metabolism of microbes, nematodes, polychaetes, and their interactions in sediment, as detected by heat flow measurements. *Marine Ecology Progress Series* **11**, 31-38.
- Pearson, T. and Rosenberg, R.** (1978). Macrobenthic succession in relation to organic enrichment and pollution of the marine environment. *Oceanography and Marine Biology: Annual Review* **16**, 229-311.
- Pechenik, J.A., Hammer, K., and Weise, C.** (1996). The effect of starvation on acquisition of competence and post-metamorphic performance in the marine prosobranch gastropod *Crepidula fornicata* (L.). *Journal of Experimental Marine Biology and Ecology* **199**, 137-152.
- Persson, T. and De Roos, A.** (2007). Interplay between individual growth and population feedback shapes body-size distribution. In *Body Size: The Structure and Function of Aquatic Ecosystems* (ed. A.G. Hildrew, D.G. Raffaelli, and R. Edmonds-Brown). pp. 225-244. New York: Cambridge University Press.
- Plese, B., Schröder, H. C., Grebenjuk, V. A., Wegener, G., Brandt, D., Natalio, F., and Müller, W. E.** (2009). Strombine dehydrogenase in the demosponge *Suberites domuncula*: characterization and kinetic properties of the enzyme crucial for anaerobic metabolism. *Comparative Biochemistry and Physiology Part B: Biochemistry and Molecular Biology* **154**, 102-107.
- Pörtner, H.** (2001). Climate change and temperature-dependent biogeography: oxygen limitation of thermal tolerance in animals. *Naturwissenschaften* **88**, 137-146.
- Pörtner, H. O.** (2002). Climate variations and the physiological basis of temperature dependent biogeography: systemic to molecular hierarchy of thermal tolerance in

animals. *Comparative Biochemistry and Physiology Part A: Molecular and Integrative Physiology* **132**, 739-761.

Pörtner, H. O., Langenbuch, M., and Michaelidis, B. (2005). Synergistic effects of temperature extremes, hypoxia, and increases in CO₂ on marine animals: From Earth history to global change. *Journal of Geophysical Research: Oceans* doi:10.1029/2004JC002561.

Pörtner, H.O. (2009). Oxygen- and capacity-limitation of thermal tolerance: a matrix for integrating climate-related stressor effects in marine ecosystems. *The Journal of Experimental Biology* **213**, 881-893.

Rabalais, N. N., Turner, R. E., and Wiseman Jr, W. J. (2002). Gulf of Mexico hypoxia, aka “The dead zone”. *Annual Review of ecology and Systematics* **33**, 235-263.

Rabalais, N. N., Turner, R. E., Díaz, R. J., and Justić, D. (2009). Global change and eutrophication of coastal waters. *ICES Journal of Marine Science: Journal du Conseil* **66**, 1528-1537.

Rakocinski, C.F. (2009). Linking allometric macrobenthic processes to hypoxia using the Peters mass balance model. *Journal of Experimental Marine Biology and Ecology* **381**, S13-S20.

Ramskov, T. and Forbes, V.E. (2008). Life history and population dynamics of the opportunistic polychaete *Capitella* sp. I in relation to sediment organic matter. *Marine Ecology Progress Series* **369**, 181-192.

Rasmussen, J. (1993). Patterns in the size structure of littoral zone macroinvertebrate

- communities. *Canadian Journal of Fisheries and Aquatic Sciences* **50**, 2192-2207.
- Razali, N. M., and Wah, Y. B.** (2011). Power comparisons of Shapiro-Wilk, Kolmogorov-Smirnov, Lilliefors and Anderson-Darling tests. *Journal of Statistical Modeling and Analytics* **2**, 21-33.
- Sagasti, A., Schaffner, L. and Duffy, J.** (2001). Effects of periodic hypoxia on mortality, feeding and predation in an estuarine epifaunal community. *Journal of Experimental Marine Biology and Ecology* **258**, 257-283.
- Sarmiento, J.L., Hughes, T.M.C, Stouffer, R.J., and Manabe, S.** (1998). Simulated response of the ocean carbon cycle to anthropogenic climate warming. *Nature* **393**, 245-249.
- Schidek, D.** (1997). *Marenzellaria viridis* (Verrill, 1873) (Polychaeta), a new benthic species within European coastal waters, some metabolic features. *Journal of Experimental Biology and Ecology* **211**, 85-101.
- Schwinghamer, P.** (1981). Characteristic size distributions of integral benthic communities. *Canadian Journal of Fisheries and Aquatic Science* **38**, 1255-1263.
- Selck, H., Decho, A. W., and Forbes, V. E.** (1999). Effects of chronic metal exposure and sediment organic matter on digestive absorption efficiency of cadmium by the deposit-feeding polychaete *Capitella* species I. *Environmental Toxicology and Chemistry* **18**, 1289-1297.
- Sherwood, G. D., Pazzia, I., Moeser, A., Hontela, A., and Rasmussen, J. B.** (2002). Shifting gears: enzymatic evidence for the energetic advantage of switching diet

- in wild-living fish. *Canadian Journal of Fisheries and Aquatic Sciences* **59**, 229-241.
- Shingleton, A.** (2010) Allometry: The Study of Biological Scaling. *Nature Education Knowledge* **3**, 2.
- Shumway, S. E.** (1979). The effects of body size, oxygen tension and mode of life on the oxygen uptake rates of polychaetes. *Comparative Biochemistry and Physiology Part A: Physiology* **64**, 273-278.
- Shumway, S.** (1983). Factors affecting oxygen consumption in the coot clam *Mulina lateralis*. *Ophelia* **22**, 143-171.
- Siegunmund, B. and Grieshaber, M.** (2002). Alanopine and strombine are end products of anaerobic glycolysis in the lugworm, *Arenicola marina* L. (Annelida, polychaete). *Comparative Biochemistry and Physiology Part B.* **82**, 337-345.
- Somero, G. N., and Childress, J. J.** (1990). Scaling of ATP-supplying enzymes, myofibrillar proteins and buffering capacity in fish muscle: relationship to locomotory habit. *Journal of Experimental Biology* **149**, 319-333.
- Sommer, A. and Porter, H.O.** (1999). Exposure of *Arenicola marina* to extreme temperatures: adaptive flexibility of a boreal and a subpolar population. *Marine Ecology Progress Series* **181**, 215-226.
- Sommer, A., Klein, B., and Pörtner, H. O.** (1997). Temperature induced anaerobiosis in two populations of the polychaete worm *Arenicola marina* (L.). *Journal of Comparative Physiology B: Biochemical, Systemic, and Environmental Physiology* **167**, 25-35.

- Stillman, J. H.** (2002). Causes and consequences of thermal tolerance limits in rocky intertidal porcelain crabs, genus *Petrolisthes*. *Integrative and Comparative Biology* **42**, 790-796.
- Storey, K. B., and Storey, J. M.** (1990). Metabolic rate depression and biochemical adaptation in anaerobiosis, hibernation and estivation. *Quarterly Review of Biology* **65**, 145-174.
- Taghon, G.L.** (1989). Modeling deposit feeding. In *Ecology of Marine Deposit Feeders* (ed. G. Lopez, G. Taghon, and J. Levinton). pp. 223-246. New York: Springer.
- Tenore, K. R.** (1983). Organic nitrogen and caloric content of detritus III. Effect on growth of a deposit-feeding polychaete, *Capitella capitata*. *Estuarine, Coastal and Shelf Science* **17**, 733-742.
- Tenore, K. R.** (1988). Nitrogen in benthic food chains. In: *Nitrogen Cycling in Coastal Marine Environments* (ed. T.H. Blackburn and J. Sorensen). pp. 191-206. New York: Wiley.
- Tenore, K.R. and Chesney, E.J.** (1985). The effects of interaction of rate of food supply and population density on the bioenergetics of the opportunistic polychaete, *Capitella capitata* (type 1). *Limnology and Oceanography* **30**, 1188-1195.
- Thuesen, E. V., and Childress, J. J.** (1994). Oxygen consumption rates and metabolic enzyme activities of oceanic California medusae in relation to body size and habitat depth. *The Biological Bulletin* **187**, 84-98.
- Tomanek, L., and Somero, G. N.** (1999). Evolutionary and acclimation-induced variation in the heat-shock responses of congeneric marine snails (genus *Tegula*)

- from different thermal habitats: implications for limits of thermotolerance and biogeography. *The Journal of Experimental Biology* **21**, 2925-2936.
- Vaquer-Sunyer, R. and Duarte, C. M.** 2011. Temperature effects on oxygen thresholds for hypoxia in marine benthic organisms. *Global Change Biology* **17**, 1788-1797.
- Vismann, B. and Hagerman, L.** (1996). Recovery from hypoxia with and without sulfide in *Saduria entomon*: oxygen debt, reduced sulfur and anaerobic metabolites. *Marine Ecology Progress Series* **143**, 131-139.
- Weber, R.** (1980). Functions of invertebrate hemoglobins with special reference to adaptations of environmental hypoxia. *American Zoologist* **20**, 79-101.
- Weiss, R. F.** 1970. The solubility of nitrogen, oxygen and argon in water and seawater. *Deep Sea Research and Oceanographic Abstracts* **17**, 721-735.
- Wells, R.M.G., Jarvis, P.J., and Shumway, S.E.** (1980). Oxygen uptake, the circulatory system, and haemoglobin function in the intertidal polychaete *Terebella haplochaeta*. *Journal of Experimental Marine Biology and Ecology* **46**, 255-277.
- White, C. R., Cassey, P., and Blackburn, T. M.** (2007). Allometric exponents do not support a universal metabolic allometry. *Ecology* **88**, 315-323.
- Wood, S. C.** (1980). Adaptation of red blood cell function to hypoxia and temperature in ectothermic vertebrates. *American Zoologist* **20**, 163-172.
- Wu, R. S.** (2002). Hypoxia: from molecular responses to ecosystem responses. *Marine Pollution Bulletin* **45**, 35-45.
- Yong, L., Weiwei, X., and Shichun, S.** (2009). Metabolism of polychaete *Neanthes japonica* Izuka: relations to temperature, salinity, and body weight. *Chinese Journal of Oceanology and Limnology* **27**, 356-364.

- Quiroga, E. Quinones, R. Gonzalez, R., Gallardo, V., and Jessen, G.** (2007). Aerobic and anaerobic metabolism of *Paraprionospio pinnata* (Polychaeta: Spionidae) in central Chile. *Journal of Marine Biological Association of the UK* **87**, 459-463.
- Zachariassen, K. E., Aunaas, T., Børseth, J. F., Einarson, S., Nordtug, T., Olsen, A., and Skjervø, G.** (1991). Physiological parameters in ecotoxicology. *Comparative Biochemistry and Physiology Part C: Comparative Pharmacology* **100**, 77-79.
- Zammit, V. A.** (1978). Possible relationship between energy metabolism of muscle and oxygen binding characteristics of haemocyanin of cephalopods. *Journal of the Marine Biological Association of the United Kingdom* **58**, 421-424.
- Zeuthen, E.** (1953). Oxygen Uptake as Related to Body Size in Organisms. *The Quarterly Review of Biology* **28**, 1-12
- Zhang, H., Shin, P.K.S., and Cheung, S.G.** (2015). Physiological responses and scope for growth upon medium-term exposure to the combined effects of ocean acidification and temperature in a subtidal scavenger *Nassarius conoidalis*. *Marine Environmental Research* **106**, 51-60.